Low-order absorbing boundary condition for two-dimensional isotropic poroelasticity

Hélène Barucq, Julien Diaz, Rose-Cloé Meyer, Ha Pham

Low-order absorbing boundary condition for two-dimensional isotropic poroelasticity

Hélène Barucq, Julien Diaz, Rose-Cloé Meyer, Ha Pham

RESEARCH REPORT

N° 9358

Mars 2020

Project-Team Magique 3D

ISSN 0249-6399 ISRN INRIA/RR--9358--FR+ENG

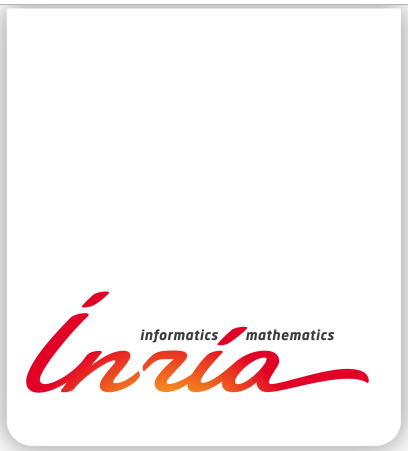

Low-order absorbing boundary condition for two-dimensional isotropic poroelasticity

Hélène Barucq*, Julien Diaz*, Rose-Cloé Meyer*, Ha Pham*

Project-Team Magique 3D

Research Report n° 9358 — Mars 2020 — 61 pages

Abstract: In this report, we construct a low order absorbing boundary condition (ABC) for two-dimensional isotropic poroelasticity in frequency domain. The ABC is obtained for circular geometry by approximating the behavior of the analytical outgoing wave solution. The ABC is then extended to general non-circular domains and implemented with Hybridizable Discontinuous Galerkin (HDG) method. In circular symmetry, using the form of the exact solution, the robustness of the ABC is evaluated for the problem of scattering of planewave by a circular obstacle. We also compare the performance of this ABC with Perfectly Matched Layers, both coupled with HDG method. All of our numerical tests are performed on geophysical realistic media.

Key-words: Absorbing boundary condition, radiation boundary condition, PML, HDG method, isotropic poroelasticity

* Inria Bordeaux Sud-Ouest, Project-Team Magique 3D, Université de Pau et des pays de l'Adour, France

RESEARCH CENTRE
BORDEAUX – SUD-OUEST

200 avenue de la Vieille Tour
33405 Talence Cedex

Condition limite absorbante de bas ordre pour les équations poroélastiques isotropes en deux dimensions

Résumé : Dans ce rapport, nous construisons une condition limite absorbante (CLA) de bas ordre pour la poroélasticit isotrope en deux dimensions et dans le domaine fréquentiel. La CLA est obtenue analytiquement pour des géométries circulaires en approximant l'expression exacte de l'onde sortante pour les équations poroélastiques. Cette condition est étendue à des géométries quelconques et mise en oeuvre numériquement avec la méthode de Galerkin Discontinue Hybridizable (HDG). La robustesse de la CLA est évaluée en géométrie circulaire pour le problème de la diffraction des ondes planes par un obstacle. Nous comparons aussi la performance de cette CLA avec celle des couches parfaitement adaptées (PML), couplées à la méthode HDG. Tous les tests numériques sont effectués sur des matériaux géophysiques réalistes.

Mots-clés : Condition limite absorbante, condition de radiation, PML, méthode HDG, poroélasticité isotrope

1 Introduction

In this report, we construct a low order radiation boundary condition for the 2D isotropic poroelastic equations in frequency domain and implement it with Hybridizable Discontinuous Galerkin method. The implementation of non-reflective boundary conditions for wave propagation is an important question in many physical applications. In our case, poroelastic media are used to model realistic geophysical materials.

The wave propagation in poroelastic materials has been first modeled by Biot in [6, 7]. We refer to [3] for more history on the equation. This document follows the results from our work on analytical solutions for poroelasticity [3], in which we had obtained expansions of generic outgoing solutions in series of Bessel functions using the potential theory. This family of outgoing solutions satisfies a relation between the trace of their solid and fluid stress tensors and the trace of their velocities on a circle. This relation is approximated to order r^{-1} to give a boundary condition of the form

$$\begin{pmatrix} \tau\,\mathbf{n} \\ p \end{pmatrix} \;=\; A \begin{pmatrix} \mathbf{u} \\ \mathbf{w} \end{pmatrix} \tag{1}$$

where A is a zero-th order operator containing no derivation. This condition is analogous to LysmerKuhlemeyer (LK) absorbing boundary condition for elasticity, that has been investigated in [21]. We have found that our condition gives results of the same order of magnitude as LK condition. Absorbing boundary conditions for poroelasticity have been given by Degrande [15, 16] and Akiyoshi [1, 2] in time domain. The methods employed in these reference are different from ours resulting in a different form of ABC. This is in particular for the second reference, whose form of ABC is not given in a compact form conducive for discretization with finite elements. On the other hand, Degrande [15, 16] works in a stratified setting, and arrives at a form comparable to ours. In our ABC, the operator A is not symmetric, while that in [15, 16] is symmetrized. In the above form, our derived ABC is natural to be coupled with HDG, since it resembles the conservativity condition of numerical traces. For discussion of HDG, we refer to [4], in which we have presented in detail the HDG formulation and discretization for poroelasticity on bounded domains. This work thus extends [4] to unbounded domains.

An other way to truncate the domain is to use Perfectly Matched Layer (PML). This has first been done for the electromagnetic wave equations by Berenger in [5]. An absorbent layer is added using two attenuation functions that prevent the reflections on the border. Due to the lack of work on ABC for poroelasticity, most works in literature e.g. [18], [23] and [20] use PML, which is readily available for most partial differential equations (PDE).

This report is organized as follows. First, we recall the poroelasticity equation in section 2. In section 3, we derive a low order radiation boundary condition (RBC). Then we obtain the expression for the exact solution associated with this condition in section 4 for an annulus domain. The performance of this condition is investigated in section 5, by comparison with the outgoing solution that we calculated in [3]. This is recalled in A. In section 6, the obtained RBC is implemented with Hybridizable discontinuous Galerkin (HDG) method for poroelastic wave equations. Then, in section 7, we consider a second method to truncate the domain by using the Perfectly Matched Layer (PML) also with HDG discretization. Finally, section 8 compares the performance of our RBC with that of PML.

2 Poroelasticity

In this section, we recall the isotropic poroelastic wave equations in frequency domain, and the porous physical parameters. Next, we present the main results obtained in [3] for the expression of the unknowns in terms of potentials and Bessel functions. Finally, we present the boundary conditions considered in a bounded domain and the parameters of the materials used for the numerical tests.

2.1 First-order harmonic equation

We consider an isotropic porous medium, composed by a solid frame, and pores filled with a fluid that follows Biot's model [8], [9]. We will use the first-order poroelastic wave equations in frequency domain. The unknowns in first order formulation are the solid velocity $\mathbf{u}$ (m.s^{-1}), the relative fluid velocity $\mathbf{w}$ (m.s^{-1}), the solid stress

$\boldsymbol{\tau}$ (MPa) and the fluid pressure p (MPa). They solve the system

$$\begin{cases} \nabla\cdot\boldsymbol{\tau} + \mathbf{f}_u &= \mathrm{i}\omega\,\rho_a\,\mathbf{u} \;+\; \mathrm{i}\omega\,\rho_f\,\mathbf{w}\,, \\ -\nabla \mathrm{p} + \mathbf{f}_{\mathrm{w}} &= \mathrm{i}\omega\,\rho_f\mathbf{u} \;+\; \mathrm{i}\omega\;\rho_{\mathrm{dyn}}\mathbf{w}\,, \\ \mathrm{i}\omega\,\boldsymbol{\tau} &= \mathbf{C}_{\mathrm{fr}} : \boldsymbol{\epsilon} \;-\; \mathrm{i}\omega\,\boldsymbol{\alpha}\,\mathrm{p}\,, \\ \mathrm{i}\omega\,\mathrm{p} &= -M\,\nabla\cdot\mathbf{w} \;-\; M\,\boldsymbol{\alpha} : \boldsymbol{\epsilon}\,. \end{cases} \tag{2}$$

with $\boldsymbol{\epsilon} = \dfrac{\nabla\mathbf{u} + (\nabla\mathbf{u})^t}{2}$, ρ_a the averaged density, ρ_f the fluid density, $\rho_{\mathrm{dyn}} = \dfrac{\mathrm{i}\,\eta}{\omega\,k(\omega)}$ the dynamic density, η being the viscosity of the fluid and k the permability, $\mathbf{C}_{\mathrm{fr}}$ the stiffness matrix, $\boldsymbol{\alpha}$ the effective-stress coefficient, M the fluid-solid coupling modulus, and $\mathbf{f}_u$, f_{w} external forces. More details on the parameters and equations of poroelasticity can be found in [10], [13], [3].

2.2 Physical parameters used for the numerical tests

We list in Table 1 the physical parameters of the porous media considered in this report. The media are filled with brine, which can be either inviscid or viscous. For some of the tests, we vary the viscosity of the material to highlight its influence on the solution.

Physical parameters	Sandstone	Sand	Shale
Porosity ϕ	0.2	0.3	0.16
Fluid Density ρ_f $(10^3 kg.m^{-3})$	1.04	1	1.04
Solid Density ρ_s $(10^3 kg.m^{-3})$	2.5	2.6	2.21
Viscosity η $(10^{-3} Pa.s)$	0	1	0
Permeability κ_0 $(10^{-9} m^2)$	0.06	0.01	0.01
Tortuosity $\mathfrak{t}$	2	3	2
Solid Bulk Modulus $\mathrm{k_s}$ $(10^9 Pa)$	40	35	7.6
Fluid Bulk Modulus $\mathrm{k_f}$ $(10^9 Pa)$	2.5	2.2	2.5
Frame Bulk Modulus $\mathrm{k_{fr}}$ $(10^9 Pa)$	20	0.4	6.6
Frame Shear Modulus $\mathrm{G_{fr}}$ $(10^9 Pa)$	12	0.5	3.96

Table 1: Summary of the physical parameters of media in consideration in this report. The parameters for sand are obtained from [19][Table 1], those for sandstone and shale from [14][Table 5]. For some tests, we will use these materials. However, we will vary some of the parameters to highlight their effect on the solution.

2.3 Boundary conditions for a fixed boundary

For a fixed boundary, we can impose four types of boundary conditions:

Type 1 "Neumann-like"
$$\begin{cases} \boldsymbol{\tau}\,\boldsymbol{n} &= f_t\,, \\ \mathbf{w}\cdot\boldsymbol{n} &= f_w\,, \end{cases} \tag{3a}$$

Type 2
$$\begin{cases} \boldsymbol{\tau}\,\boldsymbol{n} &= f_t\,, \\ \mathrm{p} &= f_p\,, \end{cases} \tag{3b}$$

Type 3 "Dirichlet-like"
$$\begin{cases} \mathbf{u} &= f_u, \\ \mathrm{p} &= f_p\,, \end{cases} \tag{3c}$$

Type 4
$$\begin{cases} \mathbf{u} &= f_u\,, \\ \mathbf{w}\cdot\boldsymbol{n} &= f_w\,, \end{cases} \tag{3d}$$

where f_u, f_w, f_t, f_p are exterior forces. In the numerical tests, we will focus mainly on the boundary condition of type 1 and 3. If $f_t\,, f_p$ are zeros in (3b), we have free surface condition. Similarly, if $f_u\,, f_w$ are zeros in (3d), the surface is a wall.

2.4 Plane wave solution

In poroelastic media, we observe three types of plane waves, two longitudinal waves, denoted P for the fast-wave and B for the slow wave, and one transverse wave, denoted S. The three slownesses sustained in a poroelastic

medium are

$$\text{S-wave-slowness} \qquad \mathsf{s}_{\mathrm{S}}^2(\omega) \;:=\; \frac{\det A(\omega)}{\mu_{\mathrm{fr}}\,\rho_{\mathrm{dyn}}(\omega)}\,, \tag{4a}$$

$$\text{'fast' P-wave-slowness} \qquad 2\,\mathsf{s}_{\mathrm{P}}^2(\omega) \;:=\; \frac{\operatorname{tr} C(\omega)}{\det B} \;-\; \sqrt{\left(\frac{\operatorname{tr} C(\omega)}{\det B}\right)^2 \;-\; 4\frac{\det A(\omega)}{\det B}}\,, \tag{4b}$$

$$\text{'slow' B-wave-slowness} \qquad 2\,\mathsf{s}_{\mathrm{B}}^2(\omega) \;:=\; \frac{\operatorname{tr} C(\omega)}{\det B} \;+\; \sqrt{\left(\frac{\operatorname{tr} C(\omega)}{\det B}\right)^2 \;-\; 4\frac{\det A(\omega)}{\det B}}\,, \tag{4c}$$

where we have defined

$$A(\omega) := \begin{pmatrix} \rho_a & \rho_f \\ \rho_f & \rho_{\mathrm{dyn}} \end{pmatrix} \quad , \quad B := \begin{pmatrix} H & \alpha\, M \\ \alpha M & M \end{pmatrix} \quad , \quad B^{\mathrm{cof}} = \begin{pmatrix} M & -\alpha\, M \\ -\alpha M & H \end{pmatrix} \quad , \quad C(\omega) := B^{\mathrm{cof}}\, A(\omega)\,, \tag{5}$$

and

$$\begin{aligned} \operatorname{tr} C(\omega) \;&=\; \rho_{\mathrm{dyn}}(\omega)\, H \;-\; 2\alpha\, M\, \rho_f \;+\; \rho_a\, M\,, \\ \det B \;&=\; M\, H \;-\; (\alpha\, M)^2 \;=\; M\,(\lambda_{\mathrm{fr}} \;+\; 2\mu_{\mathrm{fr}})\,, \\ \det A(\omega) \;&=\; \rho_a\, \rho_{\mathrm{dyn}}(\omega) \;-\; \rho_f^2\,. \end{aligned} \tag{6}$$

Remark 1. Note that these quantities can have complex values, (see [3]), and $\det A(\omega)$ cannot vanish. The slownesses should also be taken such as their real part is positive and their imaginary part is negative, for the Hankel function of type 1 to represent the outgoing solution. More details are given in Section 4 and 5 of [3].

Using the slowness expresssions from (4), the plane wave propagating in direction $\widehat{\mathbf{k}} = (\cos\alpha_{\mathrm{inc}}, \sin\alpha_{\mathrm{inc}})$ writes:

1. For the transverse wave (polarization direction perpendicular to the propagation direction):

$$\mathbf{u}_{\mathrm{S}}^{\mathrm{pw}} \;=\; e^{\mathrm{i}\,\mathbf{k}_{\mathrm{S}}\cdot\boldsymbol{x}}\;(\mathfrak{s}\,\mathrm{i}\,\omega)\;\widehat{\mathbf{d}} \quad , \quad \mathbf{w}_{\mathrm{S}}^{\mathrm{pw}} \;=\; \beta_{\mathrm{S}}\, e^{\mathrm{i}\,\mathbf{k}_{\mathrm{S}}\cdot\boldsymbol{x}}\;(\mathfrak{s}\,\mathrm{i}\,\omega)\;\widehat{\mathbf{d}}\,, \tag{7a}$$

$$\boldsymbol{\tau}_{\mathrm{S}}^{\mathrm{pw}} \;=\; \mathrm{i}\,\omega\,\mathsf{s}_{\mathrm{S}}(\omega)\, e^{\mathrm{i}\,\mathbf{k}_{\mathrm{S}}\cdot\boldsymbol{x}}\,\mu_{\mathrm{fr}}\left(\widehat{\mathbf{k}}\otimes\widehat{\mathbf{d}} \;+\; \widehat{\mathbf{d}}\otimes\widehat{\mathbf{k}}\right), \tag{7b}$$

$$\mathrm{p}_{\mathrm{S}}^{\mathrm{pw}} \;=\; 0\,. \tag{7c}$$

with polarization given by

$$\begin{cases} \mathbf{k}_{\mathrm{S}} \;=\; \omega\,\mathsf{s}_{\mathrm{S}}(\omega)\,\widehat{\mathbf{k}} \quad , \\ \mathsf{s}_{\mathrm{S}}(\omega) \text{ given by (4a)}\,, \\ \widehat{\mathbf{d}} \perp \widehat{\mathbf{k}} \quad , \quad |\widehat{\mathbf{d}}| = 1\,, \\ \beta_{\mathrm{S}} \;=\; \dfrac{\rho_f}{\rho_{\mathrm{dyn}}(\omega)}\,. \end{cases} \tag{8}$$

2. For the two types of longitudinal waves P and B (polarization direction parallel to the propagation direction), which are distinguished by subscript $\bullet \in \{\mathrm{P}\,,\mathrm{B}\}$:

$$\mathbf{u}_{\bullet}^{\mathrm{pw}} \;=\; e^{\mathrm{i}\,\mathbf{k}_{\bullet}\cdot\boldsymbol{x}}\;(\mathfrak{s}\,\mathrm{i}\,\omega)\;\widehat{\mathbf{d}} \quad , \quad \mathbf{w}_{\bullet}^{\mathrm{pw}} \;=\; \beta_{\bullet}\, e^{\mathrm{i}\,\mathbf{k}_{\bullet}\cdot\boldsymbol{x}}\;(\mathfrak{s}\,\mathrm{i}\,\omega)\;\widehat{\mathbf{d}}\,, \tag{9a}$$

$$\boldsymbol{\tau}_{\bullet}^{\mathrm{pw}} \;=\; \mathrm{i}\,\omega\,\mathsf{s}_{\bullet}(\omega)\, e^{\mathrm{i}\mathbf{k}_{\bullet}\cdot\boldsymbol{x}}\left(2\,\mu_{\mathrm{fr}}\,\widehat{\mathbf{d}}\otimes\widehat{\mathbf{d}} \;+\; \Big(\underbrace{-\tfrac{2}{3}\mu_{\mathrm{fr}} \;+\; \mathrm{k}_{\mathrm{fr}}}_{\lambda_{\mathrm{fr}}} \;+ M\,\alpha^2 \;+\; \beta_{\bullet}\,\alpha\, M\Big)\,\mathbf{Id}\right), \tag{9b}$$

$$\mathrm{p}_{\bullet}^{\mathrm{pw}} \;=\; \mathrm{i}\,\omega\,\mathsf{s}_{\bullet}(\omega)\;(-M\,\beta_{\bullet} \;-\; M\,\alpha)\, e^{\mathrm{i}\mathbf{k}_{\bullet}\cdot\boldsymbol{x}}\,. \tag{9c}$$

with polarization given by

$$\begin{cases} \mathbf{k}_{\bullet} \;=\; \omega\,\mathsf{s}_{\bullet}(\omega)\,\widehat{\mathbf{d}} \quad , \quad |\widehat{\mathbf{d}}| = 1, \\ \mathsf{s}_{\bullet}(\omega) \text{ given by (4b) or (4c)}\,, \\ \beta_{\bullet} \;=\; -\dfrac{H\,\mathsf{s}_{\bullet}^2(\omega) - \rho_a}{\alpha\, M\,\mathsf{s}_{\bullet}^2(\omega) \;-\; \rho_f}\,. \end{cases} \tag{10}$$

2.5 Polar coordinates

A point in polar coordinates $(r,\,\theta)$ is defined with the distance of the point from the origin r and an angle θ. The coordinates are linked to Cartesian coordinates by:

$$x \,=\, r\,\cos\theta\,, \qquad \text{and} \quad y \,=\, r\,\sin\theta\,. \tag{11}$$

We define the unit vectors in the polar coordinate system,

$$\mathbf{e}_r \,=\, \begin{pmatrix}\cos\theta\\ \sin\theta\end{pmatrix}\,, \qquad \text{and} \quad \mathbf{e}_\theta \,=\, \begin{pmatrix}-\sin\theta\\ \cos\theta\end{pmatrix}\,. \tag{12}$$

In this system we decompose a vector $\mathbf{a}\in\mathbb{C}^2$ as

$$\mathbf{a} \,=\, \mathbf{a}_r\,\mathbf{e}_r \,+\, \mathbf{e}_\theta\,\mathbf{e}_\theta\,. \tag{13}$$

The tensor product of two vectors in polar coordinates are

$$\mathbf{a}\otimes\mathbf{b} \,=\, \mathbf{a}_r\mathbf{b}_r\;\mathbf{e}_r\otimes\mathbf{e}_r \,+\, \mathbf{a}_r\mathbf{b}_\theta\;\mathbf{e}_r\otimes\mathbf{e}_\theta \,+\, \mathbf{a}_\theta\mathbf{b}_r\;\mathbf{e}_\theta\otimes\mathbf{e}_r \,+\, \mathbf{a}_\theta\mathbf{b}_\theta\;\mathbf{e}_\theta\otimes\mathbf{e}_\theta \tag{14}$$

We also list the action of differential operators in polar coordinates. For a scalar f, we recall the notation of **curl** first in Cartesian coordinates,

$$\mathbf{curl}\, f \;=\; \begin{pmatrix}\partial_y f\\ -\partial_x f\end{pmatrix} \tag{15}$$

In polar coordinates, the action of **curl** and gradient ∇ are,

$$\mathbf{curl}\, f = \frac{1}{r}\,\partial_\theta f\,\mathbf{e}_r - \partial_r f\,\mathbf{e}_\theta\,, \quad \text{and} \quad \nabla f \,=\partial_r f\,\mathbf{e}_r + \frac{\partial_\theta}{r}\,\mathbf{e}_\theta\,. \tag{16}$$

We will also need the following second-order operators,

$$\nabla^2 f \;:=\; \nabla\,(\nabla f) = \partial_r^2 f\,\mathbf{e}_r\otimes\mathbf{e}_r + \left(\frac{\partial^2_{r\theta} f}{r} - \frac{\partial_\theta f}{r^2}\right)\mathbf{e}_r\otimes\mathbf{e}_\theta + \left(\frac{\partial^2_{r\theta} f}{r} - \frac{\partial_\theta f}{r^2}\right)\mathbf{e}_\theta\otimes\mathbf{e}_r + \left(\frac{\partial^2_\theta f}{r} + \frac{\partial_r f}{r}\right)\mathbf{e}_\theta\otimes\mathbf{e}_\theta\,, \tag{17a}$$

$$\nabla\,(\mathbf{curl} f) = \left(\frac{\partial^2_{r\theta} f}{r} - \frac{\partial_\theta f}{r^2}\right)\mathbf{e}_r\otimes\mathbf{e}_r + \left(\frac{\partial^2_\theta f}{r^2} + \frac{\partial_r f}{r}\right)\mathbf{e}_r\otimes\mathbf{e}_\theta - \partial_r^2 f\,\mathbf{e}_\theta\otimes\mathbf{e}_r + \left(-\frac{\partial^2_{r\theta} f}{r} + \frac{\partial_\theta f}{r^2}\right)\mathbf{e}_\theta\otimes\mathbf{e}_\theta. \tag{17b}$$

2.6 Potentials and expansion of the unknowns

In [3], we have expressed the unknowns ($\mathbf{u}$, $\mathbf{w}$, $\boldsymbol{\tau}$, p) in two dimensions, using the potentials $\chi_\bullet$, $\bullet = P, B, S$, to obtain the following expressions:

$$\begin{aligned}
\mathrm{i}\,\omega\,\mathbf{u} \;&=\; \mathrm{s}_{\mathrm{P}}^{-2}\,\nabla\chi_{\mathrm{P}} \,+\, \mathrm{s}_{\mathrm{B}}^{-2}\,\nabla\chi_{\mathrm{B}} \,-\, \mathrm{s}_{\mathrm{S}}^{-2}\,\mathbf{curl}\,\chi_{\mathrm{S}}\,,\\
\mathrm{i}\,\omega\,\mathbf{w} \;&=\; \frac{\beta_{\mathrm{P}}}{\mathrm{s}_{\mathrm{P}}^2}\nabla\chi_{\mathrm{P}} \,+\, \frac{\beta_{\mathrm{B}}}{\mathrm{s}_{\mathrm{B}}^2}\nabla\chi_{\mathrm{B}} \,+\, \frac{\rho_f\,\mu_{\mathrm{fr}}}{\det A}\mathbf{curl}\,\chi_{\mathrm{S}}\,,\\
\mathrm{p} \;&=\; -M\,(\beta_{\mathrm{P}} \,+\, \alpha)\chi_{\mathrm{P}} \,-\, M\,(\beta_{\mathrm{B}} \,+\, \alpha)\chi_{\mathrm{B}}\,,\\
\omega^2\,\boldsymbol{\tau} \;&=\; \mu_{\mathrm{fr}}\left(-\frac{2}{\mathrm{s}_{\mathrm{P}}^2}\,\nabla^2\chi_{\mathrm{P}} \,-\, \frac{2}{\mathrm{s}_{\mathrm{B}}^2}\,\nabla^2\chi_{\mathrm{B}} \,+\, \frac{\nabla\mathbf{curl}\,\chi_{\mathrm{S}} \,+\, (\nabla\mathbf{curl}\,\chi_{\mathrm{S}})^t}{\mathrm{s}_{\mathrm{S}}^2}\right)\\
&\quad +\, \omega^2\,\left(-\tfrac{2}{3}\mu_{\mathrm{fr}} \,+\, \mathrm{k}_{\mathrm{fr}} \,+\, M\alpha^2\right)\,(\chi_{\mathrm{P}} \,+\, \chi_{\mathrm{B}})\;\mathbf{Id}\\
&\quad +\, \omega^2\,\alpha\,M\,(\beta_{\mathrm{P}}\,\chi_{\mathrm{P}} \,+\, \beta_{\mathrm{B}}\,\chi_{\mathrm{B}})\;\mathbf{Id}\,.
\end{aligned} \tag{18}$$

with operator **curl** defined in (15) and ∇^2 in (17b), and $\mathbf{Id} = \begin{pmatrix}1 & 0\\ 0 & 1\end{pmatrix}$.

The potentials $\chi_\bullet$ solve the Helmholtz equation,

$$\left(-\,\Delta \,-\, \omega^2\,\mathsf{s}_\bullet^2\right)\chi_\bullet \;=\; 0\,, \tag{19}$$

hence they can be expanded in terms of Bessel functions, depending on the domain considered. Denote by Z_k and $\tilde{\mathrm{Z}}_k$ a basis of linearly independent Bessel functions, we have:

$$\chi_\bullet(\boldsymbol{x}) \;=\; \sum_{k\in\mathbb{Z}} \Big(a_{\bullet,k}\, \mathrm{Z}_k(\,\omega\, \mathsf{s}_\bullet\, |\boldsymbol{x}|) \;+\; \tilde{a}_{\bullet,k} \tilde{\mathrm{Z}}_k(\,\omega\, \mathsf{s}_\bullet\, |\boldsymbol{x}|) \Big)\; e^{\mathrm{i}\, k\, \theta} \quad , \quad \bullet \in \{\mathrm{S},\mathrm{P},\mathrm{B}\}. \tag{20}$$

The Bessel functions have the following identities:

$$\mathrm{Z}_k'(z) \;=\; -\mathrm{Z}_{k+1}(z) + \frac{k}{z}\mathrm{Z}_k(z)\,, \qquad \mathrm{Z}_k''(z) \;=\; -\frac{1}{z}\mathrm{Z}_k' \;-\; \left(1 - \frac{k^2}{z^2}\right)\mathrm{Z}_k\,. \tag{21}$$

To obtain the value of ($\mathbf{u}$, $\mathbf{w}$, $\boldsymbol{\tau}$, p) on a bounded domain, we need to express one of the boundary conditions given in section 2.3 by replacing the potentials $\chi_\bullet$ with the Bessel or Hankel expansion to obtain a system on each Bessel mode, (see [3]). In appendix A, we detail the system obtained with the expansion of the potentials for the scattering of a plane wave by an impenetrable obstacle for boundary conditions of type 1 (equation (3a)) and type 3 (equation (3c)).

Definition 1 (Outgoing solutions). The fields $\mathbf{u}$ and $\mathbf{w}$ are called outgoing solutions of the poroelastic equations (2) if they satisfy the following radiations conditions.

1. Their rotational $\operatorname{curl}\mathbf{u}$ and $\operatorname{curl}\mathbf{w}$ satisfy the outgoing Sommerfeld radiation condition with wavenumber k_S, *i.e.* for $\varphi = \operatorname{curl}\mathbf{u}$ or $\operatorname{curl}\mathbf{w}$, φ satisfies

$$\lim_{r\to\infty} \sqrt{r}\, \left(\frac{\partial \varphi}{\partial r} \;-\; \mathrm{i}\, \mathsf{k}_s\, \varphi \right) \;=\; 0\,, \tag{22}$$

   uniformly in all directions.

2. Denoting $P(\omega) \;=\; \begin{pmatrix} 1 & 1 \\ \beta_\mathrm{P} & \beta_\mathrm{B} \end{pmatrix}$, and defining φ_P , φ_B as $\begin{pmatrix} \varphi_P \\ \varphi_B \end{pmatrix} = P^{-1} \begin{pmatrix} \nabla\cdot\mathbf{u} \\ \nabla\cdot\mathbf{w} \end{pmatrix}$, then φ_P and φ_B satisfies the outgoing Sommerfeld radiation condition with wavenumber k_P and k_B respectively:

$$\lim_{r\to\infty} \sqrt{r}\, \left(\frac{\partial \varphi_P}{\partial r} \;-\; \mathrm{i}\, \mathsf{k}_P\, \varphi_P \right) \;=\; 0\,, \quad \text{and} \quad \lim_{r\to\infty} \sqrt{r}\, \left(\frac{\partial \varphi_B}{\partial r} \;-\; \mathrm{i}\, \mathsf{k}_B\, \varphi_B \right) \;=\; 0\,, \tag{23}$$

   uniformly in all directions.

The potential (20) of a generic outgoing solution by the above definition contains only $\mathrm{H}_k^{(1)}$. Specifically,

$$\begin{aligned} \chi_\mathrm{P}(\boldsymbol{x}) \;&=\; \sum_{k\in\mathbb{Z}} a_k\, \mathrm{H}_k^{(1)}(\omega\, \mathsf{s}_\mathrm{P}\, |\boldsymbol{x}|)\; e^{\mathrm{i}\, k\, \theta}\,, \\ \chi_\mathrm{B}(\boldsymbol{x}) \;&=\; \sum_{k\in\mathbb{Z}} b_k\, \mathrm{H}_k^{(1)}(\omega\, \mathsf{s}_\mathrm{B}\, |\boldsymbol{x}|)\; e^{\mathrm{i}\, k\, \theta}\,, \\ \chi_\mathrm{S}(\boldsymbol{x}) \;&=\; \sum_{k\in\mathbb{Z}} c_k\, \mathrm{H}_k^{(1)}(\omega\, \mathsf{s}_\mathrm{S}\, |\boldsymbol{x}|)\; e^{\mathrm{i}\, k\, \theta}\,. \end{aligned} \tag{24}$$

3 Derivation of radiation conditions

In this section, we build artificial boundary conditions for isotropic poroelastic media. We derive the radiation conditions of an outgoing solution in order to find a relation between the stress $\boldsymbol{\tau}$, p and the velocities $\mathbf{u}$, $\mathbf{w}$.

3.1 Radiating asymptotic of Hankel functions

Let $\mathrm{H}_k^{(1)}(z)$ be the Hankel function such as $\mathrm{H}_k^{(1)}(z) = \mathrm{J}_k(z) + \mathrm{i}\mathrm{Y}_k(z)$. From equations (10.17.11) and (10.17.2) in [17], we have

$$\mathrm{H}_k^{(1)'}(z) \;\sim\; \mathrm{i} \left(\frac{2}{\pi\, z} \right)^{\frac{1}{2}}\; e^{\mathrm{i}\,(z\,-\frac{1}{2}\,k\,\pi\,-\,\frac{1}{4}\,\pi)} \left(1 \;+\; \sum_{m=1}^{\infty} (-1)^m\, \frac{b_m(k)}{z^m} \right). \tag{25}$$

Equivalently from equations (10.17.5) and (10.17.2) in [17],

$$\mathrm{H}_k^{(1)}(z) \sim \left(\frac{2}{\pi\, z}\right)^{\frac{1}{2}} e^{\mathrm{i}\,(z-\frac{1}{2}\,k\,\pi-\frac{1}{4}\,\pi)} \left(1 + \sum_{m=1}^{\infty} \mathrm{i}^m\, \frac{a_m(k)}{z^m}\right). \tag{26}$$

Hence,

$$\mathrm{H}_k^{(1)'}(z) - \mathrm{i}\,\mathrm{H}_k^{(1)}(z) \sim \left(\frac{2}{\pi\, z}\right)^{\frac{1}{2}} e^{\mathrm{i}\,(z-\frac{1}{2}\,k\,\pi-\frac{1}{4}\,\pi)} \left(\sum_{m=1}^{\infty} \mathrm{i}^m\, \frac{c_m(k)}{z^m}\right). \tag{27}$$

In the end we obtain the radiating asymptotic:

$$H_k^{(1)'}(z) - \mathrm{i}\,H_k^{(1)}(z) = O(z^{-\frac{3}{2}}), \quad z \to \infty. \tag{28}$$

This will be the main ingredient in the derivation of the absorbing boundary conditions.

3.2 Derivation

We recall from (24) the potentials $\chi_\bullet$ that define a generic outgoing solution, which only contains $\mathrm{H}_k^{(1)}$ Bessel functions via (18),

$$\begin{aligned}
\chi_{\mathrm{P}}(\boldsymbol{x}) &= \sum_{k\in\mathbb{Z}} a_k\, \mathrm{H}_k^{(1)}(\omega\, \mathsf{s}_{\mathrm{P}}\, |\boldsymbol{x}|)\; e^{\mathrm{i}\,k\,\theta}, \\
\chi_{\mathrm{B}}(\boldsymbol{x}) &= \sum_{k\in\mathbb{Z}} b_k\, \mathrm{H}_k^{(1)}(\omega\, \mathsf{s}_{\mathrm{B}}\, |\boldsymbol{x}|)\; e^{\mathrm{i}\,k\,\theta}, \\
\chi_{\mathrm{S}}(\boldsymbol{x}) &= \sum_{k\in\mathbb{Z}} c_k\, \mathrm{H}_k^{(1)}(\omega\, \mathsf{s}_{\mathrm{S}}\, |\boldsymbol{x}|)\; e^{\mathrm{i}\,k\,\theta}.
\end{aligned} \tag{29}$$

Substitute this form of potential in equation (18) and use the expression for the action of **curl** ∇ and ∇^2 in polar coordinates presented in Section 2.5, we have the following expressions for the expansion of the unknowns ($\mathbf{u}$, $\mathbf{w}$, $\boldsymbol{\tau}$, p),

$$\begin{aligned}
\mathrm{i}\,\omega\,\mathbf{u}_r &= \sum_{k\in\mathbb{Z}} a_k\, \frac{\omega}{\mathsf{s}_{\mathrm{P}}}\, \mathrm{H}_k^{(1)'}(\omega\, \mathsf{s}_{\mathrm{P}}\, |\boldsymbol{x}|) e^{\mathrm{i}k\theta} + \sum_{k\in\mathbb{Z}} b_k\, \frac{\omega}{\mathsf{s}_{\mathrm{B}}}\, \mathrm{H}_k^{(1)'}(\omega\, \mathsf{s}_{\mathrm{B}}\, |\boldsymbol{x}|) e^{\mathrm{i}k\theta} - \sum_{k\in\mathbb{Z}} c_k\, \frac{\mathrm{i}k}{\mathsf{s}_{\mathrm{S}}^2\, |\boldsymbol{x}|} \mathrm{H}_k^{(1)}(\omega\, \mathsf{s}_{\mathrm{S}}\, |\boldsymbol{x}|) e^{\mathrm{i}k\theta}, \\
\mathrm{i}\,\omega\,\mathbf{u}_\theta &= \sum_{k\in\mathbb{Z}} a_k\, \frac{\mathrm{i}k}{\mathsf{s}_{\mathrm{P}}^2\, |\boldsymbol{x}|} \mathrm{H}_k^{(1)}(\omega\, \mathsf{s}_{\mathrm{P}}\, |\boldsymbol{x}|) e^{\mathrm{i}k\theta} + \sum_{k\in\mathbb{Z}} b_k\, \frac{\mathrm{i}k}{\mathsf{s}_{\mathrm{B}}^2\, |\boldsymbol{x}|} \mathrm{H}_k^{(1)}(\omega\, \mathsf{s}_{\mathrm{B}}\, |\boldsymbol{x}|) e^{\mathrm{i}k\theta} + \sum_{k\in\mathbb{Z}} c_k\, \mathsf{s}_{\mathrm{S}}^{-1}\, \omega\, \mathrm{H}_k^{(1)'}(\omega\, \mathsf{s}_{\mathrm{S}}\, |\boldsymbol{x}|) e^{\mathrm{i}k\theta}, \\
\mathrm{i}\,\omega\,\mathbf{w}_r &= \sum_{k\in\mathbb{Z}} a_k\, \frac{\beta_{\mathrm{P}}}{\mathsf{s}_{\mathrm{P}}}\, \omega\, \mathrm{H}_k^{(1)'}(\omega\, \mathsf{s}_{\mathrm{P}}\, |\boldsymbol{x}|) e^{\mathrm{i}k\theta} + \sum_{k\in\mathbb{Z}} b_k\, \frac{\beta_{\mathrm{B}}}{\mathsf{s}_{\mathrm{B}}}\, \omega\, \mathrm{H}_k^{(1)'}(\omega\, \mathsf{s}_{\mathrm{B}}\, |\boldsymbol{x}|) e^{\mathrm{i}k\theta} + \sum_{k\in\mathbb{Z}} c_k\, \frac{\rho_f\, \mu_{\mathrm{fr}}}{\det A}\, \frac{\mathrm{i}k}{|\boldsymbol{x}|} \mathrm{H}_k^{(1)}(\omega\, \mathsf{s}_{\mathrm{S}}\, |\boldsymbol{x}|) e^{\mathrm{i}k\theta},
\end{aligned} \tag{30a}$$

For the symmetric $\boldsymbol{\tau}$, we have $\boldsymbol{\tau}_{r\theta} = \boldsymbol{\tau}_{\theta r}$. We will only be concerned with $\boldsymbol{\tau}\cdot\mathbf{e}_r = \boldsymbol{\tau}_{rr}\mathbf{e}_r + \boldsymbol{\tau}_{r\theta}\mathbf{e}_\theta$,

$$\begin{aligned}
\omega^2\boldsymbol{\tau}_{rr} = &- \sum_{k\in\mathbb{Z}} \frac{2\,\mu_{\mathrm{fr}}\,\omega}{\mathsf{s}_{\mathrm{P}}\,|\boldsymbol{x}|}\, a_k\, \mathrm{H}_{k+1}^{(1)}(\omega\, \mathsf{s}_{\mathrm{P}}\, |\boldsymbol{x}|)\; e^{\mathrm{i}\,k\,\theta} + \sum_{k\in\mathbb{Z}} \frac{2\,\mu_{\mathrm{fr}}\,k}{\mathsf{s}_{\mathrm{P}}^2\,|\boldsymbol{x}|^2}\, a_k\, \mathrm{H}_k^{(1)}(\omega\, \mathsf{s}_{\mathrm{P}}\, |\boldsymbol{x}|)\; e^{\mathrm{i}\,k\,\theta} \\
&+ \sum_{k\in\mathbb{Z}} 2\,\mu_{\mathrm{fr}}\, a_k\, \omega^2\, \mathrm{H}_k^{(1)}(\omega\, \mathsf{s}_{\mathrm{P}}\, |\boldsymbol{x}|)\; e^{\mathrm{i}\,k\,\theta} - \sum_{k\in\mathbb{Z}} \frac{2\,\mu_{\mathrm{fr}}\,k^2}{\mathsf{s}_{\mathrm{P}}^2\,|\boldsymbol{x}|^2}\, a_k\, \mathrm{H}_k^{(1)}(\omega\, \mathsf{s}_{\mathrm{P}}\, |\boldsymbol{x}|)\; e^{\mathrm{i}\,k\,\theta} \\
&- \sum_{k\in\mathbb{Z}} \frac{2\,\mu_{\mathrm{fr}}\,\omega}{\mathsf{s}_{\mathrm{B}}\,|\boldsymbol{x}|}\, b_k\, \mathrm{H}_{k+1}^{(1)}(\omega\, \mathsf{s}_{\mathrm{B}}\, |\boldsymbol{x}|)\; e^{\mathrm{i}\,k\,\theta} + \sum_{k\in\mathbb{Z}} \frac{2\,\mu_{\mathrm{fr}}\,k}{\mathsf{s}_{\mathrm{B}}^2\,|\boldsymbol{x}|^2}\, b_k\, \mathrm{H}_k^{(1)}(\omega\, \mathsf{s}_{\mathrm{B}}\, |\boldsymbol{x}|)\; e^{\mathrm{i}\,k\,\theta} \\
&+ \sum_{k\in\mathbb{Z}} 2\,\mu_{\mathrm{fr}}\, b_k\, \omega^2\, \mathrm{H}_k^{(1)}(\omega\, \mathsf{s}_{\mathrm{B}}\, |\boldsymbol{x}|)\; e^{\mathrm{i}\,k\,\theta} - \sum_{k\in\mathbb{Z}} \frac{2\,\mu_{\mathrm{fr}}\,k^2}{\mathsf{s}_{\mathrm{B}}^2\,|\boldsymbol{x}|^2}\, b_k\, \mathrm{H}_k^{(1)}(\omega\, \mathsf{s}_{\mathrm{B}}\, |\boldsymbol{x}|)\; e^{\mathrm{i}\,k\,\theta} \\
&+ \sum_{k\in\mathbb{Z}} \frac{2\,\mu_{\mathrm{fr}}}{\mathsf{s}_{\mathrm{S}}|\boldsymbol{x}|}\; c_k\, \omega\, \mathrm{i}k\, \mathrm{H}_k^{(1)'}(\omega\, \mathsf{s}_{\mathrm{S}}\, |\boldsymbol{x}|)\; e^{\mathrm{i}\,k\,\theta} \\
&+ \sum_{k\in\mathbb{Z}} \omega^2\, \left(-\tfrac{2}{3}\mu_{\mathrm{fr}} + \mathrm{k}_{\mathrm{fr}} + M\alpha^2 + \alpha\, M\beta_{\mathrm{P}}\right)\; a_k\, \mathrm{H}_k^{(1)}(\omega\, \mathsf{s}_{\mathrm{P}}\, |\boldsymbol{x}|)\; e^{\mathrm{i}\,k\,\theta} \\
&+ \sum \omega^2\, \left(-\tfrac{2}{3}\mu_{\mathrm{fr}} + \mathrm{k}_{\mathrm{fr}} + M\alpha^2 + \alpha\, M\beta_{\mathrm{B}}\right)\, b_k\, \mathrm{H}_k^{(1)}(\omega\, \mathsf{s}_{\mathrm{B}}\, |\boldsymbol{x}|)\; e^{\mathrm{i}\,k\,\theta},
\end{aligned} \tag{30b}$$

$$
\begin{aligned}
\omega^2\,\boldsymbol{\tau}_{r\theta} \;=\; & -\sum_{k\in\mathbb{Z}} \frac{2\,\mu_{\rm fr}\,\omega\,\mathrm{i}\,k}{|\boldsymbol{x}|\,\mathsf{s}_{\rm P}}\,a_k\,\mathrm{H}_k^{(1)'}(\omega\,\mathsf{s}_{\rm P}\,|\boldsymbol{x}|)\;e^{\mathrm{i}\,k\,\theta} + \sum_{k\in\mathbb{Z}} \frac{2\,\mathrm{i}\,\mu_{\rm fr}\,k}{|\boldsymbol{x}|^2\,\mathsf{s}_{\rm P}^2}\,a_k\,\mathrm{H}_k^{(1)}(\omega\,\mathsf{s}_{\rm P}\,|\boldsymbol{x}|)\;e^{\mathrm{i}\,k\,\theta} \\
& -\sum_{k\in\mathbb{Z}} \frac{2\,\mu_{\rm fr}\omega\,\mathrm{i}\,k}{|\boldsymbol{x}|\,\mathsf{s}_{\rm B}}\,b_k\,\mathrm{H}_k^{(1)'}(\omega\,\mathsf{s}_{\rm B}\,|\boldsymbol{x}|)\;e^{\mathrm{i}\,k\,\theta} + \sum_{k\in\mathbb{Z}} \frac{2\,\mathrm{i}\,\mu_{\rm fr}\,k}{|\boldsymbol{x}|^2\,\mathsf{s}_{\rm B}^2}\,b_k\,\mathrm{H}_k^{(1)}(\omega\,\mathsf{s}_{\rm B}\,|\boldsymbol{x}|)\;e^{\mathrm{i}\,k\,\theta} \\
& -\sum_{k\in\mathbb{Z}} \frac{\mu_{\rm fr}\,k^2}{|\boldsymbol{x}|^2\,\mathsf{s}_{\rm S}^2}\,c_k\,\mathrm{H}_k^{(1)}(\omega\,\mathsf{s}_{\rm S}\,|\boldsymbol{x}|)\;e^{\mathrm{i}\,k\,\theta} + \sum_{k\in\mathbb{Z}} \frac{\mu_{\rm fr}\,\omega}{|\boldsymbol{x}|\,\mathsf{s}_{\rm S}}\,c_k\,\mathrm{H}_k^{(1)'}(\omega\,\mathsf{s}_{\rm S}\,|\boldsymbol{x}|)\;e^{\mathrm{i}\,k\,\theta} \\
& -\sum_{k\in\mathbb{Z}} \mu_{\rm fr}\,\frac{\omega}{\mathsf{s}_{\rm S}\,|\boldsymbol{x}|}\,c_k\,\mathrm{H}_{k+1}^{(1)}(\omega\,\mathsf{s}_{\rm S}\,|\boldsymbol{x}|)\;e^{\mathrm{i}\,k\,\theta} + \sum_{k\in\mathbb{Z}} \mu_{\rm fr}\,\frac{k}{\mathsf{s}_{\rm S}^2\,|\boldsymbol{x}|^2}\,c_k\,\mathrm{H}_k^{(1)}(\omega\,\mathsf{s}_{\rm S}\,|\boldsymbol{x}|)\;e^{\mathrm{i}\,k\,\theta} \\
& +\sum_{k\in\mathbb{Z}} \mu_{\rm fr}\,\omega^2\,c_k\,\mathrm{H}_k^{(1)}(\omega\,\mathsf{s}_{\rm S}\,|\boldsymbol{x}|)\;e^{\mathrm{i}\,k\,\theta} - \sum_{k\in\mathbb{Z}} \mu_{\rm fr}\,\frac{k^2}{\mathsf{s}_{\rm S}^2\,|\boldsymbol{x}|^2}\,c_k\,\mathrm{H}_k^{(1)}(\omega\,\mathsf{s}_{\rm S}\,|\boldsymbol{x}|)\;e^{\mathrm{i}\,k\,\theta}\,,
\end{aligned}
\tag{30c}
$$

$$
\mathrm{p} \;=\; -\sum_{k\in\mathbb{Z}} a_k M\,(\beta_{\rm P}\;+\;\alpha)\mathrm{H}_k^{(1)}(\omega\,\mathsf{s}_{\rm P}\,|\boldsymbol{x}|)\,e^{\mathrm{i}k\theta} \;-\; \sum_{k\in\mathbb{Z}} b_k M\,(\beta_{\rm B}\;+\;\alpha)\mathrm{H}_k^{(1)}(\,\omega\,\mathsf{s}_{\rm B}\,|\boldsymbol{x}|)\,e^{\mathrm{i}k\theta}\,. \tag{30d}
$$

In order to find a relation between the unknowns $\boldsymbol{\tau}$, p and $\mathbf{u}$, $\mathbf{w}$, we choose to approximate the components by truncating at the first order in $\frac{1}{|\boldsymbol{x}|} = \frac{1}{r}$. We obtain:

$$
\begin{aligned}
\mathbf{u}_r \;&=\; -\sum_{k\in\mathbb{Z}} a_k\,\frac{\mathrm{i}}{\mathsf{s}_{\rm P}}\,\mathrm{H}_k^{(1)'}(\omega\,\mathsf{s}_{\rm P}\,|\boldsymbol{x}|)e^{\mathrm{i}k\theta} \;-\; \sum_{k\in\mathbb{Z}} b_k\,\frac{\mathrm{i}}{\mathsf{s}_{\rm B}}\,\mathrm{H}_k^{(1)'}(\omega\,\mathsf{s}_{\rm B}\,|\boldsymbol{x}|)e^{\mathrm{i}k\theta} + \mathsf{O}(r^{-\frac{3}{2}})\,, \\
\mathbf{w}_r \;&=\; -\sum_{k\in\mathbb{Z}} a_k\,\frac{\mathrm{i}\,\beta_{\rm P}}{\mathsf{s}_{\rm P}}\,\mathrm{H}_k^{(1)'}(\omega\,\mathsf{s}_{\rm P}\,|\boldsymbol{x}|)e^{\mathrm{i}k\theta} \;-\; \sum_{k\in\mathbb{Z}} b_k\,\frac{\mathrm{i}\,\beta_{\rm B}}{\mathsf{s}_{\rm B}}\,\mathrm{H}_k^{(1)'}(\omega\,\mathsf{s}_{\rm B}\,|\boldsymbol{x}|)e^{\mathrm{i}k\theta} \;+\; \mathsf{O}(r^{-\frac{3}{2}})\,, \\
\mathbf{u}_\theta \;&=\; -\sum_{k\in\mathbb{Z}} c_k\,\frac{\mathrm{i}}{\mathsf{s}_{\rm S}}\,\mathrm{H}_k^{(1)'}(\omega\,\mathsf{s}_{\rm S}\,|\boldsymbol{x}|) + \mathsf{O}(r^{-\frac{3}{2}})\,,
\end{aligned}
\tag{31}
$$

and

$$
\begin{aligned}
\boldsymbol{\tau}_{rr} &= \left(\frac{4}{3}\mu_{\rm fr} \;+\; \mathrm{k}_{\rm fr} \;+\; \alpha(M\alpha \;+\; M\beta_{\rm P})\right) \sum_{k\in\mathbb{Z}}\; a_k\,\mathrm{H}_k^{(1)}(\omega\,\mathsf{s}_{\rm P}\,|\boldsymbol{x}|)\;e^{\mathrm{i}\,k\,\theta} \\
&\quad + \left(\frac{4}{3}\mu_{\rm fr} \;+\; \mathrm{k}_{\rm fr} \;+\; \alpha(M\alpha \;+\; M\beta_{\rm B})\right) \sum_{k\in\mathbb{Z}}\; b_k\,\mathrm{H}_k^{(1)}(\omega\,\mathsf{s}_{\rm B}\,|\boldsymbol{x}|)\;e^{\mathrm{i}\,k\,\theta} \;+\; \mathsf{O}(r^{-\frac{3}{2}})\,, \\
\boldsymbol{\tau}_{r\theta} &= \sum_{k\in\mathbb{Z}} \mu_{\rm fr}\,c_k\,\mathrm{H}_k^{(1)}(\omega\,\mathsf{s}_{\rm S}\,|\boldsymbol{x}|)\,e^{\mathrm{i}\,k\,\theta} \;+\; \mathsf{O}(r^{-\frac{3}{2}})\,, \\
\mathrm{p} &= -\sum_{k\in\mathbb{Z}} a_k M\,(\beta_{\rm P}\;+\;\alpha)\mathrm{H}_k^{(1)}(\,\omega\,\mathsf{s}_{\rm P}\,|\boldsymbol{x}|)\,e^{\mathrm{i}k\theta} \;-\; \sum_{k\in\mathbb{Z}} b_k M\,(\beta_{\rm B}\;+\;\alpha)\mathrm{H}_k^{(1)}(\omega\,\mathsf{s}_{\rm B}\,|\boldsymbol{x}|)\,e^{\mathrm{i}k\theta}\,.
\end{aligned}
\tag{32}
$$

Important identity Using the expressions of the radial velocities in equation (31), we can write the system:

$$
\begin{pmatrix} \mathrm{i}\,\mathbf{u}_r \\ \mathrm{i}\,\mathbf{w}_r \end{pmatrix} = \begin{pmatrix} \frac{1}{\mathsf{s}_{\rm P}} & \frac{1}{\mathsf{s}_{\rm B}} \\ \frac{\beta_{\rm P}}{\mathsf{s}_{\rm P}} & \frac{\beta_{\rm B}}{\mathsf{s}_{\rm B}} \end{pmatrix} \begin{pmatrix} \sum\limits_{k\in\mathbb{Z}} a_k\;\mathrm{H}_k^{(1)'}(\omega\,\mathsf{s}_{\rm P}\,|\boldsymbol{x}|)e^{\mathrm{i}k\theta} \\ \sum\limits_{k\in\mathbb{Z}} b_k\;\mathrm{H}_k^{(1)'}(\omega\,\mathsf{s}_{\rm B}\,|\boldsymbol{x}|)e^{\mathrm{i}k\theta} \end{pmatrix} + \mathsf{O}(r^{-\frac{3}{2}})\,. \tag{33}
$$

We can express the inverse matrix of the above matrix:

$$
\begin{pmatrix} \frac{1}{\mathsf{s}_{\rm P}} & \frac{1}{\mathsf{s}_{\rm B}} \\ \frac{\beta_{\rm P}}{\mathsf{s}_{\rm P}} & \frac{\beta_{\rm B}}{\mathsf{s}_{\rm B}} \end{pmatrix}^{-1} = \frac{1}{\beta_{\rm B}-\beta_{\rm P}} \begin{pmatrix} \mathsf{s}_{\rm P}\,\beta_{\rm B} & -\mathsf{s}_{\rm P} \\ -\beta_{\rm P}\,\mathsf{s}_{\rm B} & \mathsf{s}_{\rm B} \end{pmatrix}.
$$

Hence, equation (33) becomes

$$
\begin{pmatrix} \sum\limits_{k\in\mathbb{Z}} a_k\;\mathrm{H}_k^{(1)'}(\omega\,\mathsf{s}_{\rm P}\,|\boldsymbol{x}|)e^{\mathrm{i}k\theta} \\ \sum\limits_{k\in\mathbb{Z}} b_k\;\mathrm{H}_k^{(1)'}(\omega\,\mathsf{s}_{\rm B}\,|\boldsymbol{x}|)e^{\mathrm{i}k\theta} \end{pmatrix} = \frac{1}{\beta_{\rm B}-\beta_{\rm P}} \begin{pmatrix} \mathsf{s}_{\rm P}\,\beta_{\rm B} & -\mathsf{s}_{\rm P} \\ -\beta_{\rm P}\,\mathsf{s}_{\rm B} & \mathsf{s}_{\rm B} \end{pmatrix} \begin{pmatrix} \mathrm{i}\,\mathbf{u}_r \\ \mathrm{i}\,\mathbf{w}_r \end{pmatrix} + \mathsf{O}(r^{-\frac{3}{2}})\,. \tag{34}
$$

In the following subsections, we will express the radial component of the solid stress, the tangential component of the solid stress and the fluid pressure using the velocities $\mathbf{u}$ and $\mathbf{w}$.

3.2.1 Radial component of the solid stress

With the approximate values of $\boldsymbol{\tau}_{rr}$ and p given in equation (32), we have:

$$\begin{aligned}\boldsymbol{\tau}_{rr} - \left(\tfrac{4}{3}\mu_{\rm fr} + {\rm k}_{\rm fr} + \alpha(M\alpha + M\beta_{\rm P})\right) \sum_{k\in\mathbb{Z}} a_k \, {\rm H}_k^{(1)}(\omega \, {\rm s}_{\rm P} \, |\boldsymbol{x}|) \; e^{{\rm i}\, k\, \theta} \\ - \left(\tfrac{4}{3}\mu_{\rm fr} + {\rm k}_{\rm fr} + \alpha(M\alpha + M\beta_{\rm B})\right) \sum_{k\in\mathbb{Z}} b_k \, {\rm H}_k^{(1)}(\omega \, {\rm s}_{\rm B} \, |\boldsymbol{x}|) \; e^{{\rm i}\, k\, \theta} \; = \; \mathsf{O}(r^{-\frac{3}{2}}) \, .\end{aligned}$$

Using equation (28), we replace ${\rm H}_k^{(1)}(z)$ by

$$\mathrm{H}_k^{(1)}(z) \; = -{\rm i}\, \mathrm{H}_k^{(1)'}(z) + \; \mathsf{O}(z^{-\frac{3}{2}}) \, , \tag{35}$$

to obtain

$$\begin{aligned}\boldsymbol{\tau}_{rr} + \left(\tfrac{4}{3}\mu_{\rm fr} + {\rm k}_{\rm fr} + \alpha(M\alpha + M\beta_{\rm P})\right) \sum_{k\in\mathbb{Z}} a_k \, {\rm i}\, {\rm H}_k^{(1)'}(\omega \, {\rm s}_{\rm P} \, |\boldsymbol{x}|) \; e^{{\rm i}\, k\, \theta} \\ + \left(\tfrac{4}{3}\mu_{\rm fr} + {\rm k}_{\rm fr} + \alpha(M\alpha + M\beta_{\rm B})\right) \sum_{k\in\mathbb{Z}} b_k \, {\rm i}\, {\rm H}_k^{(1)'}(\omega \, {\rm s}_{\rm B} \, |\boldsymbol{x}|) \; e^{{\rm i}\, k\, \theta} \; = \; \mathsf{O}(r^{-\frac{3}{2}}) \, .\end{aligned}$$

Finally, using equation (34), we obtain a relation between $\boldsymbol{\tau}_{rr}$, frv_r and $\mathbf{w}_r$:

$$\begin{aligned}\boldsymbol{\tau}_{rr} - \frac{\frac{4}{3}\mu_{\rm fr} + {\rm k}_{\rm fr} + \alpha(M\alpha + M\beta_{\rm P})}{\beta_{\rm B} - \beta_{\rm P}} \left({\rm s}_{\rm P} \, \beta_{\rm B} \, \mathbf{u}_r - {\rm s}_{\rm P} \mathbf{w}_r \right) \\ - \frac{\frac{4}{3}\mu_{\rm fr} + {\rm k}_{\rm fr} + \alpha(M\alpha + M\beta_{\rm B})}{\beta_{\rm B} - \beta_{\rm P}} \left(- \beta_{\rm P} \, {\rm s}_{\rm B} \, \mathbf{u}_r + {\rm s}_{\rm B} \mathbf{w}_r \right) = \; \mathsf{O}(r^{-\frac{3}{2}}) \, .\end{aligned}$$

3.2.2 Tangential component of the solid stress

The tangent solid velocity $\mathbf{u}_\theta$ and $\boldsymbol{\tau}_{r\theta}$ are expressed with equations (31) and (32). Replace ${\rm H}_k^{(1)}$, using the identity (28), we obtain:

$$\boldsymbol{\tau}_{r\theta} \; - \; {\rm s}_{\rm S} \, \mu_{\rm fr} \, \mathbf{u}_\theta = \; \mathsf{O}(r^{-\frac{3}{2}})$$

3.2.3 Fluid pressure

From the expression of p in (32) and the radiating assymptotic (28), we have:

$$-{\rm p} + M \left(\beta_{\rm P} \; + \; \alpha\right) \sum_{k\in\mathbb{Z}} a_k {\rm i} {\rm H}_k^{(1)'}(\, \omega \, {\rm s}_{\rm P} \, |\boldsymbol{x}|) \, e^{{\rm i}k\theta} \; + \; M \left(\beta_{\rm B} \; + \; \alpha\right) \sum_{k\in\mathbb{Z}} b_k {\rm i} {\rm H}_k^{(1)'}(\, \omega \, {\rm s}_{\rm B} \, |\boldsymbol{x}|) \, e^{{\rm i}k\theta} = \; \mathsf{O}(r^{-\frac{3}{2}}) \, .$$

Using equation (34), we obtain,

$$-{\rm p} \; - \frac{M \left(\beta_{\rm P} \; + \; \alpha\right)}{\beta_{\rm B} - \beta_{\rm P}} ({\rm s}_{\rm P} \, \beta_{\rm B} \, \mathbf{u}_r \; - {\rm s}_{\rm P} \mathbf{w}_r) - \frac{M \left(\beta_{\rm B} \; + \; \alpha\right)}{\beta_{\rm B} - \beta_{\rm P}} \left(- {\rm s}_{\rm B} \, \beta_{\rm P} \, \mathbf{u}_r \; + {\rm s}_{\rm B} \mathbf{w}_r \right) = \; \mathsf{O}(r^{-\frac{3}{2}}) \, .$$

3.2.4 Summary

We have built the three conditions:

$$\begin{aligned}\boldsymbol{\tau}_{rr} = \frac{\frac{4}{3}\mu_{\rm fr} + {\rm k}_{\rm fr} + \alpha(M\alpha + M\beta_{\rm P})}{\beta_{\rm B} - \beta_{\rm P}} \left({\rm s}_{\rm P} \, \beta_{\rm B} \, \mathbf{u}_r - {\rm s}_{\rm P} \mathbf{w}_r \right) \\ + \frac{\frac{4}{3}\mu_{\rm fr} + {\rm k}_{\rm fr} + \alpha(M\alpha + M\beta_{\rm B})}{\beta_{\rm B} - \beta_{\rm P}} \left(- \beta_{\rm P} \, {\rm s}_{\rm B} \, \mathbf{u}_r + {\rm s}_{\rm B} \mathbf{w}_r \right), \\ \boldsymbol{\tau}_{r\theta} \; = \; {\rm s}_{\rm S} \, \mu_{\rm fr} \, \mathbf{w}_\theta, \\ {\rm p} \; = - \frac{M \left(\beta_{\rm P} \; + \; \alpha\right)}{\beta_{\rm B} - \beta_{\rm P}} ({\rm s}_{\rm P} \, \beta_{\rm B} \, \mathbf{u}_r \; - {\rm s}_{\rm P} \mathbf{w}_r) - \frac{M \left(\beta_{\rm B} \; + \; \alpha\right)}{\beta_{\rm B} - \beta_{\rm P}} \left(- {\rm s}_{\rm B} \, \beta_{\rm P} \, \mathbf{u}_r \; + {\rm s}_{\rm B} \mathbf{w}_r \right) .\end{aligned}$$

We denote:

$$\begin{aligned}
\mathbf{X}_1 &= -\frac{\frac{4}{3}\mu_{\rm fr} + {\rm k}_{\rm fr} + \alpha(M\alpha + M\beta_{\rm P})}{\beta_{\rm B} - \beta_{\rm P}}\,{\rm s}_{\rm P}\,\beta_{\rm B} + \frac{\frac{4}{3}\mu_{\rm fr} + {\rm k}_{\rm fr} + \alpha(M\alpha + M\beta_{\rm B})}{\beta_{\rm B} - \beta_{\rm P}}\,\beta_{\rm P}\,{\rm s}_{\rm B}\,,\\
\mathbf{X}_2 &= \frac{\frac{4}{3}\mu_{\rm fr} + {\rm k}_{\rm fr} + \alpha(M\alpha + M\beta_{\rm P})}{\beta_{\rm B} - \beta_{\rm P}}\,{\rm s}_{\rm P} - \frac{\frac{4}{3}\mu_{\rm fr} + {\rm k}_{\rm fr} + \alpha(M\alpha + M\beta_{\rm B})}{\beta_{\rm B} - \beta_{\rm P}}\,{\rm s}_{\rm B}\,,\\
\mathbf{X}_3 &= -\,{\rm s}_{\rm S}\,\mu_{\rm fr}\,,\\
\mathbf{X}_4 &= \frac{M\left(\beta_{\rm P} + \alpha\right)}{\beta_{\rm B} - \beta_{\rm P}}{\rm s}_{\rm P}\,\beta_{\rm B} - \frac{M\left(\beta_{\rm B} + \alpha\right)}{\beta_{\rm B} - \beta_{\rm P}}\,{\rm s}_{\rm B}\,\beta_{\rm P}\,,\\
\mathbf{X}_5 &= -\frac{M\left(\beta_{\rm P} + \alpha\right)}{\beta_{\rm B} - \beta_{\rm P}}{\rm s}_{\rm P} + \frac{M\left(\beta_{\rm B} + \alpha\right)}{\beta_{\rm B} - \beta_{\rm P}}\,{\rm s}_{\rm B}\,.
\end{aligned} \tag{36}$$

We have hence obtained a radiation condition, written as follows:

$$\begin{cases}
\boldsymbol{\tau}_{rr} + \mathbf{X}_1\mathbf{u}_r + \mathbf{X}_2\mathbf{w}_r = 0\,,\\
\boldsymbol{\tau}_{r\theta} + \mathbf{X}_3\mathbf{u}_\theta = 0\,,\\
{\rm p} + \mathbf{X}_4\mathbf{u}_r + \mathbf{X}_5\mathbf{w}_r = 0\,.
\end{cases} \tag{37}$$

Recall that on a circle, we have:

$$\begin{aligned}
&\mathbf{u}_r = \mathbf{u}\cdot\boldsymbol{n}\,, \quad \mathbf{w}_r = \mathbf{w}\cdot\boldsymbol{n}\,,\\
&\mathbf{u}_\theta = \mathbf{u}\cdot\mathbf{t}\,, \quad \boldsymbol{\tau}\,\boldsymbol{n} = \boldsymbol{\tau}_{rr}\mathbf{e}_r + \boldsymbol{\tau}_{r\theta}\mathbf{e}_\theta\,,
\end{aligned}$$

with $\mathbf{t} = \begin{pmatrix} -n_y \\ n_x \end{pmatrix} = \mathbf{e}_\theta$. The derivation has been done for a circular geometry. Here we propose the general boundary condition, that will be tested in section 8.

$$\begin{cases}
\boldsymbol{\tau}\,\boldsymbol{n} + \left(\mathbf{X}_1(\mathbf{u}\cdot\boldsymbol{n}) + \mathbf{X}_2(\mathbf{w}\cdot\boldsymbol{n})\right)\boldsymbol{n} + \mathbf{X}_3(\mathbf{u}\cdot\mathbf{t})\,\mathbf{t} = 0\,,\\
{\rm p} + \mathbf{X}_4(\mathbf{u}\cdot\boldsymbol{n}) + \mathbf{X}_5(\mathbf{w}\cdot\boldsymbol{n}) = 0\,.
\end{cases} \tag{38}$$

Remark 2. Results from Degrande: In [15], they work with the displacements instead of the velocities. We cannot compare our formulations, because they also use different values for $\beta_{\rm P}$, $\beta_{\rm B}$, $\beta_{\rm S}$. They obtain a general form for the boundary condition, which is of the form:

$$\begin{cases}
\boldsymbol{\tau}_{rr} + \tilde{\mathbf{X}}_1\mathbf{u}_r + \tilde{\mathbf{X}}_2\mathbf{w}_r = 0\,,\\
\boldsymbol{\tau}_{r\theta} + \tilde{\mathbf{X}}_3\mathbf{u}_\theta = 0\,,\\
{\rm p} + \tilde{\mathbf{X}}_2\mathbf{u}_r + \tilde{\mathbf{X}}_5\mathbf{w}_r = 0\,.
\end{cases} \tag{39}$$

Remark 3. In the elastic case, the form of LK absorbing boundary condition is (see [21, 12, 11]):

$$\boldsymbol{\tau}\,\boldsymbol{n} + \mathbf{Y}_1(\mathbf{u}\cdot\boldsymbol{n})\,\boldsymbol{n} + \mathbf{Y}_2(\mathbf{u}\cdot\mathbf{t})\,\mathbf{t} = 0\,.$$

In equation (38), without $\mathbf{w}$ and p, we retrieve the same form of the condition.

Definition 2 (Truncated solution). Considering a domain Ω with $\partial\Omega = \Gamma_{abs} \cup \Gamma_n$, and $\Gamma_{abs} \cap \Gamma_n = 0$. We define the truncated solution of the poroelastic equations on Ω as follows:

($\mathbf{u}$, $\mathbf{w}$, $\boldsymbol{\tau}$, p) solves the poroelastic equations (2) on Ω, the ABC equation (38) on Γ_{abs}, and one of the four boundary conditions from equation (3) on Γ_n.

4 Analytical solutions for the scattering of impenetrable obstacle by plane wave

We consider the scattering of a solid circular obstacle immersed in an infinite porous medium by a plane wave. We denote by $\mathbf{D}_{\mathfrak{a}}$ the obstacle whose radius is $\mathfrak{a}$. Its boundary is denoted by $\Gamma_1 = \partial\mathbf{D}_{\mathfrak{a}}$. For the solution with

ABC, we put an artificial boundary at radius $\mathfrak{b}$, denoted by $\Gamma_2 = \partial\mathbf{D}_\mathfrak{b}$, with $\mathfrak{b} > \mathfrak{a}$, cf. Figure 1. We use notation $\mathfrak{U}$ to denote the ordered tuple ($\mathbf{u}$, $\mathbf{w}$, $\boldsymbol{\tau}$, p). For $i = 1, \dots, 4$, we will discuss two analytic solutions, an outgoing solution $\mathfrak{U}^{\infty-\mathrm{Ti}}$, that is defined on the whole exterior domain $\mathbb{R}^2 \setminus \mathbf{D}_\mathfrak{a}$ and $\mathfrak{U}^{\text{abc-Ti}}$ obtained with ABC defined on the annulus $\Omega_{\mathfrak{a}\mathfrak{b}} := \mathbf{D}_\mathfrak{b} \setminus \mathbf{D}_\mathfrak{a}$. The superscript '$Ti$' denotes the type of boundary condition, given in section 2.3 equation (3), placed on the boundary of the obstacle, to describe its interaction with the incident wave.

The truncated solution $\mathfrak{U}^{\text{abc -Ti}}$ solves the following problem

$$\begin{cases} \text{the poroelastic equations (2) on } \Omega_{\mathfrak{a}\mathfrak{b}}, \\ \text{boundary condition Type i given equation (3) on } r = \mathfrak{a}\,, \\ \boldsymbol{\tau}_{rr} + \mathbf{X}_1\mathbf{u}_r + \mathbf{X}_2\mathbf{w}_r = 0\,, \\ \boldsymbol{\tau}_{r\theta} + \mathbf{X}_3\mathbf{u}_\theta = 0\,, \qquad\qquad \text{on } r = \mathfrak{b}\,. \\ \mathrm{p} + \mathbf{X}_4\mathbf{u}_r + \mathbf{X}_5\mathbf{w}_r = 0\,., \end{cases} \tag{40}$$

On the other hand, the outgoing solution $\mathfrak{U}^{\infty-\mathrm{Ti}}$ solves

$$\begin{cases} \text{the poroelastic equations (2) on } \mathbb{R}^2 \setminus \mathbf{D}_\mathfrak{a}, \\ \text{boundary condition Type i given in 2.3 on } r = \mathfrak{a}\,, \\ \mathfrak{U}^{\infty-\mathrm{Ti}} \text{ is outgoing by Definition 1}\,. \end{cases} \tag{41}$$

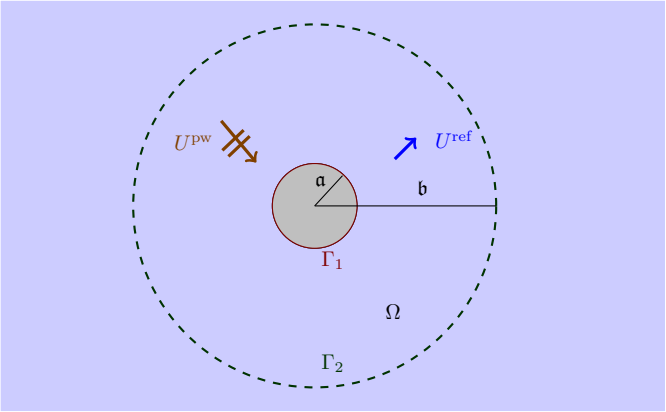

Figure 1: Scattering of a plane wave by an impenetrable solid immersed in a porous medium. The cross section of the obstacle is a disc parameterized by $r = \mathfrak{a}$. The artificial boundary is set on $\Gamma_2 = \{r = \mathfrak{b}\}$.

Potential representation We also recall that that the solutions $\mathfrak{U}$ are completely determined by their potentials $\chi_\bullet$, cf. (18),

$$\begin{aligned} \mathrm{i}\,\omega\,\mathbf{u} &= \mathrm{s}_\mathrm{P}^{-2}\,\nabla\chi_\mathrm{P} + \mathrm{s}_\mathrm{B}^{-2}\,\nabla\chi_\mathrm{B} - \mathrm{s}_\mathrm{S}^{-2}\,\mathbf{curl}\,\chi_\mathrm{S}\,, \\ \mathrm{i}\,\omega\,\mathbf{w} &= \frac{\beta_\mathrm{P}}{\mathrm{s}_\mathrm{P}^2}\nabla\chi_\mathrm{P} + \frac{\beta_\mathrm{B}}{\mathrm{s}_\mathrm{B}^2}\nabla\chi_\mathrm{B} + \frac{\rho_f\,\mu_\mathrm{fr}}{\det A}\mathbf{curl}\,\chi_\mathrm{S}\,, \\ \mathrm{p} &= -M\,(\beta_\mathrm{P} + \alpha)\chi_\mathrm{P} - M\,(\beta_\mathrm{B} + \alpha)\chi_\mathrm{B}\,, \\ \omega^2\,\boldsymbol{\tau} &= \mu_\mathrm{fr}\left(-\frac{2}{\mathrm{s}_\mathrm{P}^2}\,\nabla^2\chi_\mathrm{P} - \frac{2}{\mathrm{s}_\mathrm{B}^2}\,\nabla^2\chi_\mathrm{B} + \frac{\nabla\mathbf{curl}\,\chi_\mathrm{S} + (\nabla\mathbf{curl}\,\chi_\mathrm{S})^t}{\mathrm{s}_\mathrm{S}^2}\right) \\ &\quad + \omega^2\,\left(-\tfrac{2}{3}\mu_\mathrm{fr} + \mathrm{k}_\mathrm{fr} + M\alpha^2\right)(\chi_\mathrm{P} + \chi_\mathrm{B})\,\mathbf{Id} \\ &\quad + \omega^2\,\alpha\,M\,(\beta_\mathrm{P}\,\chi_\mathrm{P} + \beta_\mathrm{B}\,\chi_\mathrm{B})\,\mathbf{Id}\,. \end{aligned} \tag{42}$$

We write the potentials corresponding to $\mathfrak{U}^{\text{abc-Ti}}$ and $\mathfrak{U}^{\infty-\mathrm{Ti}}$ as

$$\chi_\bullet^{\text{abc-Ti}} \quad \text{and} \quad \chi_\bullet^{\infty-\mathrm{Ti}}\,, \qquad i = 1, 2, 3, 4\,. \tag{43}$$

The potentials $\chi_\bullet^{\infty-\mathrm{Ti}}$ corresponding to $\mathfrak{U}^{\infty-\mathrm{Ti}}$ are given by

$$\begin{aligned}
\chi_{\mathrm{P}}^{\infty-\mathrm{Ti}}(|\boldsymbol{x}|) &= \sum_{k\in\mathbb{Z}} a_k^\infty \, \mathrm{H}_k^{(1)}(\omega\, \mathsf{s}_{\mathrm{P}}\, |\boldsymbol{x}|)\; e^{\mathrm{i}\, k\, \theta}\,, \\
\chi_{\mathrm{B}}^{\infty-\mathrm{Ti}}(|\boldsymbol{x}|) &= \sum_{k\in\mathbb{Z}} b_k^\infty \, \mathrm{H}_k^{(1)}(\omega\, \mathsf{s}_{\mathrm{B}}\, |\boldsymbol{x}|)\; e^{\mathrm{i}\, k\, \theta}\,, \\
\chi_{\mathrm{S}}^{\infty-\mathrm{Ti}}(|\boldsymbol{x}|) &= \sum_{k\in\mathbb{Z}} c_k^\infty \, \mathrm{H}_k^{(1)}(\omega\, \mathsf{s}_{\mathrm{S}}\, |\boldsymbol{x}|)\; e^{\mathrm{i}\, k\, \theta}\,.
\end{aligned} \tag{44}$$

The solution $\mathfrak{U}^{\infty-\mathrm{Ti}}$ is now represented by the coefficients

$$(a_k^\infty,\, b_k^\infty,\, c_k^\infty) \;=\; (a_k^{\infty-\mathrm{Ti}},\, b_k^{\infty-\mathrm{Ti}},\, c_k^{\infty-\mathrm{Ti}})\,. \tag{45}$$

In the first notation, we have suppressed the dependence on the boundary condition for lighter exposition. They solve the linear system,

$$\mathbb{A}^{\infty-\mathrm{Ti}} \begin{pmatrix} a_k^\infty \\ b_k^\infty \\ c_k^\infty \end{pmatrix} = \mathfrak{f}_{\mathrm{Ti}}\,. \tag{46}$$

The components of $\mathbb{A}^{\infty-\mathrm{Ti}}$ and right-hand-side $\mathfrak{f}_{\mathrm{Ti}}$ are determined using boundary conditions on $r = \mathfrak{a}$. Derivation of the above linear system for each of the boundary condition are discussed in Section 8 of [3]. For convenience, we relist the derivation for Type 1 and 3, i.e. $\mathbb{A}^{\infty-\mathrm{T1}}$ and $\mathbb{A}^{\infty-\mathrm{T3}}$ in Appendix A.

The potentials $\chi_\bullet^{\text{abc-Ti}}$ are given by

$$\begin{aligned}
\chi_{\mathrm{P}}^{\text{abc-Ti}}(|\boldsymbol{x}|) &= \sum_{k\in\mathbb{Z}} a_k \, \mathrm{H}_k^{(1)}(\omega\, \mathsf{s}_{\mathrm{P}}\, |\boldsymbol{x}|)\; e^{\mathrm{i}\, k\, \theta} + \sum_{k\in\mathbb{Z}} \tilde{a}_k \, \mathrm{H}_k^{(2)}(\omega\, \mathsf{s}_{\mathrm{P}}\, |\boldsymbol{x}|)\; e^{\mathrm{i}\, k\, \theta}\,, \\
\chi_{\mathrm{B}}^{\text{abc-Ti}}(|\boldsymbol{x}|) &= \sum_{k\in\mathbb{Z}} b_k \, \mathrm{H}_k^{(1)}(\omega\, \mathsf{s}_{\mathrm{B}}\, |\boldsymbol{x}|)\; e^{\mathrm{i}\, k\, \theta} + \sum_{k\in\mathbb{Z}} \tilde{b}_k \, \mathrm{H}_k^{(2)}(\omega\, \mathsf{s}_{\mathrm{B}}\, |\boldsymbol{x}|)\; e^{\mathrm{i}\, k\, \theta}\,, \\
\chi_{\mathrm{S}}^{\text{abc-Ti}}(|\boldsymbol{x}|) &= \sum_{k\in\mathbb{Z}} c_k \, \mathrm{H}_k^{(1)}(\omega\, \mathsf{s}_{\mathrm{S}}\, |\boldsymbol{x}|)\; e^{\mathrm{i}\, k\, \theta} + \sum_{k\in\mathbb{Z}} \tilde{c}_k \, \mathrm{H}_k^{(2)}(\omega\, \mathsf{s}_{\mathrm{S}}\, |\boldsymbol{x}|)\; e^{\mathrm{i}\, k\, \theta}\,.
\end{aligned} \tag{47}$$

The solution $\mathfrak{U}^{\text{abc-Ti}}$ is now represented by the coefficients

$$a_k,\, b_k,\, c_k,\, \tilde{a}_k,\, \tilde{b}_k,\, \tilde{c}_k\,, \tag{48}$$

which solve the linear system

$$\mathbb{A}^{\text{abc-Ti}} \begin{pmatrix} a_k \\ b_k \\ c_k \\ \tilde{a}_k \\ \tilde{b}_k \\ \tilde{c}_k \end{pmatrix} = \begin{pmatrix} \mathfrak{f}_{\mathrm{Ti}}^{\text{abc}} \\ 0 \\ 0 \\ 0 \end{pmatrix}\,. \tag{49}$$

Note that in the above notation for the coefficients, we have suppressed the dependence on type of boundary condition on Γ_1. The components of $\mathbb{A}^{\text{abc-Ti}}$ (of size 6×6) and the right-hand-side are determined using boundary conditions on $r = \mathfrak{a}$ and $r = \mathfrak{b}$. In particular, the first three rows of the linear system are determined by one of the boundary condition imposed on Γ_1 (the boundary of the obstacle) while the last three rows are determined by the ABC imposed on Γ_2 the artificial boundary. We also have $\mathfrak{f}_{\mathrm{Ti}}^{\text{abc}} = \mathfrak{f}_{\mathrm{Ti}}$.

Derivation of $\mathbb{A}^{\text{abc-T3}}$: As an example, we list below the derivation associated to type 3 boundary condition imposed on the obstacle. Since the derivation of the first three lines are similar to that for $\mathbb{A}^{\infty-\mathrm{T3}}$,

we only list the derivation associated to the ABC i.e. the last three lines. On $r = \mathfrak{b}$, we replace the unknowns using equation (18) and we apply condition (38) to obtain:

$$\begin{aligned}
&\Bigg(\frac{\mathrm{i}\,\mu_{\mathrm{fr}}}{\omega} \Big(-\frac{2}{\mathsf{s}_{\mathrm{P}}^2}\,\partial_{r^2}\chi_{\mathrm{P}} \;-\; \frac{2}{\mathsf{s}_{\mathrm{B}}^2}\,\partial_{r^2}\chi_{\mathrm{B}} \;+\; \frac{2}{\mathsf{s}_{\mathrm{S}}^2} \Big(\frac{1}{\mathfrak{b}}\partial_{r\theta} - \frac{1}{\mathfrak{b}^2}\partial_\theta \Big) \chi_{\mathrm{S}} \Big) \\
&\quad + \mathrm{i}\,\omega \left(-\tfrac{2}{3}\mu_{\mathrm{fr}} + \mathrm{k}_{\mathrm{fr}} + M\alpha^2 \right) (\chi_{\mathrm{P}} \;+\; \chi_{\mathrm{B}}) \quad + \mathrm{i}\,\omega\alpha\, M\, (\beta_{\mathrm{P}}\,\chi_{\mathrm{P}} \;+\; \beta_{\mathrm{B}}\,\chi_{\mathrm{B}}) \Bigg) \\
&+ \mathbf{X}_1 \Big(\frac{1}{\mathsf{s}_{\mathrm{P}}^2}\,\partial_r\chi_{\mathrm{P}} \;+\; \frac{1}{\mathsf{s}_{\mathrm{B}}^2}\,\partial_r\chi_{\mathrm{B}} \;-\; \frac{1}{\mathsf{s}_{\mathrm{S}}^2\,\mathfrak{b}}\,\partial_\theta\chi_{\mathrm{S}} \Big) + \mathbf{X}_2 \Big(\frac{\beta_{\mathrm{P}}}{\mathsf{s}_{\mathrm{P}}^2}\partial_r\chi_{\mathrm{P}} \;+\; \frac{\beta_{\mathrm{B}}}{\mathsf{s}_{\mathrm{B}}^2}\partial_r\chi_{\mathrm{B}} \;+\; \frac{\rho_f\,\mu_{\mathrm{fr}}}{\det A\,\mathfrak{b}}\partial_\theta\,\chi_{\mathrm{S}} \Big) \;=\; 0\,,
\end{aligned}$$

$$\begin{aligned}
&\mu_{\mathrm{fr}} \Big(-\frac{2}{\mathsf{s}_{\mathrm{P}}^2} \Big(\frac{1}{\mathfrak{b}}\partial_{r\theta} - \frac{1}{\mathfrak{b}^2}\partial_\theta \Big) \chi_{\mathrm{P}} \;-\; \frac{2}{\mathsf{s}_{\mathrm{B}}^2} \Big(\frac{1}{\mathfrak{b}}\partial_{r\theta} - \frac{1}{\mathfrak{b}^2}\partial_\theta \Big) \chi_{\mathrm{B}} \;+\; \frac{1}{\mathsf{s}_{\mathrm{S}}^2} \Big(\frac{1}{\mathfrak{b}^2}\partial_{\theta\theta} + \frac{1}{\mathfrak{b}}\partial_r - \partial_{r^2} \Big) \chi_{\mathrm{S}} \Big) \\
&\quad + \frac{\mathbf{X}_3\,\omega}{\mathrm{i}} \Big(\mathsf{s}_{\mathrm{P}}^{-2}\,\frac{1}{\mathfrak{b}}\partial_\theta\chi_{\mathrm{P}} \;+\; \mathsf{s}_{\mathrm{B}}^{-2}\,\frac{1}{\mathfrak{b}}\partial_\theta\chi_{\mathrm{B}} \;+\; \mathsf{s}_{\mathrm{S}}^{-2}\,\partial_r\chi_{\mathrm{S}} \Big) = 0\,,
\end{aligned}$$

and

$$\begin{aligned}
&-\,\mathrm{i}\,\omega\, M\,(\beta_{\mathrm{P}} \;+\; \alpha)\chi_{\mathrm{P}} \;-\; \mathrm{i}\,\omega\, M\,(\beta_{\mathrm{B}} \;+\; \alpha)\chi_{\mathrm{B}} \\
&+ \mathbf{X}_4 \Big(\frac{1}{\mathsf{s}_{\mathrm{P}}^2}\,\partial_r\chi_{\mathrm{P}} \;+\; \frac{1}{\mathsf{s}_{\mathrm{B}}^2}\,\partial_r\chi_{\mathrm{B}} \;-\; \frac{1}{\mathsf{s}_{\mathrm{S}}^2\,\mathfrak{b}}\,\partial_\theta\chi_{\mathrm{S}} \Big) + \mathbf{X}_5 \Big(\frac{\beta_{\mathrm{P}}}{\mathsf{s}_{\mathrm{P}}^2}\partial_r\chi_{\mathrm{P}} \;+\; \frac{\beta_{\mathrm{B}}}{\mathsf{s}_{\mathrm{B}}^2}\partial_r\chi_{\mathrm{B}} \;+\; \frac{\rho_f\,\mu_{\mathrm{fr}}}{\det A\,\mathfrak{b}}\partial_\theta\,\chi_{\mathrm{S}} \Big) \;=\; 0\,,
\end{aligned}$$

Below, for clarity, we keep the first and second Hankel function derivatives, they can however be replaced with the identities given in (21). The linear system is

$$\mathbb{A}_k^{\text{abc-T3}} \begin{pmatrix} a_k \\ b_k \\ c_k \\ \tilde{a}_k \\ \tilde{b}_k \\ \tilde{c}_k \end{pmatrix} = \begin{pmatrix} \mathrm{i}\,\omega\,\mathbf{u}_r^{\mathrm{pw}} \\ \mathrm{i}\,\omega\,\mathbf{u}_\theta^{\mathrm{pw}} \\ \mathrm{p}^{\mathrm{pw}} \\ 0 \\ 0 \\ 0 \end{pmatrix}, \tag{50}$$

with components A_{ij},

$$\begin{aligned}
&A_{11} = \mathsf{s}_{\mathrm{P}}^{-1}\,\omega\,\mathrm{H}_k^{(1)'}(\omega\,\mathsf{s}_{\mathrm{P}}\,\mathfrak{a})\,, \quad A_{12} = \mathsf{s}_{\mathrm{B}}^{-1}\,\omega\,\mathrm{H}_k^{(1)'}(\omega\,\mathsf{s}_{\mathrm{B}}\,\mathfrak{a})\,, \quad A_{13} = -\,\mathsf{s}_{\mathrm{S}}^{-2}\,\frac{\mathrm{i}k}{\mathfrak{a}}\mathrm{H}_k^{(1)}(\omega\,\mathsf{s}_{\mathrm{S}}\,\mathfrak{a})\,, \\
&A_{14} = \mathsf{s}_{\mathrm{P}}^{-1}\,\omega\,\mathrm{H}_k^{(2)'}(\omega\,\mathsf{s}_{\mathrm{P}}\,\mathfrak{a})\,, \quad A_{15} = \mathsf{s}_{\mathrm{B}}^{-1}\,\omega\,\mathrm{H}_k^{(2)'}(\omega\,\mathsf{s}_{\mathrm{B}}\,\mathfrak{a})\,, \quad A_{16} = -\,\mathsf{s}_{\mathrm{S}}^{-2}\,\frac{\mathrm{i}k}{\mathfrak{a}}\mathrm{H}_k^{(2)}(\omega\,\mathsf{s}_{\mathrm{S}}\,\mathfrak{a})\,,
\end{aligned}$$

$$\begin{aligned}
&A_{21} = \mathsf{s}_{\mathrm{P}}^{-2}\,\frac{\mathrm{i}k}{\mathfrak{a}}\mathrm{H}_k^{(1)}(\omega\,\mathsf{s}_{\mathrm{P}}\,\mathfrak{a})\,, \quad A_{22} = \mathsf{s}_{\mathrm{B}}^{-2}\,\frac{\mathrm{i}k}{\mathfrak{a}}\mathrm{H}_k^{(1)}(\omega\,\mathsf{s}_{\mathrm{B}}\,\mathfrak{a})\,, \quad A_{23} = \mathsf{s}_{\mathrm{S}}^{-1}\,\omega\,\mathrm{H}_k^{(1)'}(\omega\,\mathsf{s}_{\mathrm{S}}\,\mathfrak{a})\,, \\
&A_{24} = \mathsf{s}_{\mathrm{P}}^{-2}\,\frac{\mathrm{i}k}{\mathfrak{a}}\mathrm{H}_k^{(2)}(\omega\,\mathsf{s}_{\mathrm{P}}\,\mathfrak{b})\,, \quad A_{25} = \mathsf{s}_{\mathrm{B}}^{-2}\,\frac{\mathrm{i}k}{\mathfrak{a}}\mathrm{H}_k^{(2)}(\omega\,\mathsf{s}_{\mathrm{B}}\,\mathfrak{a})\,, \quad A_{26} = \mathsf{s}_{\mathrm{S}}^{-1}\,\omega\,\mathrm{H}_k^{(2)'}(\omega\,\mathsf{s}_{\mathrm{S}}\,\mathfrak{a})\,,
\end{aligned}$$

$$\begin{aligned}
&A_{31} = -M\,(\beta_{\mathrm{P}} \;+\; \alpha)\,\mathrm{H}_k^{(1)}(\omega\,\mathsf{s}_{\mathrm{P}}\,\mathfrak{a})\,, \quad A_{32} = -\,M\,(\beta_{\mathrm{B}} \;+\; \alpha)\,\mathrm{H}_k^{(1)}(\omega\,\mathsf{s}_{\mathrm{P}}\,\mathfrak{a})\,, \quad A_{33} = 0\,, \\
&A_{34} = -M\,(\beta_{\mathrm{P}} \;+\; \alpha)\,\mathrm{H}_k^{(2)}(\omega\,\mathsf{s}_{\mathrm{P}}\,\mathfrak{a})\,, \quad A_{35} = -\,M\,(\beta_{\mathrm{B}} \;+\; \alpha)\,\mathrm{H}_k^{(2)}(\omega\,\mathsf{s}_{\mathrm{P}}\,\mathfrak{a})\,, \quad A_{36} = 0\,,
\end{aligned}$$

$$A_{41} = -2\,\mathrm{i}\,\mu_{\rm fr}\,\omega\,\mathrm{H}_k^{(1)''}(\omega\,\mathsf{s}_{\rm P}\,\mathfrak{b}) + \mathrm{i}\omega(-\frac{2}{3}\mu_{\rm fr} + \mathrm{k}_{\rm fr} + M\,\alpha(\alpha+\beta_{\rm P})\,\mathrm{H}_k^{(1)}(\omega\,\mathsf{s}_{\rm P}\,\mathfrak{b}) + \frac{\boldsymbol{X}_1\,\omega}{\mathsf{s}_{\rm P}}\mathrm{H}_k^{(1)'}(\omega\,\mathsf{s}_{\rm P}\,\mathfrak{b}) + \frac{\boldsymbol{X}_2\,\omega\beta_{\rm P}}{\mathsf{s}_{\rm P}}\,\mathrm{H}_k^{(1)'}(\omega\,\mathsf{s}_{\rm P}\,\mathfrak{b}),$$

$$A_{42} = -2\,\mathrm{i}\,\mu_{\rm fr}\,\omega\,\mathrm{H}_k^{(1)''}(\omega\,\mathsf{s}_{\rm B}\,\mathfrak{b}) + \mathrm{i}\omega(-\frac{2}{3}\mu_{\rm fr} + \mathrm{k}_{\rm fr} + M\,\alpha(\alpha+\beta_{\rm B})\,\mathrm{H}_k^{(1)}(\omega\,\mathsf{s}_{\rm B}\,\mathfrak{b}) + \frac{\boldsymbol{X}_1\,\omega}{\mathsf{s}_{\rm B}}\mathrm{H}_k^{(1)'}(\omega\,\mathsf{s}_{\rm B}\,\mathfrak{b}) + \frac{\boldsymbol{X}_2\,\omega\beta_{\rm B}}{\mathsf{s}_{\rm B}}\,\mathrm{H}_k^{(1)'}(\omega\,\mathsf{s}_{\rm B}\,\mathfrak{b}),$$

$$A_{43} = -\frac{2\,\mu_{\rm fr}\,k}{\mathsf{s}_{\rm S}\,\mathfrak{b}}\,\mathrm{H}_k^{(1)'}(\omega\,\mathsf{s}_{\rm S}\,\mathfrak{b}) + \frac{2\,\mu_{\rm fr}\,k}{\omega\mathsf{s}_{\rm S}^2\,\mathfrak{b}^2}\,\mathrm{H}_k^{(1)}(\omega\,\mathsf{s}_{\rm S}\,\mathfrak{b}) - \frac{\boldsymbol{X}_1\,\mathrm{i}\,k}{\mathsf{s}_{\rm S}^2\,\mathfrak{b}}\,\mathrm{H}_k^{(1)}(\omega\,\mathsf{s}_{\rm S}\,\mathfrak{b}) + \frac{\boldsymbol{X}_2\,\rho_f\,\mu_{\rm fr}\,\mathrm{i}\,k}{\mathrm{detA}\,\mathfrak{b}}\,\mathrm{H}_k^{(1)}(\omega\,\mathsf{s}_{\rm S}\,\mathfrak{b}),$$

$$A_{44} = -2\,\mathrm{i}\,\mu_{\rm fr}\,\omega\,\mathrm{H}_k^{(2)''}(\omega\,\mathsf{s}_{\rm P}\,\mathfrak{b}) + \mathrm{i}\omega(-\frac{2}{3}\mu_{\rm fr} + \mathrm{k}_{\rm fr} + M\,\alpha(\alpha+\beta_{\rm P})\,\mathrm{H}_k^{(2)}(\omega\,\mathsf{s}_{\rm P}\,\mathfrak{b}) + \frac{\boldsymbol{X}_1\,\omega}{\mathsf{s}_{\rm P}}\mathrm{H}_k^{(2)'}(\omega\,\mathsf{s}_{\rm P}\,\mathfrak{b}) + \frac{\boldsymbol{X}_2\,\omega\beta_{\rm P}}{\mathsf{s}_{\rm P}}\,\mathrm{H}_k^{(2)'}(\omega\,\mathsf{s}_{\rm P}\,\mathfrak{b}),$$

$$A_{45} = -2\,\mathrm{i}\,\mu_{\rm fr}\,\omega\,\mathrm{H}_k^{(2)''}(\omega\,\mathsf{s}_{\rm B}\,\mathfrak{b}) + \mathrm{i}\omega(-\frac{2}{3}\mu_{\rm fr} + \mathrm{k}_{\rm fr} + M\,\alpha(\alpha+\beta_{\rm B})\,\mathrm{H}_k^{(2)}(\omega\,\mathsf{s}_{\rm B}\,\mathfrak{b}) + \frac{\boldsymbol{X}_1\,\omega}{\mathsf{s}_{\rm B}}\mathrm{H}_k^{(2)'}(\omega\,\mathsf{s}_{\rm B}\,\mathfrak{b}) + \frac{\boldsymbol{X}_2\,\omega\beta_{\rm B}}{\mathsf{s}_{\rm B}}\,\mathrm{H}_k^{(2)'}(\omega\,\mathsf{s}_{\rm B}\,\mathfrak{b}),$$

$$A_{46} = -\frac{2\,\mu_{\rm fr}\,k}{\mathsf{s}_{\rm S}\,\mathfrak{b}}\,\mathrm{H}_k^{(2)'}(\omega\,\mathsf{s}_{\rm S}\,\mathfrak{b}) + \frac{2\,\mu_{\rm fr}\,k}{\omega\mathsf{s}_{\rm S}^2\,\mathfrak{b}^2}\,\mathrm{H}_k^{(2)}(\omega\,\mathsf{s}_{\rm S}\,\mathfrak{b}) - \frac{\boldsymbol{X}_1\,\mathrm{i}\,k}{\mathsf{s}_{\rm S}^2\,\mathfrak{b}}\,\mathrm{H}_k^{(2)}(\omega\,\mathsf{s}_{\rm S}\,\mathfrak{b}) + \frac{\boldsymbol{X}_2\,\rho_f\,\mu_{\rm fr}\,\mathrm{i}\,k}{\mathrm{detA}\,\mathfrak{b}}\,\mathrm{H}_k^{(2)}(\omega\,\mathsf{s}_{\rm S}\,\mathfrak{b}),$$

$$A_{51} = -\frac{2\,\mu_{\rm fr}\,\omega\,\mathrm{i}\,k}{\mathsf{s}_{\rm P}\,\mathfrak{b}}\,\mathrm{H}_k^{(1)'}(\omega\,\mathsf{s}_{\rm P}\,\mathfrak{b}) + \frac{2\,\mu_{\rm fr}\,\mathrm{i}\,k}{\mathsf{s}_{\rm P}^2\,\mathfrak{b}^2}\,\mathrm{H}_k^{(1)}(\omega\,\mathsf{s}_{\rm P}\,\mathfrak{b}) + \frac{\boldsymbol{X}_3\,\omega\,k}{\mathsf{s}_{\rm P}^2\mathfrak{b}}\mathrm{H}_k^{(1)}(\omega\,\mathsf{s}_{\rm P}\,\mathfrak{b}),$$

$$A_{52} = -\frac{2\,\mu_{\rm fr}\,\omega\,\mathrm{i}\,k}{\mathsf{s}_{\rm B}\,\mathfrak{b}}\,\mathrm{H}_k^{(1)'}(\omega\,\mathsf{s}_{\rm B}\,\mathfrak{b}) + \frac{2\,\mu_{\rm fr}\,\mathrm{i}\,k}{\mathsf{s}_{\rm B}^2\,\mathfrak{b}^2}\,\mathrm{H}_k^{(1)}(\omega\,\mathsf{s}_{\rm B}\,\mathfrak{b}) + \frac{\boldsymbol{X}_3\,\omega\,k}{\mathsf{s}_{\rm B}^2\mathfrak{b}}\mathrm{H}_k^{(1)}(\omega\,\mathsf{s}_{\rm B}\,\mathfrak{b}),$$

$$A_{53} = -\frac{k^2\,\mu_{\rm fr}}{\mathsf{s}_{\rm S}^2\,\mathfrak{b}^2}\,\mathrm{H}_k^{(1)}(\omega\,\mathsf{s}_{\rm S}\,\mathfrak{b}) + \frac{\omega\,\mu_{\rm fr}}{\mathsf{s}_{\rm S}\,\mathfrak{b}}\,\mathrm{H}_k^{(1)'}(\omega\,\mathsf{s}_{\rm S}\,\mathfrak{b}) - \omega^2\,\mu_{\rm fr}\,\mathrm{H}_k^{(1)''}(\omega\,\mathsf{s}_{\rm S}\,\mathfrak{b}) - \frac{\boldsymbol{X}_3\,\omega^2\,\mathrm{i}}{\mathsf{s}_{\rm S}}\,\mathrm{H}_k^{(1)'}(\omega\,\mathsf{s}_{\rm S}\,\mathfrak{b}),$$

$$A_{54} = -\frac{2\,\mu_{\rm fr}\,\omega\,\mathrm{i}\,k}{\mathsf{s}_{\rm P}\,\mathfrak{b}}\,\mathrm{H}_k^{(2)'}(\omega\,\mathsf{s}_{\rm P}\,\mathfrak{b}) + \frac{2\,\mu_{\rm fr}\,\mathrm{i}\,k}{\mathsf{s}_{\rm P}^2\,\mathfrak{b}^2}\,\mathrm{H}_k^{(2)}(\omega\,\mathsf{s}_{\rm P}\,\mathfrak{b}) + \frac{\boldsymbol{X}_3\,\omega\,k}{\mathsf{s}_{\rm P}^2\mathfrak{b}}\mathrm{H}_k^{(2)}(\omega\,\mathsf{s}_{\rm P}\,\mathfrak{b}),$$

$$A_{55} = -\frac{2\,\mu_{\rm fr}\,\omega\,\mathrm{i}\,k}{\mathsf{s}_{\rm B}\,\mathfrak{b}}\,\mathrm{H}_k^{(2)'}(\omega\,\mathsf{s}_{\rm B}\,\mathfrak{b}) + \frac{2\,\mu_{\rm fr}\,\mathrm{i}\,k}{\mathsf{s}_{\rm B}^2\,\mathfrak{b}^2}\,\mathrm{H}_k^{(2)}(\omega\,\mathsf{s}_{\rm B}\,\mathfrak{b}) + \frac{\boldsymbol{X}_3\,\omega\,k}{\mathsf{s}_{\rm B}^2\mathfrak{b}}\mathrm{H}_k^{(2)}(\omega\,\mathsf{s}_{\rm B}\,\mathfrak{b}),$$

$$A_{56} = -\frac{k^2\,\mu_{\rm fr}}{\mathsf{s}_{\rm S}^2\,\mathfrak{b}^2}\,\mathrm{H}_k^{(2)}(\omega\,\mathsf{s}_{\rm S}\,\mathfrak{b}) + \frac{\omega}{\mathsf{s}_{\rm S}\,\mathfrak{b}}\,\mathrm{H}_k^{(2)'}(\omega\,\mathsf{s}_{\rm S}\,\mathfrak{b}) - \omega^2\,\mu_{\rm fr}\,\mathrm{H}_k^{(2)''}(\omega\,\mathsf{s}_{\rm S}\,\mathfrak{b}) - \frac{\boldsymbol{X}_3\,\omega^2\,\mathrm{i}}{\mathsf{s}_{\rm S}}\,\mathrm{H}_k^{(2)'}(\omega\,\mathsf{s}_{\rm S}\,\mathfrak{b}),$$

and

$$A_{61} = -\mathrm{i}\,\omega\,M\,(\beta_{\rm P}+\alpha)\mathrm{H}_k^{(1)}(\omega\,\mathsf{s}_{\rm P}\,\mathfrak{b}) + \frac{\boldsymbol{X}_4\,\omega}{\mathsf{s}_{\rm P}}\mathrm{H}_k^{(1)'}(\omega\,\mathsf{s}_{\rm P}\,\mathfrak{b}) + \frac{\boldsymbol{X}_5\,\omega\,\beta_{\rm P}}{\mathsf{s}_{\rm P}}\,\mathrm{H}_k^{(1)'}(\omega\,\mathsf{s}_{\rm P}\,\mathfrak{b}),$$

$$A_{62} = -\mathrm{i}\,\omega\,M\,(\beta_{\rm B}+\alpha)\mathrm{H}_k^{(1)}(\omega\,\mathsf{s}_{\rm B}\,\mathfrak{b}) + \frac{\boldsymbol{X}_4\,\omega}{\mathsf{s}_{\rm B}}\mathrm{H}_k^{(1)'}(\omega\,\mathsf{s}_{\rm B}\,\mathfrak{b}) + \frac{\boldsymbol{X}_5\,\omega\,\beta_{\rm B}}{\mathsf{s}_{\rm B}}\,\mathrm{H}_k^{(1)'}(\omega\,\mathsf{s}_{\rm B}\,\mathfrak{b}),$$

$$A_{63} = -\frac{\boldsymbol{X}_4\,\mathrm{i}\,k}{\mathsf{s}_{\rm S}^2\,\mathfrak{b}}\,\mathrm{H}_k^{(1)}(\omega\,\mathsf{s}_{\rm S}\,\mathfrak{b}) + \frac{\boldsymbol{X}_5\,\rho_f\,\mu_{\rm fr}\,\mathrm{i}\,k}{\mathrm{detA}\,\mathfrak{b}}\,\mathrm{H}_k^{(1)}(\omega\,\mathsf{s}_{\rm S}\,\mathfrak{b}),$$

$$A_{64} = -\mathrm{i}\,\omega\,M\,(\beta_{\rm P}+\alpha)\mathrm{H}_k^{(2)}(\omega\,\mathsf{s}_{\rm P}\,\mathfrak{b}) + \frac{\boldsymbol{X}_4\,\omega}{\mathsf{s}_{\rm P}}\mathrm{H}_k^{(2)'}(\omega\,\mathsf{s}_{\rm P}\,\mathfrak{b}) + \frac{\boldsymbol{X}_5\,\omega\,\beta_{\rm P}}{\mathsf{s}_{\rm P}}\,\mathrm{H}_k^{(2)'}(\omega\,\mathsf{s}_{\rm P}\,\mathfrak{b}),$$

$$A_{65} = -\mathrm{i}\,\omega\,M\,(\beta_{\rm B}+\alpha)\mathrm{H}_k^{(2)}(\omega\,\mathsf{s}_{\rm B}\,\mathfrak{b}) + \frac{\boldsymbol{X}_4\,\omega}{\mathsf{s}_{\rm B}}\mathrm{H}_k^{(2)'}(\omega\,\mathsf{s}_{\rm B}\,\mathfrak{b}) + \frac{\boldsymbol{X}_5\,\omega\,\beta_{\rm B}}{\mathsf{s}_{\rm B}}\,\mathrm{H}_k^{(2)'}(\omega\,\mathsf{s}_{\rm B}\,\mathfrak{b}),$$

$$A_{66} = -\frac{\boldsymbol{X}_4\,\mathrm{i}\,k}{\mathsf{s}_{\rm S}^2\,\mathfrak{b}}\,\mathrm{H}_k^{(2)}(\omega\,\mathsf{s}_{\rm S}\,\mathfrak{b}) + \frac{\boldsymbol{X}_5\,\rho_f\,\mu_{\rm fr}\,\mathrm{i}\,k}{\mathrm{detA}\,\mathfrak{b}}\,\mathrm{H}_k^{(2)}(\omega\,\mathsf{s}_{\rm S}\,\mathfrak{b}).$$

5 Performance assessment of the absorbing boundary condition in the setting of an obstacle scattering

In the previous section, we have built analytical outgoing solution $\mathfrak{U}^{\infty-\mathrm{Ti}}$ and the truncated solution $\mathfrak{U}^{\text{abc-Ti}}$ for the scattering of a plane wave by an impenetrable circular obstacle. From now on, we denote by $\mathfrak{U}^{\infty-\mathrm{Ti}}$ the restriction of $\mathfrak{U}^{\infty-\mathrm{Ti}}$ on $\Omega_{\mathfrak{ab}}$. In this section, we study the robustness of the ABC by comparing $\mathfrak{U}^{\infty-\mathrm{Ti}}$ with $\mathfrak{U}^{\text{abc-Ti}}$.

The domain is an annulus described in Fig. 1 composed of sandstone (see Table 1). The boundary of the obstacle $\{r = \mathfrak{a}\}$ is denoted by Γ_1. We set an artificial boundary at radius $\mathfrak{b}$. We will consider the scattering of the three porous plane waves of type (P,B,S) by the obstacle, for boundary condition of type 1 ("Neumann-like") and 3 ("Dirichlet-like") on $\mathfrak{a}$. In all of our numerical experiments, the radius of the obstacle is kept 1 m, i.e. $\mathfrak{a} = 1\mathrm{m}$, while the value of the viscosity in the material η, of the frequency f and of the exterior radius $\mathfrak{b}$ will vary.

Recall that solution $\mathfrak{U}^{\text{abc-Ti}}$ is represented by the series of coefficients a_k, b_k, c_k, $\tilde{a}_k$, $\tilde{b}_k$, $\tilde{c}_k$, and the solution $\mathfrak{U}^{\infty-\mathrm{Ti}}$ by the coefficients a_k^∞, b_k^∞, c_k^∞ (see equations (44), to (49)). In the numerical tests, the Hankel functions are infinite series truncated to the first N terms of the series, with $N \geq 2\mathbf{k}\mathfrak{a} + 1$ (cf. [22]), where $\mathbf{k} = \max(\mathfrak{k}_\mathrm{P}, \max(\mathfrak{k}_\mathrm{B}, \max(\mathfrak{k}_\mathrm{S}$.

The comparisons are carried out in terms of the following quantities:

- Comparison mode by mode of a_k^∞, b_k^∞, c_k^∞ with a_k, b_k, c_k. Module of $\tilde{a}_k$, $\tilde{b}_k$, $\tilde{c}_k$.
- Errors on the coefficients:

$$e^2_{\text{coeff}} = \frac{\sum_{k=-N}^{k=N} \left((a_k^\infty - a_k)^2 + (b_k^\infty - b_k)^2 + (c_k^\infty - c_k)^2 + \tilde{a_k}^2 + \tilde{b_k}^2 + \tilde{c_k}^2\right)}{\sum_{k=-N}^{k=N} (a_k^{\infty 2} + b_k^{\infty 2} + c_k^{\infty 2})}, \qquad (52)$$

$$e^2_{\text{scatt}} = \sum_{k=-N}^{k=N} \left(\tilde{a_k}^2 + \tilde{b_k}^2 + \tilde{c_k}^2\right).$$

- Relative L2 error of $\mathbf{u}_x$:

$$e_h(\mathbf{u}_x^{\text{abc -Ti}}) = \frac{||\mathbf{u}_x^{\text{abc -Ti}} - \mathbf{u}_x^{\infty-\mathrm{Ti}}||_2}{||\mathbf{u}_x^{\infty-\mathrm{Ti}}||_2}. \qquad (53)$$

  The L2 norm is theoretically equals to

$$||\mathbf{u}_x^{\text{abc -Ti}} - \mathbf{u}_x^{\infty-\mathrm{Ti}}||_2 = \left(\int_\Omega |\mathbf{u}_x^{\text{abc -Ti}} - \mathbf{u}_x^{\infty-\mathrm{Ti}}|^2\right)^{\frac{1}{2}},$$

  In practice, we approximate the above equation by

$$||\mathbf{u}_x^{\text{abc -Ti}} - \mathbf{u}_x^{\infty-\mathrm{Ti}}||_2 = \left(\sum_{K\in\mathcal{T}_h} \int_K |\mathbf{u}_x^{\text{abc -Ti}} - \mathbf{u}_x^{\infty-\mathrm{Ti}}|^2\right)^{\frac{1}{2}},$$

  where we have defined a mesh $\mathcal{T}_h$ of Ω with N_{elem} elements K which are triangles. We define on each element the 10 Lagrange degrees of freedom corresponding with an interpolation of degree 3 on a triangle, and compute the norm using this interpolation. We focus on the component $\mathbf{u}_x$, but the other components have the same behaviour.

We will study the effect of different factors on the performance of the ABC:

- presence of viscosity,
- size of the exterior radius $\mathfrak{b}$.
- frequency,
- type of incident-wave (P,B,S),

- type of boundary condition on the interior radius $\mathfrak{a}$. We will focus on type 1 ("Neumann-like") and type 3 ("Dirichlet-like").

In the following, we first present in section 5.1 the modules of the coefficients for $\mathfrak{b} = 10$m and $f = 1$kHz, for many configurations. Then in section 5.2, we compare the truncated solution with the outgoing solution potential by potential by using a decomposition of the potentials. In section 5.3, we investigate the influence of the size of the domain used for the truncated solution by varying the value of $\mathfrak{b}$. Afterwards, in order to highlight the influence of the viscosity on the performance of the ABC, we compare the truncated solution with the outgoing solution for a material by varying only its viscosity in section 5.4. Finally, in section 5.5 the performance of the ABC is studied for a range of frequencies.

5.1 Comparison between the coefficients of outgoing solution and truncated solution

In the following, we display the values of the coefficients series a_k^∞, b_k^∞, c_k^∞ and a_k, b_k c_k, $\tilde{a_k}$, $\tilde{b_k}$, $\tilde{c_k}$ for several configurations:

- Scattering of a P,B,S incident plane wave for sandstone with viscosity $\eta = 10^{-3}$ Pa.s^{-1} and boundary condition of type 1 ("Neumann-like") on $r = \mathfrak{a}$ (*cf.* equation (3a)), respectively in figures 2, 3, 4 for exterior radius $\mathfrak{b} = 10$m.
- Scattering of a P,B,S incident plane wave for sandstone with viscosity $\eta = 10^{-3}$ Pa.s^{-1} and boundary condition of type 3 ("Dirichlet-like") on $r = \mathfrak{a}$ (*cf.* equation (3c)), respectively in figures 5, 6, 7, for exterior radius $\mathfrak{b} = 10$m.
- Scattering of a P,B,S incident plane wave for sandstone with no viscosity $\eta = 0$ Pa.s^{-1} and boundary condition of type 1 ("Neumann-like") on $r = \mathfrak{a}$ (*cf.* equation (3a)), respectively in figures 8, 9, 10 for exterior radius $\mathfrak{b} = 10$m.
- Scattering of a P,B,S incident plane wave for sandstone with no viscosity $\eta = 0$ Pa.s^{-1} and boundary condition of type 3 ("Dirichlet-like") on $r = \mathfrak{a}$ (*cf.* equation (3c)), respectively in figures 11, 12, 13, for exterior radius $\mathfrak{b} = 10$m.

Remark 4. Even though the value $\mathfrak{b} = 10$m may seem high compared to the size of $\mathfrak{a}$, we have for the experiments: $k_{\mathrm{P}}\,\mathfrak{b} = 14.76$, $k_{\mathrm{B}}\,\mathfrak{b} = 61.48$, $k_{\mathrm{S}}\,\mathfrak{b} = 26.25$. This means that for the fastest wave, we have $\dfrac{k_{\mathrm{P}}\,\mathfrak{b}}{2\,\pi} = 2.35$ wavelengths for 10m, which is low. The rule of thumb recommends indeed to set the boundary at least at two wavelengths of the obstacle.

From Fig. 2 to 13, we observe the following. The coefficients a_k, b_k, c_k, obtained by solving the system with absorbing boundaries seem to approximate well the coefficients obtained for the exact solution. The coefficients $\tilde{a}_k$ and $\tilde{b}_k$ are close to zero. When the incident plane wave is a B-wave, the values of the coefficients b_k, b_k^∞ are larger than the other coefficients (Fig. 3 and 6), however, the reflected coefficient $\tilde{b}_k$ remains low. The coefficients $\tilde{c}_k$ are greater than $\tilde{a}_k$ and $\tilde{b}_k$ in every cases. The value of $\tilde{c}_k$ is always at least 10% of the coefficients a_k, b_k, c_k, it can also be of the same order or higher than them (see Fig. 10 and 13). This means that the reflection of the S-wave has more influence on the error of the absorbing boundary condition. For most cases, the behaviour of $\tilde{c}_k$ is related to the one of c_k, *e.g.* Fig. 2-7, in other cases for an incident B-wave, it seems to be linked to b_k (fig. 12). Finally, as in Fig.s 7, 9 and 13, the behaviour of $\tilde{c}_k$ seems to be a combination of the behaviours of b_k and c_k. The errors of the absorbing boundary condition will hence be due mainly by the conversion of S-wave to S-waves and of B-wave to S-waves.

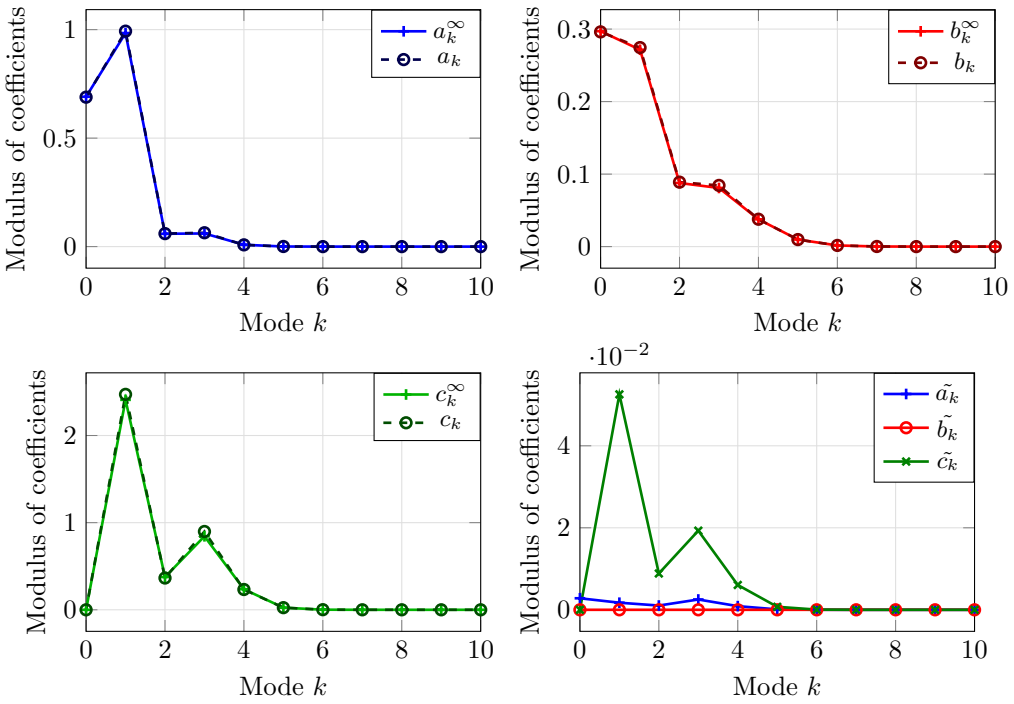

Figure 2: Obstacle scattering of an incident plane P-wave type 1 ("Neumann-like") for the boundary condition on $r = \mathfrak{a}$ (3a) at a frequency $f = 1$kHz for a sandstone medium with viscosity. The domain is an annulus with the interior radius $\mathfrak{a} = 1$m and the exterior radius $\mathfrak{b} = 10$m. The coefficients with ∞ superscript correspond to the exact outgoing solution. a_k^∞ —+—, a_k - -⊙- -, and $\tilde{a}_k$ —+— are the coefficients corresponding to the potential of the P-wave, b_k^∞ —+—, b_k - -⊙- -, and $\tilde{b}_k$ —⊙— are the to the potential of the B-wave, and c_k^∞ —+—, c_k - -⊙- -, and $\tilde{c}_k$ —×— to the potential of the S-wave (see equation (47)).

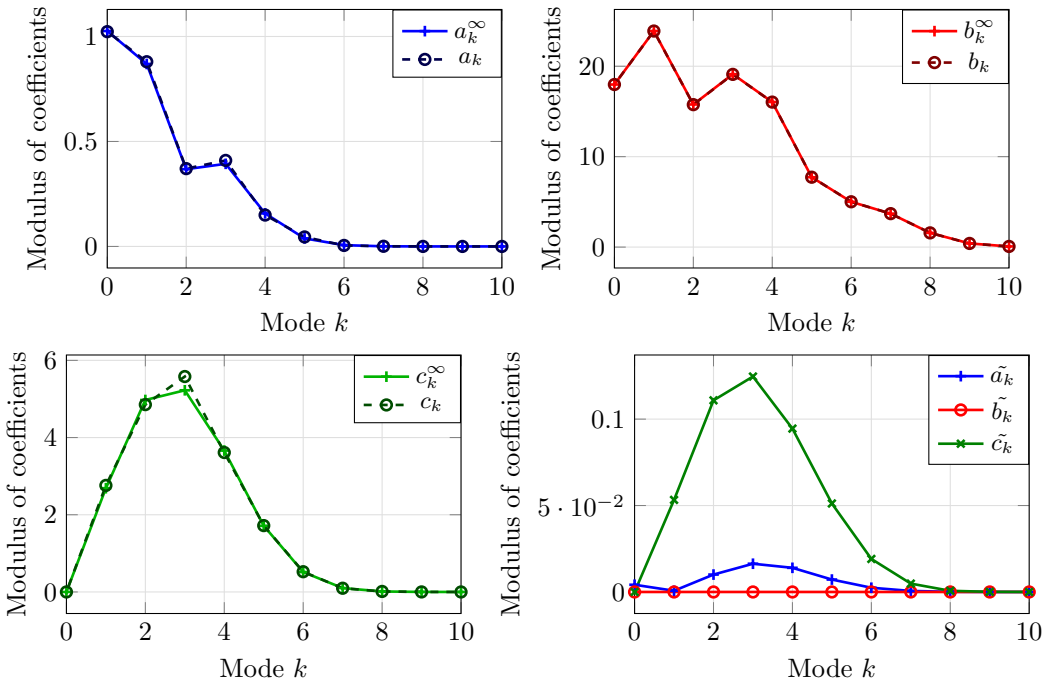

Figure 3: Obstacle scattering of an incident plane B-wave with the type 1 ("Neumann-like") for the boundary condition on $r = \mathfrak{a}$ (3a) at a frequency $f = 1$kHz for a sandstone medium with viscosity $\eta = 10^{-3}$ Pa.s^{-1}. The domain is an annulus with the interior radius $\mathfrak{a} = 1$m and the exterior radius $\mathfrak{b} = 10$m. The coefficients with ∞ superscript correspond to the exact outgoing solution. a_k^∞ —, a_k - o -, and $\tilde{a}_k$ — are the coefficients corresponding to the potential of the P-wave, b_k^∞ —, b_k - o -, and $\tilde{b}_k$ — are the to the potential of the B-wave, and c_k^∞ —, c_k - o -, and $\tilde{c}_k$ — to the potential of the S-wave (see equation (47)).

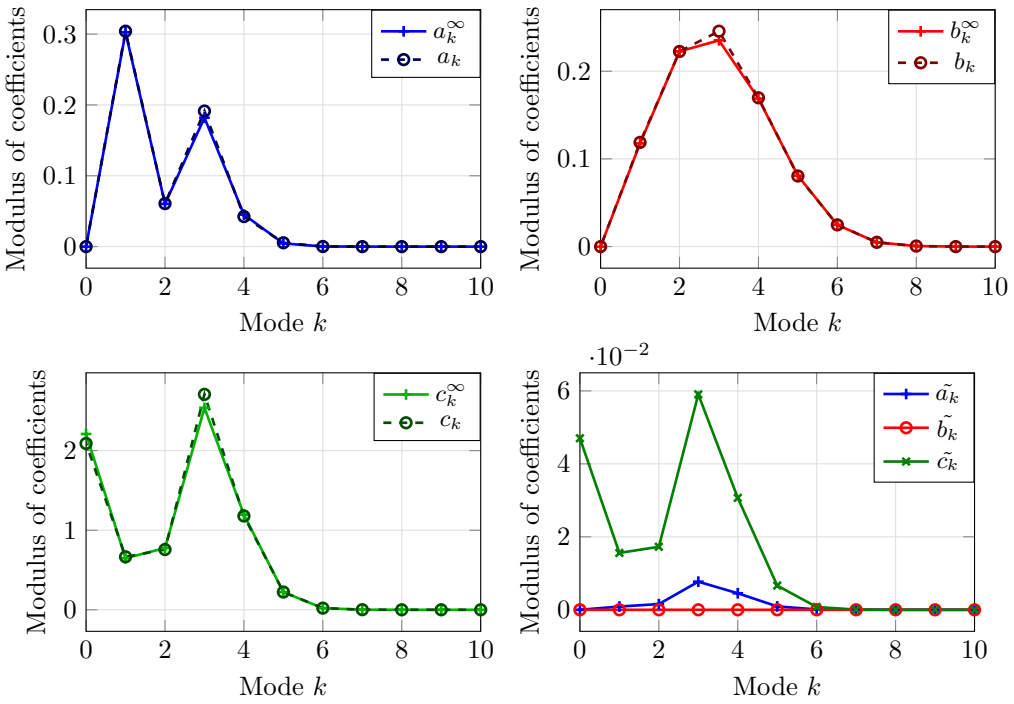

Figure 4: Obstacle scattering of an incident plane S-wave with the type 1 ("Neumann-like") for the boundary condition on $r = \mathfrak{a}$ (3a). at a frequency $f = 1$kHz for a sandstone medium with viscosity $\eta = 10^{-3}$ Pa.s^{-1}. The domain is an annulus with the interior radius $\mathfrak{a} = 1$m and the exterior radius $\mathfrak{b} = 10$m. The coefficients with ∞ superscript correspond to the exact outgoing solution. a_k^∞ —+—, a_k - -o- -, and $\tilde{a}_k$ —+— are the coefficients corresponding to the potential of the P-wave, b_k^∞ —+—, b_k - -o- -, and $\tilde{b}_k$ —o— are the to the potential of the B-wave, and c_k^∞ —+—, c_k - -o- -, and $\tilde{c}_k$ —x— to the potential of the S-wave (see equation (47)).

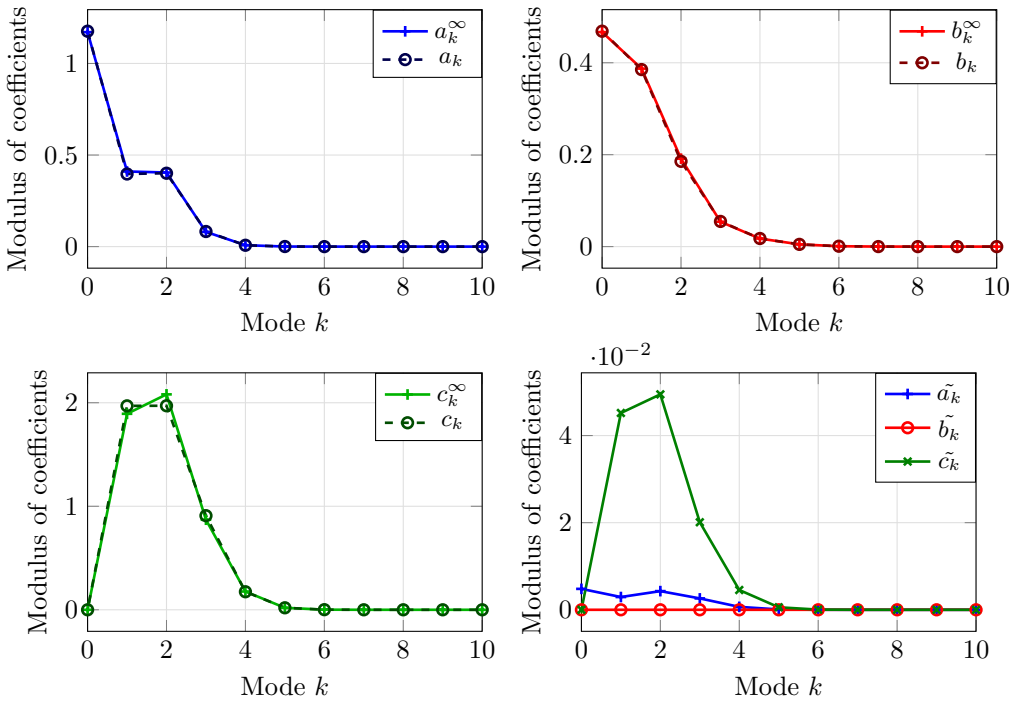

Figure 5: Obstacle scattering of an incident plane P-wave type 3 ("Dirichlet-like") for the boundary condition on $r = \mathfrak{a}$ (3c) at a frequency $f = 1$kHz for a sandstone medium with viscosity $\eta = 10^{-3}$ Pa.s^{-1}. The domain is an annulus with the interior radius $\mathfrak{a} = 1$m and the exterior radius $\mathfrak{b} = 10$m. The coefficients with ∞ superscript correspond to the exact outgoing solution. a_k^∞ —+—, a_k - -o- -, and $\tilde{a}_k$ —+— are the coefficients corresponding to the potential of the P-wave, b_k^∞ —+—, b_k - -o- -, and $\tilde{b}_k$ —o— are the to the potential of the B-wave, and c_k^∞ —+—, c_k - -o- -, and $\tilde{c}_k$ —x— to the potential of the S-wave (see equation (47)).

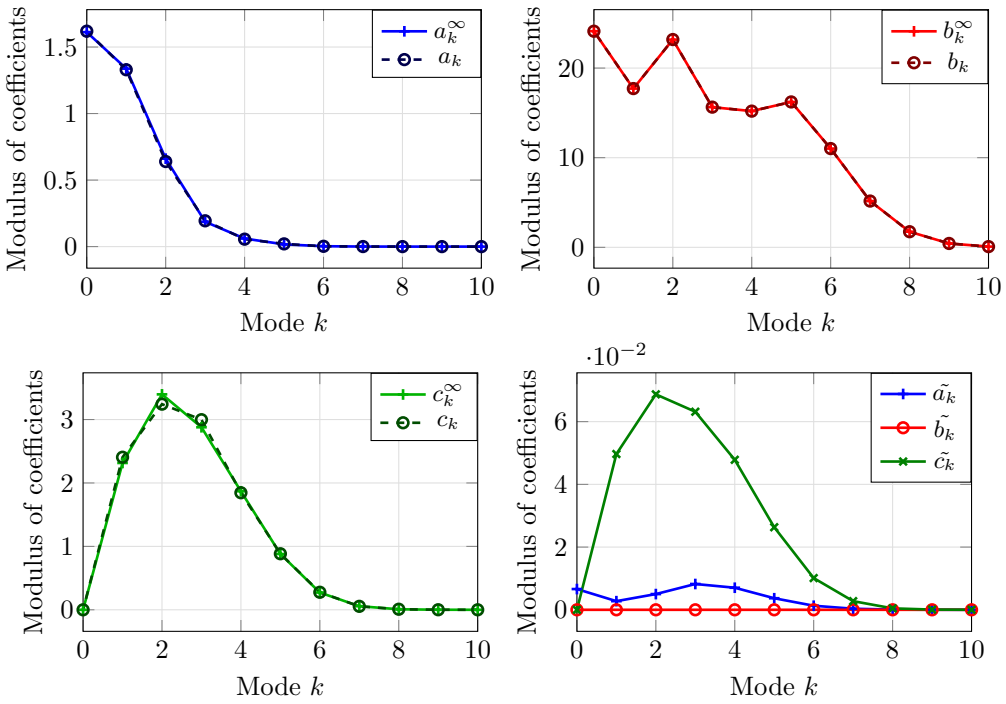

Figure 6: Obstacle scattering of an incident plane B-wave with the type 3 ("Dirichlet-like") for the boundary condition on $r = \mathfrak{a}$ (3c) at a frequency $f = 1$kHz for a sandstone medium with viscosity $\eta = 10^{-3}$ Pa.s^{-1}. The domain is an annulus with the interior radius $\mathfrak{a} = 1$m and the exterior radius $\mathfrak{b} = 10$m. The coefficients with ∞ superscript correspond to the exact outgoing solution. a_k^∞ —, a_k - o -, and $\tilde{a}_k$ — are the coefficients corresponding to the potential of the P-wave, b_k^∞ —, b_k - o -, and $\tilde{b}_k$ — are the to the potential of the B-wave, and c_k^∞ —, c_k - o -, and $\tilde{c}_k$ — to the potential of the S-wave (see equation (47)).

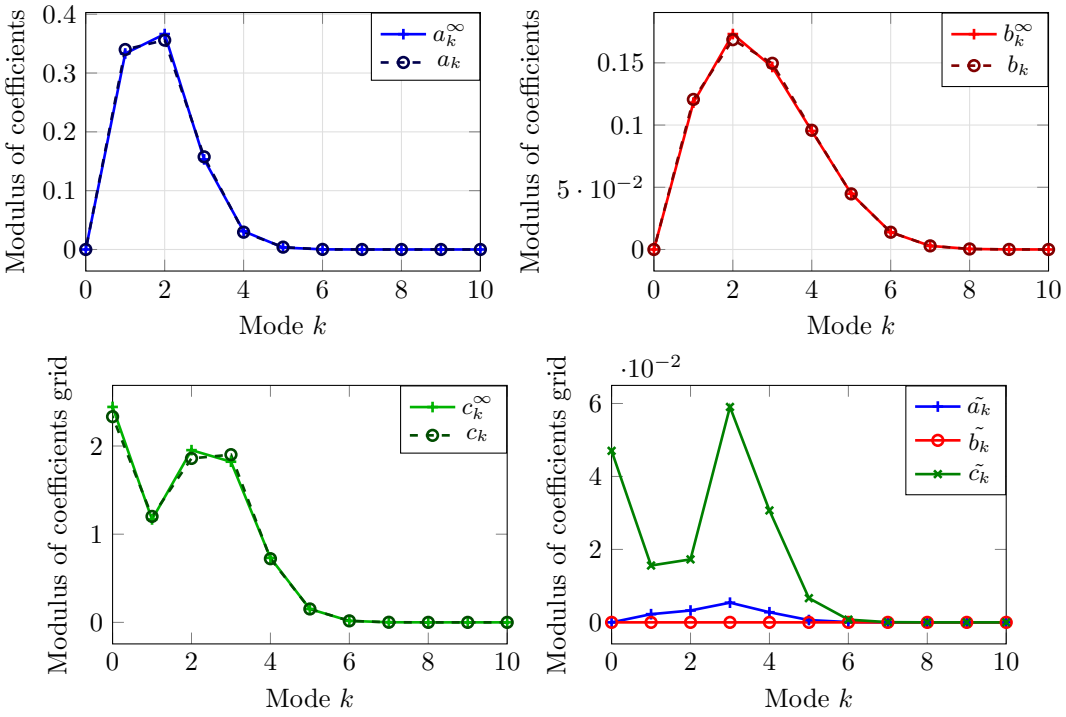

Figure 7: Obstacle scattering of an incident plane S-wave with the type 3 ("Dirichlet-like") for the boundary condition on $r = \mathfrak{a}$ (3c) at a frequency $f = 1$kHz for a sandstone medium with viscosity $\eta = 10^{-3}$ Pa.s^{-1}. The domain is an annulus with the interior radius $\mathfrak{a} = 1$m and the exterior radius $\mathfrak{b} = 10$m. The coefficients with ∞ superscript correspond to the exact outgoing solution. a_k^∞ —+—, a_k - -o- -, and $\tilde{a}_k$ —+— are the coefficients corresponding to the potential of the P-wave, b_k^∞ —+—, b_k - -o- -, and $\tilde{b}_k$ —o— are the to the potential of the B-wave, and c_k^∞ —+—, c_k - -o- -, and $\tilde{c}_k$ —x— to the potential of the S-wave (see equation (47)).

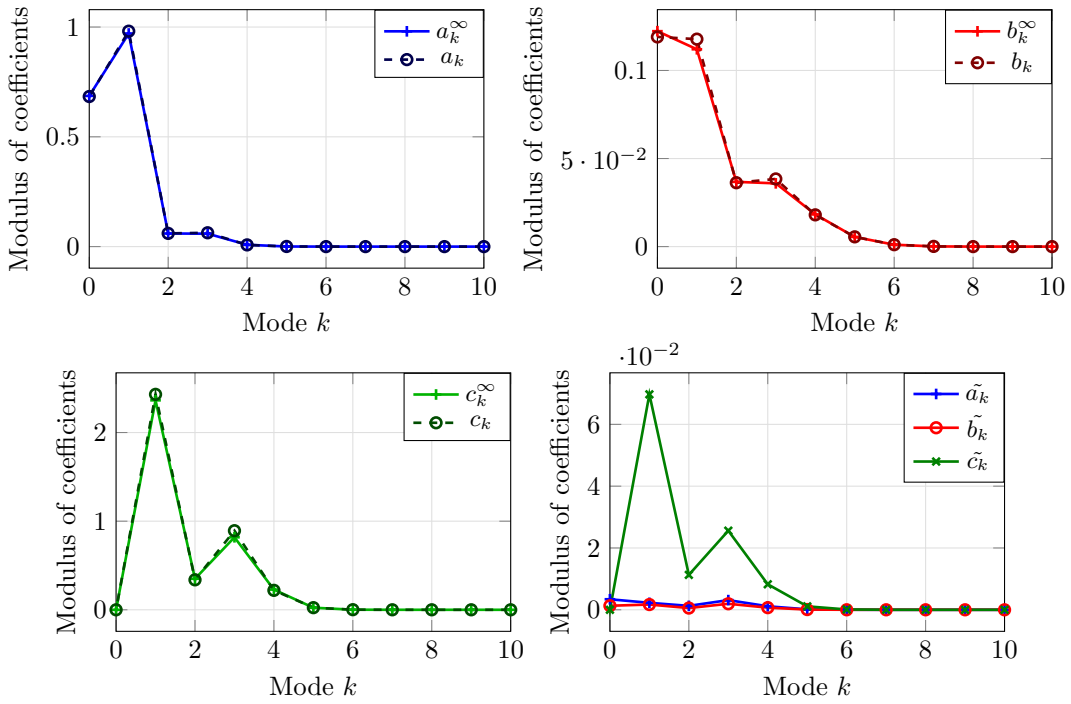

Figure 8: Obstacle scattering of an incident plane P-wave type 1 ("Neumann-like") for the boundary condition on $r = \mathfrak{a}$ (3a) at a frequency $f = 1$kHz for a sandstone medium with no viscosity. The domain is an annulus with the interior radius $\mathfrak{a} = 1$m and the exterior radius $\mathfrak{b} = 10$m. The coefficients with ∞ superscript correspond to the exact outgoing solution. a_k^∞ —+—, a_k - -o- -, and $\tilde{a}_k$ —+— are the coefficients corresponding to the potential of the P-wave, b_k^∞ —+—, b_k - -o- -, and $\tilde{b}_k$ —o— are the to the potential of the B-wave, and c_k^∞ —+—, c_k - -o- -, and $\tilde{c}_k$ —×— to the potential of the S-wave (see equation (47)).

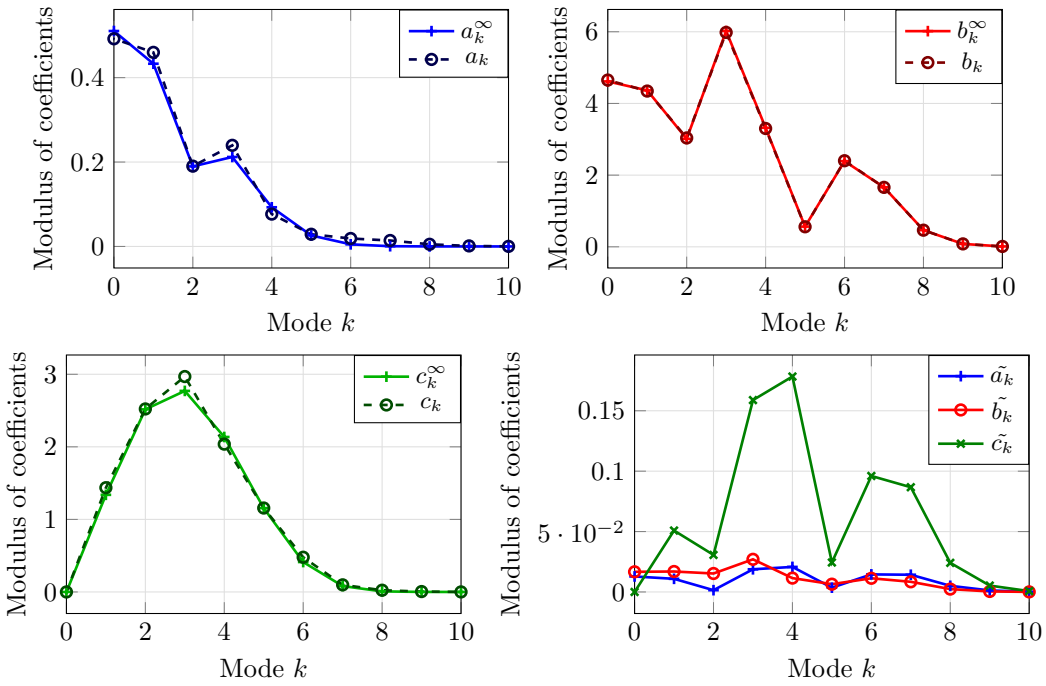

Figure 9: Obstacle scattering of an incident plane B-wave with the type 1 ("Neumann-like") for the boundary condition on $r = \mathfrak{a}$ (3a) at a frequency $f = 1$kHz for a sandstone medium with no viscosity $\eta = 0$ Pa.s^{-1}. The domain is an annulus with the interior radius $\mathfrak{a} = 1$m and the exterior radius $\mathfrak{b} = 10$m. The coefficients with ∞ superscript correspond to the exact outgoing solution. a_k^∞ —, a_k - -, and $\tilde{a}_k$ — are the coefficients corresponding to the potential of the P-wave, b_k^∞ —, b_k - -, and $\tilde{b}_k$ — are the to the potential of the B-wave, and c_k^∞ —, c_k - -, and $\tilde{c}_k$ — to the potential of the S-wave (see equation (47)).

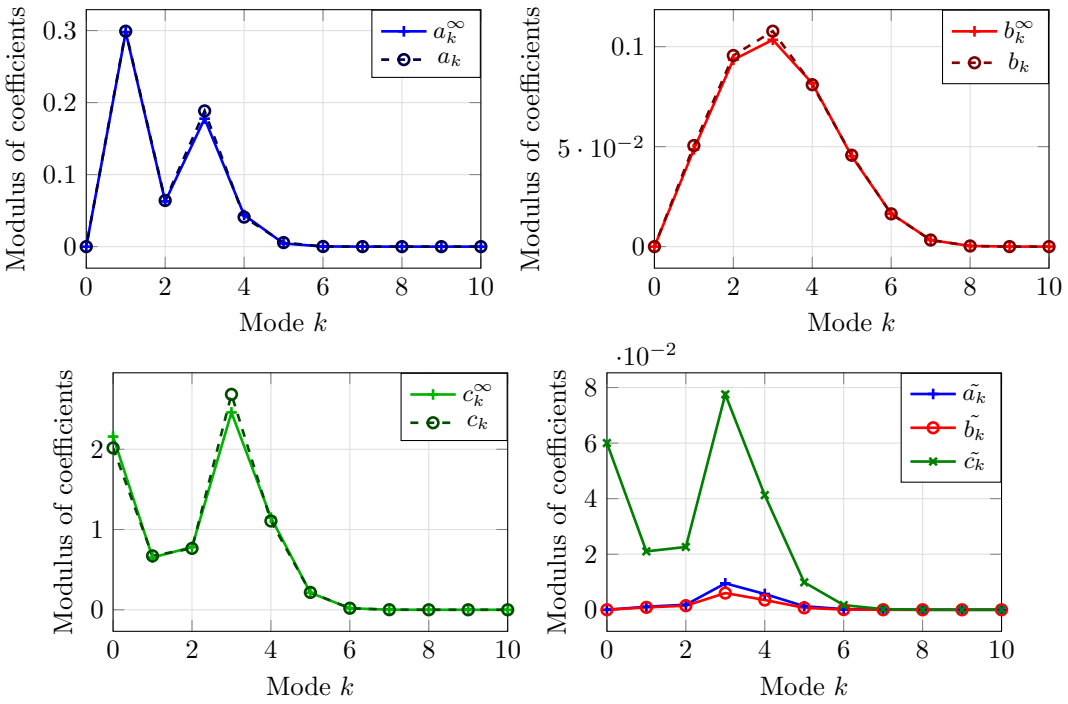

Figure 10: Obstacle scattering of an incident plane S-wave with the type 1 ("Neumann-like") for the boundary condition on $r = \mathfrak{a}$ (3a). at a frequency $f = 1$kHz for a sandstone medium with no viscosity $\eta = 0$ Pa.s^{-1}. The domain is an annulus with the interior radius $\mathfrak{a} = 1$m and the exterior radius $\mathfrak{b} = 10$m. The coefficients with ∞ superscript correspond to the exact outgoing solution. a_k^∞ —+—, a_k - -o- -, and $\tilde{a}_k$ —+— are the coefficients corresponding to the potential of the P-wave, b_k^∞ —+—, b_k - -o- -, and $\tilde{b}_k$ —o— are the to the potential of the B-wave, and c_k^∞ —+—, c_k - -o- -, and $\tilde{c}_k$ —x— to the potential of the S-wave (see equation (47)).

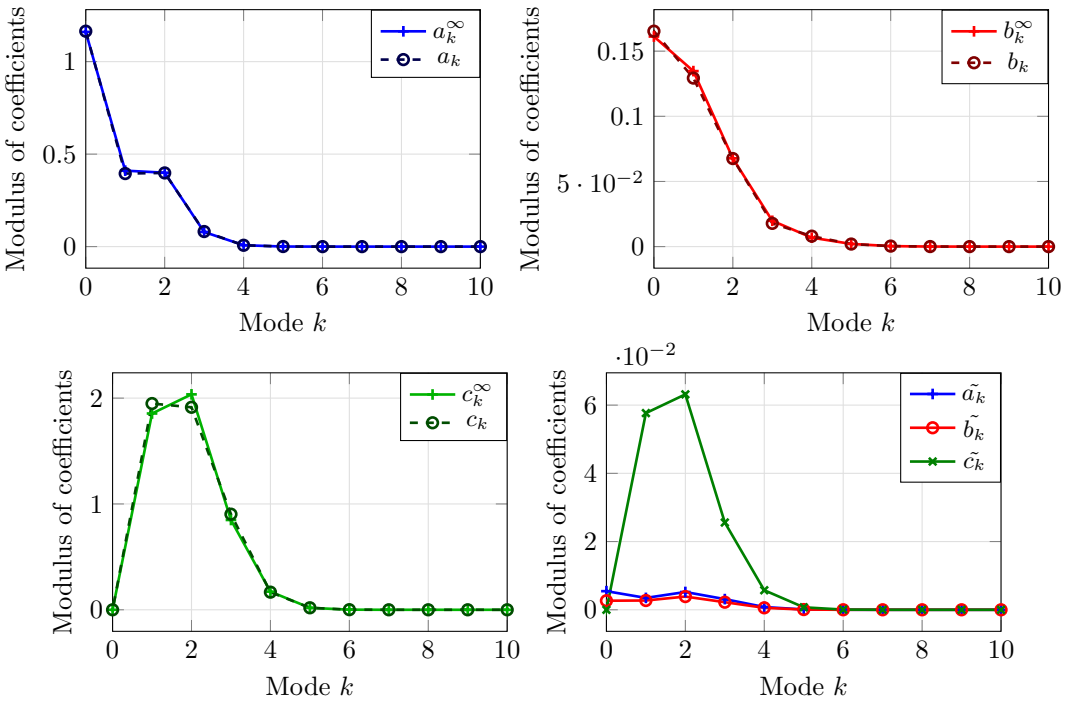

Figure 11: Obstacle scattering of an incident plane P-wave type 3 ("Dirichlet-like") for the boundary condition on $r = \mathfrak{a}$ (3c) at a frequency $f = 1$kHz for a sandstone medium with no viscosity $\eta = 0$ Pa.s^{-1}. The domain is an annulus with the interior radius $\mathfrak{a} = 1$m and the exterior radius $\mathfrak{b} = 10$m. The coefficients with ∞ superscript correspond to the exact outgoing solution. a_k^∞ —+—, a_k - -o- -, and $\tilde{a}_k$ —+— are the coefficients corresponding to the potential of the P-wave, b_k^∞ —+—, b_k - -o- -, and $\tilde{b}_k$ —o— are the to the potential of the B-wave, and c_k^∞ —+—, c_k - -o- -, and $\tilde{c}_k$ —x— to the potential of the S-wave (see equation (47)).

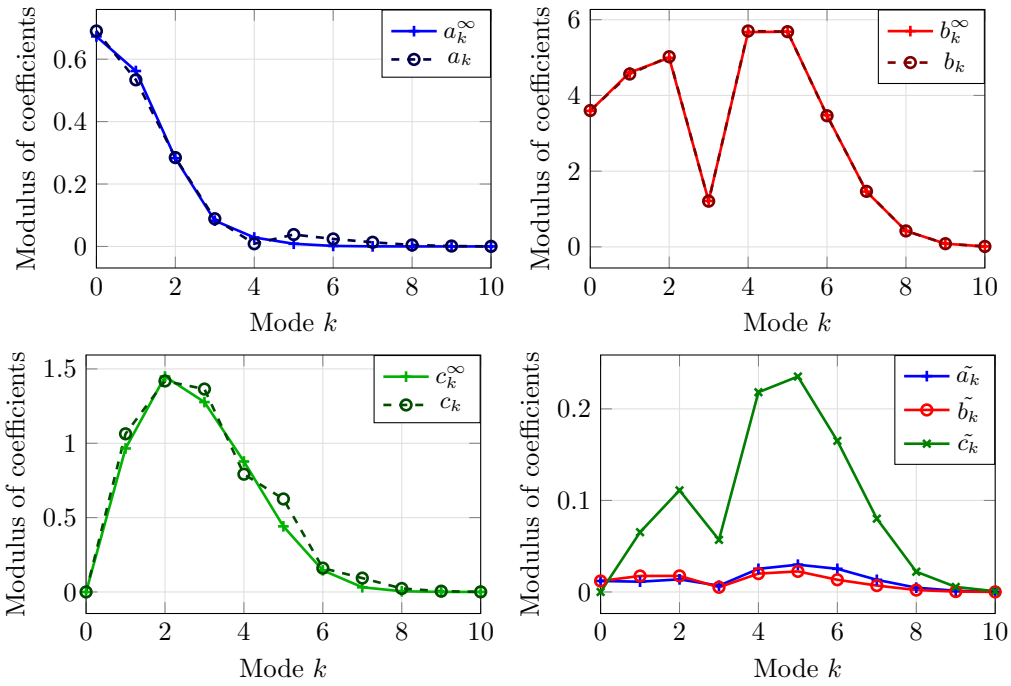

Figure 12: Obstacle scattering of an incident plane B-wave with the type 3 ("Dirichlet-like") for the boundary condition on $r = \mathfrak{a}$ (3c) at a frequency $f = 1$kHz for a sandstone medium with no viscosity $\eta = 0$ Pa.s^{-1}. The domain is an annulus with the interior radius $\mathfrak{a} = 1$m and the exterior radius $\mathfrak{b} = 10$m. The coefficients with ∞ superscript correspond to the exact outgoing solution. a_k^∞ —+—, a_k - -o- -, and $\tilde{a}_k$ —+— are the coefficients corresponding to the potential of the P-wave, b_k^∞ —+—, b_k - -o- -, and $\tilde{b}_k$ —o— are the to the potential of the B-wave, and c_k^∞ —+—, c_k - -o- -, and $\tilde{c}_k$ —×— to the potential of the S-wave (see equation (47)).

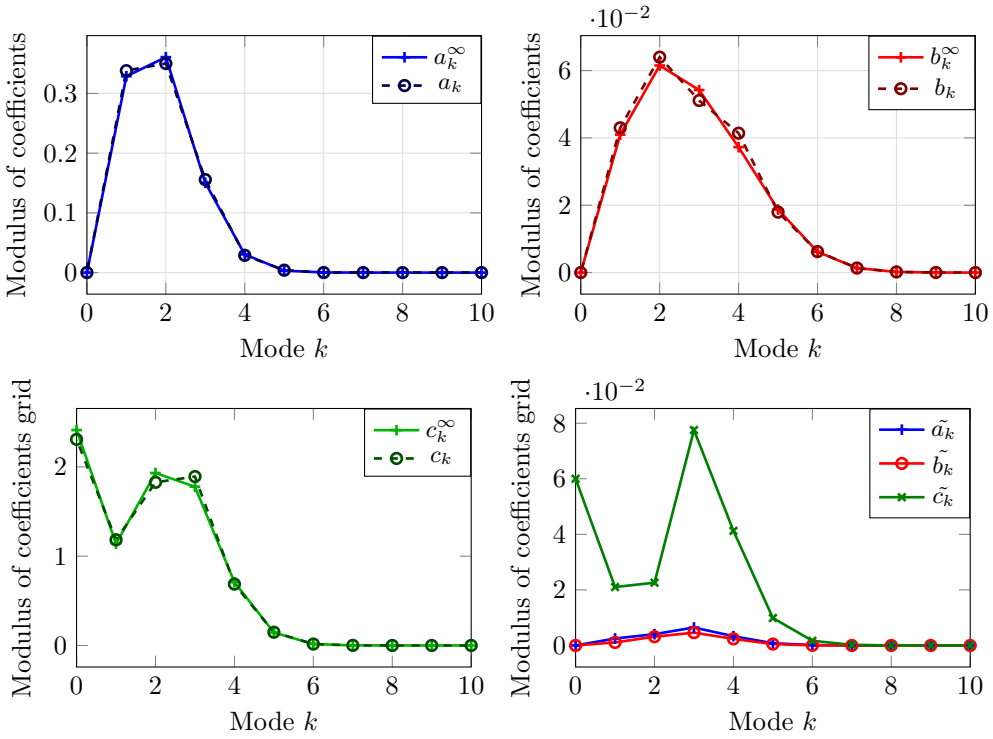

Figure 13: Obstacle scattering of an incident plane S-wave with the type 3 ("Dirichlet-like") for the boundary condition on $r = \mathfrak{a}$ (3c) at a frequency $f = 1$kHz for a sandstone medium with no viscosity $\eta = 0$ Pa.s^{-1}. The domain is an annulus with the interior radius $\mathfrak{a} = 1$m and the exterior radius $\mathfrak{b} = 10$m. The coefficients with ∞ superscript correspond to the exact outgoing solution. a_k^∞ —, a_k - -, and $\tilde{a}_k$ — are the coefficients corresponding to the potential of the P-wave, b_k^∞ —, b_k - -, and $\tilde{b}_k$ — are the to the potential of the B-wave, and c_k^∞ —, c_k - -, and $\tilde{c}_k$ — to the potential of the S-wave (see equation (47)).

5.2 Potential decomposition

To illustrate better the effect of the ABC on each of the type of waves, we will use the natural decomposition in (18). We recall that this equation gives a complete description of the components of the solution $\mathfrak{U}$ in terms of the potentials χ_{P}, χ_{B}, χ_{S}. In this section, we will focus on the displacement component $\mathbf{u}$ for type of boundary 1 ("Neumann-like") on $r = \mathfrak{a}$. The wave decomposition for $\mathbf{u}$ of $\mathfrak{U}^{\text{abc-T1}}$ is given by

$$\begin{aligned}
&\mathbf{u}^{\text{abc-T1}} = \mathbf{u}^{\chi_{\mathrm{P}}^{\text{abc-T1}}} + \mathbf{u}^{\chi_{\mathrm{P}}^{\text{abc-T1}}} + \mathbf{u}^{\chi_{\mathrm{P}}^{\text{abc-T1}}}, \\
&\mathbf{u}^{\chi_{\mathrm{P}}^{\text{abc-T1}}} = -\frac{\mathrm{i}}{\omega \mathsf{s}_{\mathrm{P}}^2} \nabla \chi_{\mathrm{P}}^{\text{abc-T1}}, \qquad \mathbf{u}^{\chi_{\mathrm{B}}^{\text{abc-T1}}} = -\frac{\mathrm{i}}{\omega \mathsf{s}_{\mathrm{B}}^2} \nabla \chi_{\mathrm{B}}^{\text{abc-T1}}, \qquad \mathbf{u}^{\chi_{\mathrm{S}}^{\text{abc-T1}}} = \frac{\mathrm{i}}{\omega \mathsf{s}_{\mathrm{S}}^2} \mathbf{curl}\, \chi_{\mathrm{S}}^{\text{abc-T1}}.
\end{aligned} \tag{54}$$

Recall that these potentials are represented by the coefficients $(a_k, b_k, c_k, \tilde{a}_k, \tilde{b}_k, \tilde{c}_k)$, cf.(47), (48), (49). We will also compare with the decomposition of $\mathbf{u}^{\infty}$ coming from $\mathfrak{U}^{\infty-\mathrm{T1}}$

$$\begin{aligned}
&\mathbf{u}^{\infty-\mathrm{T1}} = \mathbf{u}^{\chi_{\mathrm{P}}^{\infty-\mathrm{T1}}} + \mathbf{u}^{\chi_{\mathrm{B}}^{\infty-\mathrm{T1}}} + \mathbf{u}^{\chi_{\mathrm{S}}^{\infty-\mathrm{T1}}}, \\
&\mathbf{u}^{\chi_{\mathrm{P}}^{\infty-\mathrm{T1}}} = -\frac{\mathrm{i}}{\omega \mathsf{s}_{\mathrm{P}}^2} \nabla \chi_{\mathrm{P}}^{\infty-\mathrm{T1}}, \qquad \mathbf{u}^{\chi_{\mathrm{B}}^{\infty-\mathrm{T1}}} = -\frac{\mathrm{i}}{\omega \mathsf{s}_{\mathrm{B}}^2} \nabla \chi_{\mathrm{B}}^{\infty-\mathrm{T1}}, \qquad \mathbf{u}^{\chi_{\mathrm{S}}^{\infty-\mathrm{T1}}} = \frac{\mathrm{i}}{\omega \mathsf{s}_{\mathrm{S}}^2} \mathbf{curl}\, \chi_{\mathrm{S}}^{\infty-\mathrm{T1}}.
\end{aligned} \tag{55}$$

Recall that these potentials are represented by the coefficients $(a_k^{\infty}, b_k^{\infty}, c_k^{\infty})$, cf. (44), (45), (46).

In Fig. 14, we present the decomposition of the solid velocity in the three potentials.

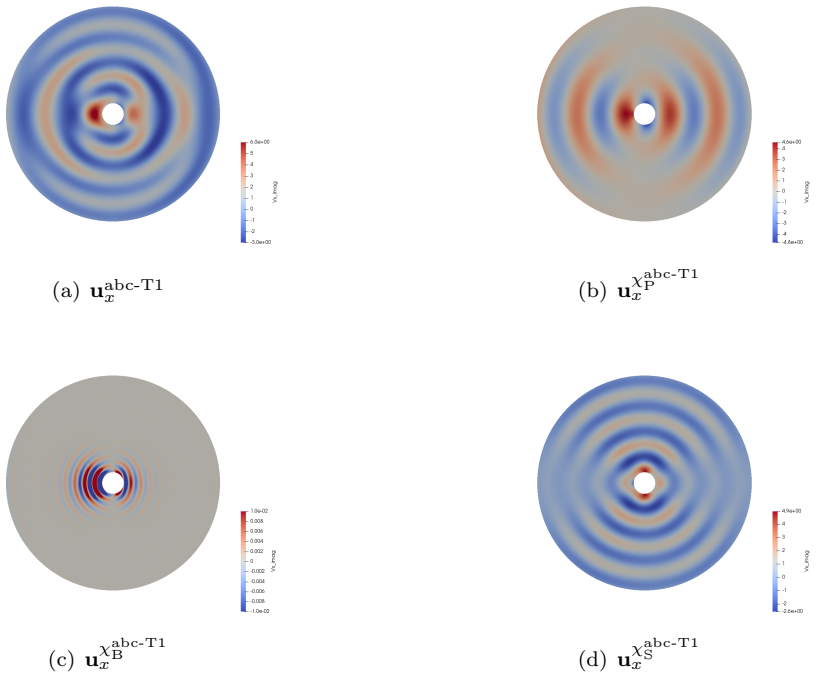

(a) $\mathbf{u}_x^{\text{abc-T1}}$ (b) $\mathbf{u}_x^{\chi_{\mathrm{P}}^{\text{abc-T1}}}$

(c) $\mathbf{u}_x^{\chi_{\mathrm{B}}^{\text{abc-T1}}}$ (d) $\mathbf{u}_x^{\chi_{\mathrm{S}}^{\text{abc-T1}}}$

Figure 14: Truncated solution: Decomposition of $\mathbf{u}$ (10^3 m.s^{-1}) in the case of the scattering of a P-wave by an impenetrable obstacle with boundary condition of type 1 ("Neumann-like") on $r = \mathfrak{a}$ cf. (3a) at a frequency $f = 1$kHz for a sandstone medium with viscosity $\eta = 10^{-3}$ Pa.s^{-1}. The absorbing boundary condition is set at $\mathfrak{b} = 10$m.

In Fig. 14, the weak reflections are barely visible. Comparing to the outgoing solution (Fig. 15), we cannot see significant differences. This is also confirmed by Table 2, where the global error is low and the error on the potentials are included between 1 and 3%. We can also observe the effect of the viscosity on the B-wave, (figs. 14(c), 16(c)) where the wave is absorbed and the energy is mainly around the obstacle when there is viscosity. This effect is not clearly seen for the P and S-waves.

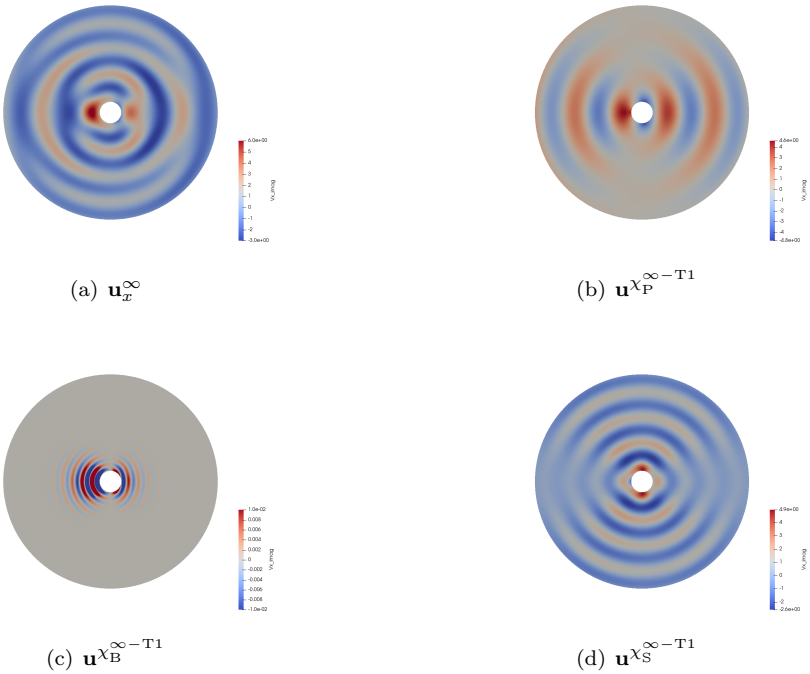

(a) $\mathbf{u}_x^{\infty}$ (b) $\mathbf{u}^{\chi_{\mathrm{P}}^{\infty-\mathrm{T1}}}$

(c) $\mathbf{u}^{\chi_{\mathrm{B}}^{\infty-\mathrm{T1}}}$ (d) $\mathbf{u}^{\chi_{\mathrm{S}}^{\infty-\mathrm{T1}}}$

Figure 15: Outgoing solution: Decomposition of $\mathbf{u}$ (10^3 m.s^{-1}) in the case of the scattering of a P-wave by an impenetrable obstacle with boundary condition of type 1 ("Neumann-like") on $r = \mathfrak{a}$, cf. (3a) at a frequency $f = 1$kHz for a sandstone medium with viscosity $\eta = 10^{-3}$ Pa.s^{-1}.

	$\mathbf{u}$	$\mathbf{u}^{\chi_{\mathrm{P}}}$	$\mathbf{u}^{\chi_{\mathrm{B}}}$	$\mathbf{u}^{\chi_{\mathrm{S}}}$
Relative L2 error (%)	2.30	2.73	1.22	3.17

Table 2: L2 error (%) on $\mathbf{u}_x$ between the analytic solution with absorbing condition and the outgoing solution for the decomposition in potentials.

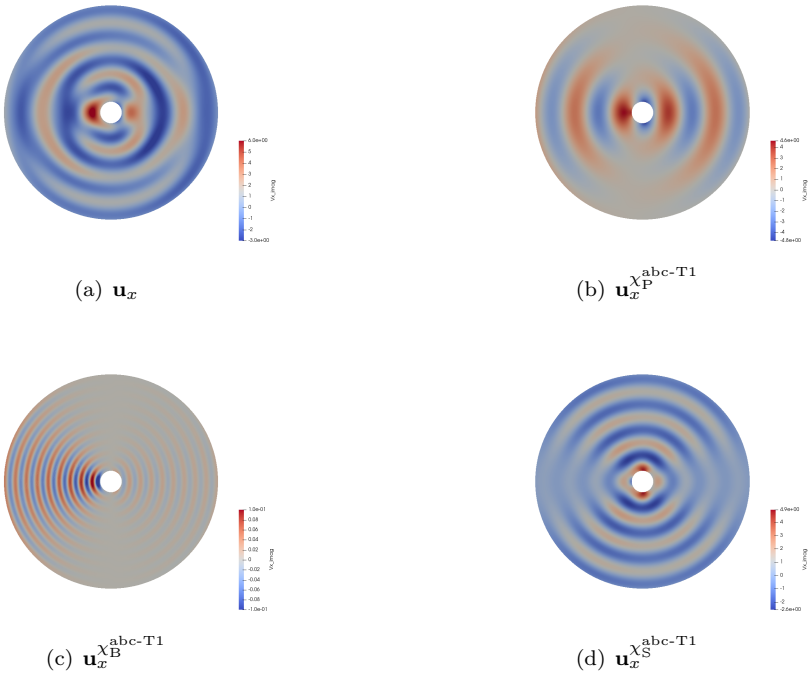

(a) $\mathbf{u}_x$ (b) $\mathbf{u}_x^{\chi_{\mathrm{P}}^{\text{abc-T1}}}$

(c) $\mathbf{u}_x^{\chi_{\mathrm{B}}^{\text{abc-T1}}}$ (d) $\mathbf{u}_x^{\chi_{\mathrm{S}}^{\text{abc-T1}}}$

Figure 16: Truncated solution: Decomposition of $\mathbf{u}$ (10^3 m.s^{-1}) in the case of the scattering of a P-wave by an impenetrable obstacle with boundary condition of type 1 ("Neumann-like") on $r = \mathfrak{a}$ cf. (3a) at a frequency $f = 1$kHz for a sandstone medium with no viscosity ($\eta = 0$ Pa.s^{-1}). The absorbing boundary condition is set at $\mathfrak{b} = 10$m.

5.3 Effect of the size of the truncated domain

We have observed previously that the absorbing boundary condition has good performance for $\mathfrak{b} = 10$m. In this section, we want to investigate the errors of the condition when the size of the truncated domain varies. Fig. 17 presents the results of the analytical solution for several sizes of exterior radius. The L2 error and the errors on the coefficients (e_{coeff}, e_{scatt}) defined in equations (52) and (53), for incident waves P,B,S, are reported in Fig. 18 to 20. As expected, we observe that when the size of the truncated domain decreases, the error grows. Note that all the components of the variables have the same behavior. The presence of viscosity seems to lower the errors. This will be confirmed by the results of section 5.4. In most cases of our tests, the L2 error is lower than 5% from $\mathfrak{b} = 10$m. We observe two cases where the error remains high (Fig. 18) for a B incident wave with no viscosity and for types of boundary condition 1 ("Neumann-like") and 3 ("Dirichlet-like"). This confirms the results from Fig. 9 and 12 where the values of $\tilde{c}_k$ is high compared to the other coefficients. This shows that the ABC depends also on the kind of incident wave.

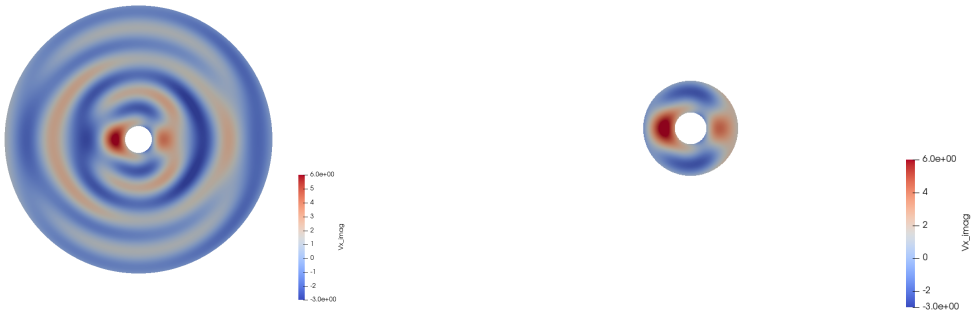

(a) Truncated solution with $\mathfrak{b} = 10$m

(b) Truncated solution with $\mathfrak{b} = 3$m

Figure 17: Truncated solution: imaginary part of $\mathbf{u}_x$ (10^3 m.s^{-1}) for the scattering of a P-wave by a porous obstacle composed of sandstone with viscosity $\eta = 10^{-3}$ Pa.s^{-1}, $f = 1$kHz and boundary condition of type 1 ("Neumann-like") on $\mathfrak{a}$, for different values of $\mathfrak{b}$.

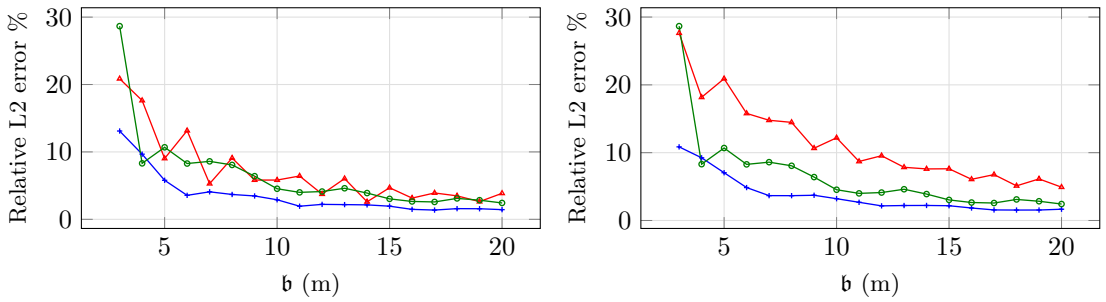

(a) Viscosity $\eta = 0$ Pa.s^{-1}, BC1

(b) Viscosity $\eta = 0$ Pa.s^{-1}, BC3

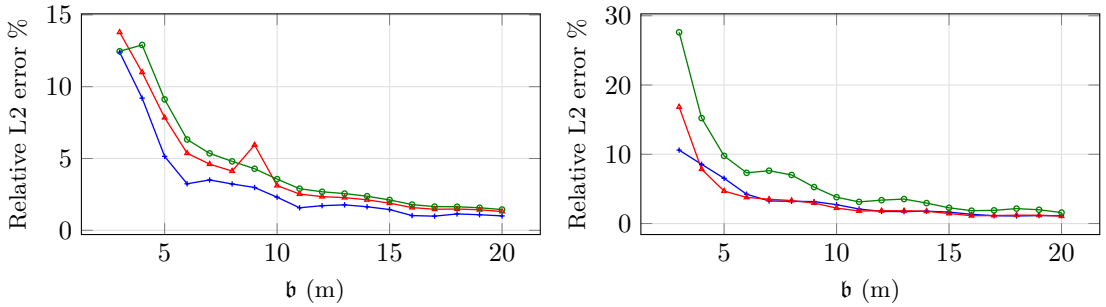

(c) Viscosity $\eta = 10^{-3}$ Pa.s^{-1}, BC1

(d) Viscosity $\eta = 10^{-3}$ Pa.s^{-1}, BC3

Figure 18: Relative L2 error (%) between the solution with absorbing condition and the exact analytic solution function of the size of the radius $\mathfrak{b}$ for $\eta = 0$ Pa.s^{-1} and $\eta = 10^{-3}$ Pa.s^{-1} for $f = 1$kHz for boundary condition of type 1 ("Neumann-like") and 3 ("Dirichlet-like") on the interior radius. The solutions are represented in blue —+— for the incident P-wave, in red —▲— for the incident B-wave and in green —○— for the incident S-wave.

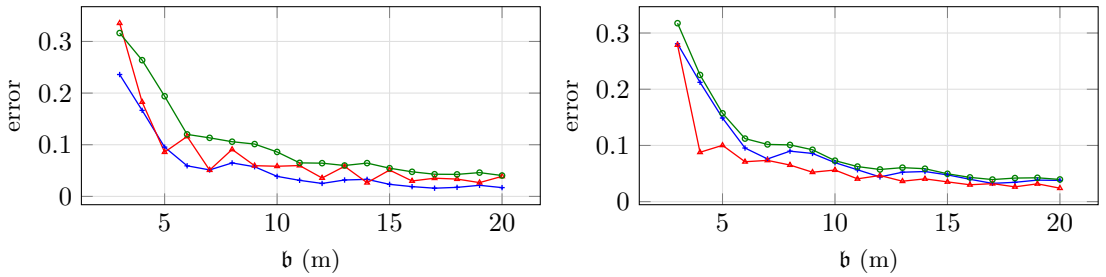

(a) Viscosity $\eta = 0$ Pa.s^{-1}, BC1

(b) Viscosity $\eta = 0$ Pa.s^{-1}, BC3

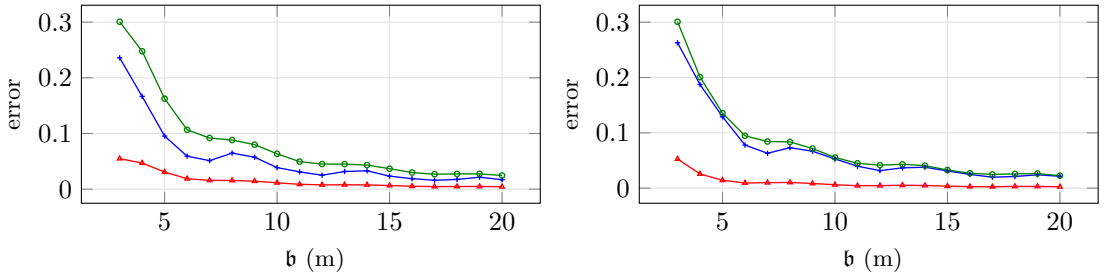

(c) Viscosity $\eta = 10^{-3}$ Pa.s^{-1}, BC1

(d) Viscosity $\eta = 10^{-3}$ Pa.s^{-1}, BC3

Figure 19: Error e_{coeff} function of the size of the radius $\mathfrak{b}$ for $\eta = 0$ Pa.s^{-1} and $\eta = 10^{-3}$ Pa.s^{-1} for $f = 1$kHz for boundary condition of type 1 ("Neumann-like") and 3 ("Dirichlet-like") on the interior radius. The solutions are represented in blue —+— for the incident P-wave, in red —▲— for the incident B-wave and in green —○— for the incident S-wave.

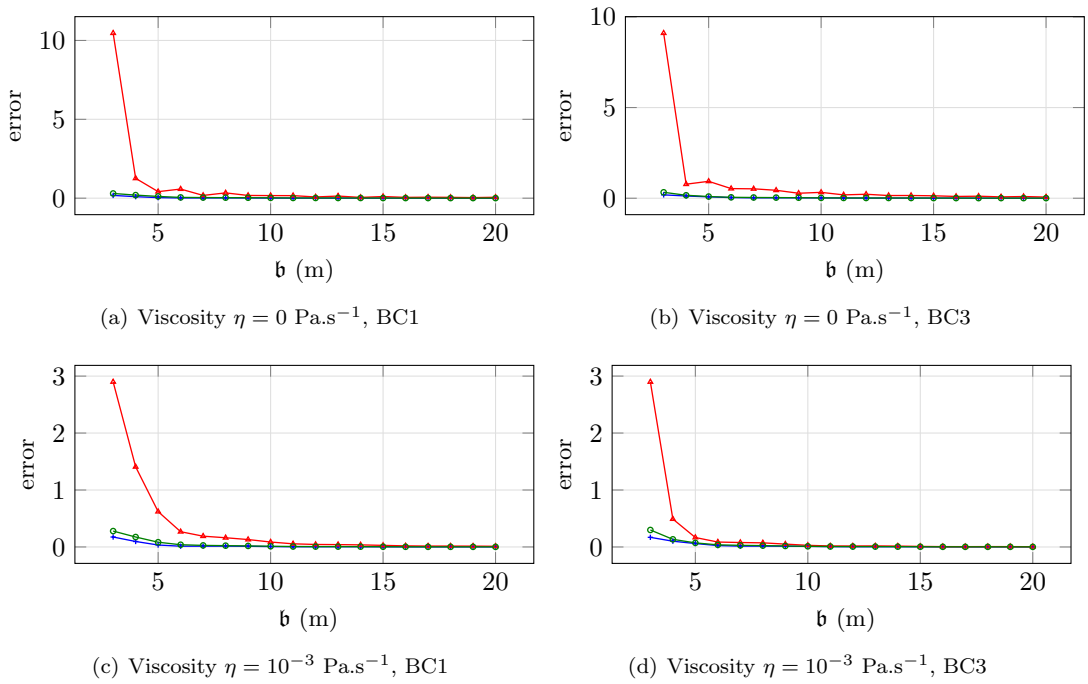

(a) Viscosity $\eta = 0$ Pa.s^{-1}, BC1

(b) Viscosity $\eta = 0$ Pa.s^{-1}, BC3

(c) Viscosity $\eta = 10^{-3}$ Pa.s^{-1}, BC1

(d) Viscosity $\eta = 10^{-3}$ Pa.s^{-1}, BC3

Figure 20: Error e_{scatt} function of the size of the radius $\mathfrak{b}$ for $\eta = 0$ Pa.s^{-1} and $\eta = 10^{-3}$ Pa.s^{-1} for $f = 1$kHz for boundary condition of type 1 ("Neumann-like") and 3 ("Dirichlet-like") on the interior radius. The solutions are represented in blue —+— for the incident P-wave, in red —▲— for the incident B-wave and in green —○— for the incident S-wave.

For the tests in the following sections, we set $\mathfrak{b} = 10$m, in order to keep the same domain and observe the influence of other parameters. We have seen in the previous figures that this value is sufficient to limit the reflections.

5.4 Effect of the viscosity

For the domain described in figure 1, we consider a medium composed of sandstone (*cf.* Table 1) and vary the value of the viscosity in the material. We compare the analytical solution with the exact outgoing solution for the scattering of the three kinds of plane waves at $f = 1$kHz. The truncated solutions is presented in Fig. 21 for the scattering of a B wave for two values of viscosity. We see that when there is viscosity in the material, the wave is absorbed, and the majority of the energy is around the obstacle. As there is less signal near the artificial boundary, we can expect the absorbing condition to be more efficient. The presence of the viscosity impacts mainly the B-wave, as we already observed in Fig. 14. In Fig. 22, we show the L2 error between the solution with absorbing condition and the exact analytic solution for the scattering of the three plane waves (P,B,S) for a fixed frequency. We observe that the errors decrease when the viscosity grows, as expected. Moreover, the error is slightly greater for boundary condition of type 3. As mentioned previously, the presence of viscosity has a greater impact on the B-wave than on the other waves, however, as seen in Fig. 22, the global error decreases, this means that the viscosity causes also absorption on the P and S-waves.

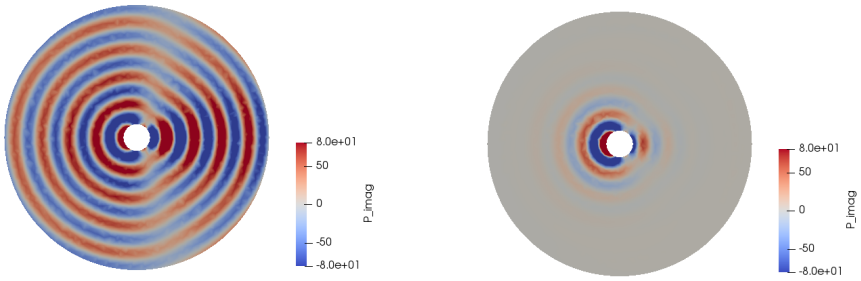

(a) $\eta = 0$Pa.s (b) $\eta = 1.10^{-3}$Pa.s

Figure 21: Imaginary part of the pressure p (MPa) of the reflected wave of the scattering by a B plane wave for type of boundary condition 3 ("Dirichlet-like") on the interior radius (*cf.* (3c)) with absorbing boundary condition on $\mathfrak{b} = 10$m for a porous medium composed of sandstone with two different values of viscosity and with $f = 500$ Hz.

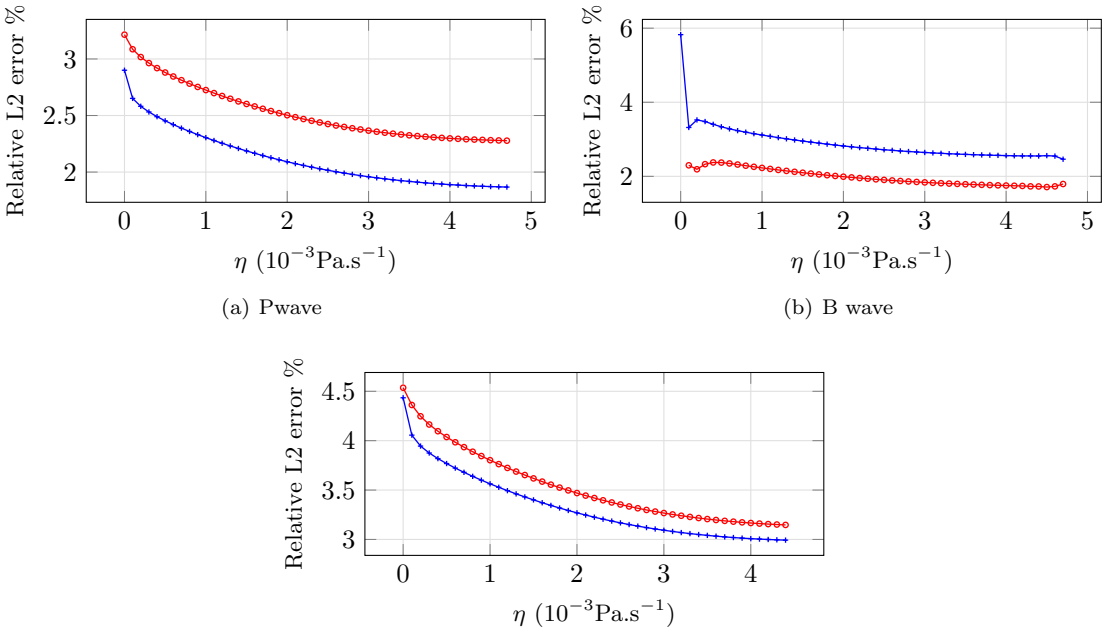

(a) Pwave

(b) B wave

(c) S wave

Figure 22: Relative L2 error (%) between the solution with absorbing condition and the exact analytic solution with $f = 1$kHz function of the viscosity of the medium for the scattering of a plane wave for type of boundary condition 1 ("Neumann-like" eq. 3a) and 3 ("Dirichlet-like" eq. 3c) on $\mathfrak{a}$, respectively represented in blue —+— and in red —○—. The results are given for $\mathfrak{a} = 1$m and $\mathfrak{b} = 10$m.

5.5 Effect of the frequency

In this section, we study the influence of the frequency on the performance of the ABC. The results for the scattering of a P-wave are presented in figure 23 for two different frequencies. When the frequency is low, we observe the truncated solution does not approach the outgoing solution, particularly around the obstacle where the energy explodes. In Fig. 24, we show the L2 error between the solution with absorbing condition and the exact analytic solution for a range of frequency. We display the results for two values of viscosity $\eta = 0$Pa.s^{-1} and $\eta = 10^{-3}$Pa.s^{-1}, and for the boundary condition of type 1 ("Neumann-like") and 3 ("Dirichlet-like"). When ω increases, the ABC performs better. In the case of incident B-wave with no viscosity, we observe some oscillations on the errors that are no longer present when the material is viscous. Moreover, for the boundary condition of type 3 ("Dirichlet-like"), the error is around 10%.

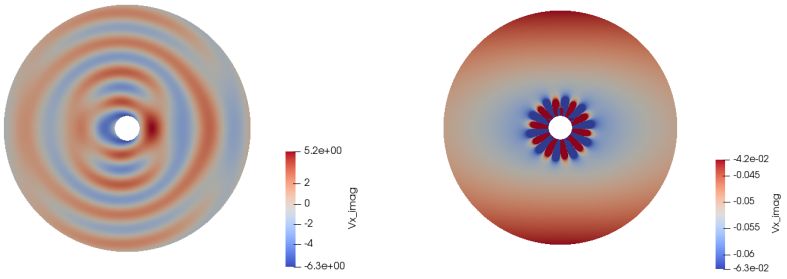

(a) $f = 1$kHz

(b) $f = 0.1$kHz

Figure 23: Scattering of a P plane wave: Imaginary part of the solid velocity $\mathbf{u}_x$ (10^3 m.s^{-1}) of truncated solution for a porous medium composed of inviscid sandstone for type of boundary condition 3 ("Neumann-like") on the interior radius (*cf.* (3c)), with $f = 1$kHz and $f = 0.1$ kHz.

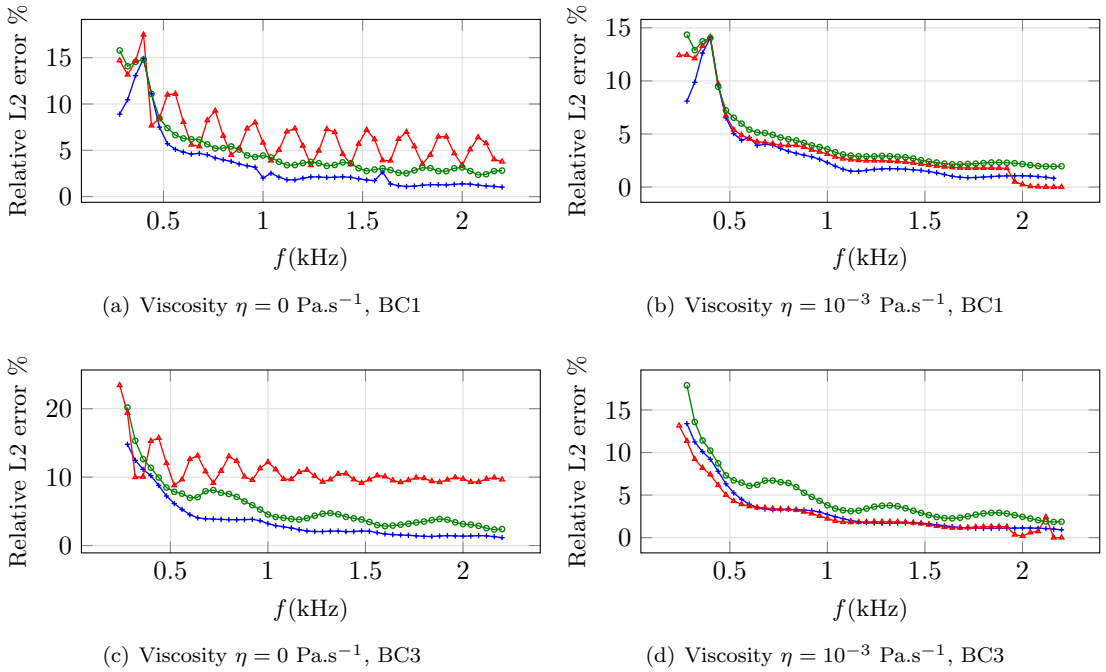

(a) Viscosity $\eta = 0$ Pa.s^{-1}, BC1

(b) Viscosity $\eta = 10^{-3}$ Pa.s^{-1}, BC1

(c) Viscosity $\eta = 0$ Pa.s^{-1}, BC3

(d) Viscosity $\eta = 10^{-3}$ Pa.s^{-1}, BC3

Figure 24: Relative L2 error (%) between the solution with absorbing condition and the exact analytic solution function of the pulsation ω in sandstone for the scattering of a plane wave for boundary condition of type 1 ("Neumann-like" equation (3a)), and type 3 ("Dirichlet-like" equation (3c)) on $\mathfrak{a}$. The results are given for $\mathfrak{a} = 1$m and $\mathfrak{b} = 10$m for $\eta = 0$ Pa.s^{-1} and $\eta = 10^{-3}$ Pa.s^{-1}. The incident P-wave is represented in blue —+—, the incident B-wave in red —▲— and the incident S-wave in green —○—.

Observations of the tests In the following, we summarize the observations for the tests in sections 5.3, 5.4, 5.5:

- The absorbing condition is efficient for the scattering of the three types of plane waves (P,B,S) and the different types of boundary condition on the scattered obstacle. The percentage of the L2 error is of the same order as for first-order ABC in acoustic or elasticity.

- As expected, we have observed that the error decreases when we consider more wavelengths, either by using a greater frequency or by setting the artificial boundaries further from the obstacle. This is also the case in acoustic or elasticity. This is however limited by the space discretization of the domain.

- The higher the viscosity is, the more the ABC is efficient. This result can lead to another idea to construct ABC: raising artificially the viscosity of the media near the absorbing boundary in order to absorb the incident waves. We do not discuss this idea in the paper, it will be the topic of a future work.

6 HDG method using Absorbing Boundary conditions

This section draws on the HDG discretization for poroelastic equations presented in report [4], on which we apply the low-order absorbing boundary condition derivate in section 3. We consider a porous domain Ω with the boundary $\Gamma = \Gamma_l \cup \Gamma_{\text{abs}}$. $(\mathbf{u}, \mathbf{w}, \boldsymbol{\tau}, \mathrm{p})$ solves the poroelastic equations (2) on Ω. On Γ_l, we impose one of the four conditions from section 2.3. From section 3, equation (38), we impose on the absorbing boundary Γ_{abs}:

$$\begin{cases} \boldsymbol{\tau}\,\boldsymbol{n} + \big(\mathbf{X}_1(\mathbf{u}\cdot\boldsymbol{n}) + \mathbf{X}_2(\mathbf{w}\cdot\boldsymbol{n})\big)\,\boldsymbol{n} + \mathbf{X}_3(\mathbf{u}\cdot\mathbf{t})\,\mathbf{t} = 0\,, \\ \mathrm{p} + \mathbf{X}_4(\mathbf{u}\cdot\boldsymbol{n}) + \mathbf{X}_5(\mathbf{w}\cdot\boldsymbol{n}) \;= 0\,. \end{cases} \tag{56}$$

On a domain $\mathcal{D}$, we define the following function spaces,

$$\begin{aligned}
&L^2(\mathcal{D}),\ \text{the space of square-integrable functions on the domain } \mathcal{D}\,,\\
&V^p(\mathcal{D}),\ \text{the set of polynomials of degree at most } p \text{ on } \mathcal{D}\,,\\
&\boldsymbol{V}^p(\mathcal{D}) = (V^p(\mathcal{D}))^2\,,\\
&\boldsymbol{\Sigma}^p(\mathcal{D}) = \{\boldsymbol{\tau} \in (V^p(\mathcal{D}))^4 \,|\, \tau_{yx} = \tau_{xy}\}\,.
\end{aligned} \tag{57}$$

We consider a triangulation $\mathcal{T}_h$ of the domain Ω of dimension 2. K denotes an element of the mesh, which in 2D is a triangle. We denote by F an edge of the element K, and $\boldsymbol{n}$ the unit normal vector to F. We define the following spaces associated to triangulation $\mathcal{T}_h$:

$$\begin{aligned}
V_h^p &= \{v \in L^2(\Omega) : v|_K \in V^p(K)\,,\ \forall K \in \mathcal{T}_h\}\,,\\
\boldsymbol{V}_h^p &= \{\boldsymbol{v} \in (L^2(\Omega))^2 : \boldsymbol{v}|_K \in V^p(K)\,,\ \forall K \in \mathcal{T}_h\}\,,\\
\boldsymbol{\Sigma}_h^p &= \{\boldsymbol{\tau} \in L^2(\Omega)^4 : \boldsymbol{\tau}|_K \in \boldsymbol{\Sigma}^p(K)\,,\ \forall K \in \mathcal{T}_h\}\,,\\
M_h &= \{\eta \in L^2(\mathcal{F}_h) : \eta|_F \in V^p(F),\ ,\ \forall K \in \mathcal{F}_h\}\,,\\
\boldsymbol{M}_h &= \{\xi \in (L^2(\mathcal{F}_h))^2 : \xi|_F \in (V^p(F))^2\,,\ \forall K \in \mathcal{F}_h\}\,.
\end{aligned} \tag{58}$$

The local unknowns $(\mathbf{u}_h,\, \mathbf{w}_h,\, \boldsymbol{\tau}_h,\, \mathrm{p}_h) \in (\boldsymbol{V}_h^p \times \boldsymbol{V}_h^p \times \boldsymbol{\Sigma}_h^p \times V_h^p)$ solve the poroelastic equations (2) on $\mathcal{T}_h$. We introduce two unknowns $\boldsymbol{\lambda}_1 \in \boldsymbol{M}_h,\ \lambda_2 \in M_h$ to replace the numerical traces $\hat{\mathbf{u}}_h$ and $\hat{\mathrm{p}}_h$. The other two traces $(\hat{\boldsymbol{\tau}}_h, \hat{\mathbf{w}}_h)$ are expressed in terms of the Lagrange multipliers $\boldsymbol{\lambda}_1,\, \lambda_2$. The numerical traces of $(\mathbf{u}_h,\, \mathbf{w}_h,\, \boldsymbol{\tau}_h,\, \mathrm{p}_h)$ on an edge are defined as:

$$\begin{aligned}
\hat{\mathbf{u}}_h &= \boldsymbol{\lambda}_1\,,\\
\hat{\boldsymbol{\tau}}_h &= \boldsymbol{\tau}_h - \boldsymbol{S}_1(\mathbf{u}_h - \boldsymbol{\lambda}_1) \otimes \boldsymbol{n} - (\mathrm{p}_h - \lambda_2)\boldsymbol{S}_3\,,\\
\hat{\mathbf{w}}_h &= \mathbf{w}_h - (\mathrm{p}_h - \lambda_2)\boldsymbol{S}_2\boldsymbol{n} - \boldsymbol{S}_4(\mathbf{u}_h - \boldsymbol{\lambda}_1)\,,\\
\hat{\mathrm{p}}_h &= \lambda_2\,,
\end{aligned} \tag{59}$$

with $\boldsymbol{S}_1$, $\boldsymbol{S}_3$, $\boldsymbol{S}_2$, $\boldsymbol{S}_4$ the stabilization matrices, that we consider to be of the form $\boldsymbol{S}_i = \gamma_i\, \mathbf{Id}$.

The HDG discretization of the poroelastic equations (2), given in details in [4], is composed of two systems of equations, the local problem on each element, and the transmission conditions which connects the elements using the numerical fluxes. They were given as:

$$\mathbb{A}^K\, \underline{W}^K \,+\, \mathbb{B}^K\, \underline{\Lambda}^K \,=\, \mathbb{C}^K_{\text{source}}\,, \qquad \text{Local problem,} \tag{60a}$$

$$\mathbb{P}^K\, \underline{W}^K \,+\, \mathbb{T}^K\, \underline{\Lambda}^K + \mathcal{R}^K \,= 0\,, \qquad \text{Transmission conditions,} \tag{60b}$$

with

$$\underline{W}^K = (\underline{\mathrm{u}}_x^K,\, \underline{\mathrm{u}}_y^K,\, \underline{\mathrm{w}}_x^K,\, \underline{\mathrm{w}}_y^K,\, \underline{\tau}_{xx}^K,\, \underline{\tau}_{yy}^K,\, \underline{\tau}_{xy}^K,\, \underline{\mathrm{p}}^K)^T\,, \tag{61a}$$

and

$$\underline{\Lambda}^K = (\underline{\lambda}_{1x}^{\beta(K,1)}, \underline{\lambda}_{1x}^{\beta(K,2)}, \underline{\lambda}_{1x}^{\beta(K,3)}, \underline{\lambda}_{1y}^{\beta(K,1)} \underline{\lambda}_{1y}^{\beta(K,2)}, \underline{\lambda}_{1y}^{\beta(K,3)}, \underline{\lambda}_{2}^{\beta(K,1)}, \underline{\lambda}_{2}^{\beta(K,2)}, \underline{\lambda}_{2}^{\beta(K,3)})^T\,, \tag{61b}$$

with $\beta(K, f)$ the global index of the f-th face of the element K, and where the local solutions and the local Lagrange unknowns are decomposed as:

$$\mathrm{u}_l^K = \sum_{j=1}^{d_i^K} \underline{\mathrm{u}}_{l,j}^K\, \varphi_j^K\,,\ \mathrm{w}_l^K = \sum_{j=1}^{d_i^K} \underline{\mathrm{w}}_{l,j}^K\, \varphi_j^K\,,\ \tau_{kl}^K = \sum_{j=1}^{d_i^K} \underline{\tau}_{kl,j}^K\, \varphi_j^K\,,\ \mathrm{p}^K = \sum_{j=1}^{d_i^K} \underline{\mathrm{p}}^K\, \varphi_j^K\,,\ \text{with } k = x, y \text{ and } l = x, y\,, \tag{62a}$$

and

$$\lambda_{1l}^F = \sum_{j=1}^{d_i^F} \underline{\lambda_{1l}}_j^F \psi_j^F\,, \qquad \lambda_2^F = \sum_{j=1}^{d_i^F} \underline{\lambda_2}_j^F \psi_j^F \ \text{ with } l = x, y\,. \tag{62b}$$

Here, d_i^K denotes the number of degrees of freedom of an element, d_i^F the number of degrees of freedom of an edge, and φ_j^K, ψ_j^F are basis functions of the element K and the edge F respectively. The expressions of $\mathbb{A}^K$, $\mathbb{B}^K$, $\mathbb{C}^K_{\text{source}}$, $\mathbb{P}^K$, $\mathbb{T}^K$, $\mathcal{R}^K$ are given in [4] for a bounded domain. The resolution was also given and is recalled in algorithm 1. Here, the presence of absorbing boundary conditions affect the expression of the transmission conditions, while the local problem is not modified for the elements on the boundaries of the mesh. Hence, we do not detail the discretization of the local problem, and we focus on the expression of the transmission conditions on an absorbing boundary.

On Γ_{abs}, the transmission conditions are replaced by absorbing conditions obtained by integrating equation (56). This gives:

$$\sum_{F\in\mathcal{F}_{\text{abc}}}\int_F (\hat{\boldsymbol{\tau}}_h\,\boldsymbol{n} + (\mathbf{X}_1(\hat{\mathbf{u}}_h\cdot\boldsymbol{n}) + \mathbf{X}_2(\hat{\mathbf{w}}_h\cdot\boldsymbol{n}))\,\boldsymbol{n} + \mathbf{X}_3(\hat{\mathbf{u}}_h\cdot\mathbf{t})\,\mathbf{t})\cdot\eta = 0\,, \tag{63a}$$

$$\sum_{F\in\mathcal{F}_{\text{abc}}}\int_F (\hat{\mathrm{p}}_h + \mathbf{X}_4(\hat{\mathbf{u}}_h\cdot\boldsymbol{n}) + \mathbf{X}_5(\hat{\mathbf{w}}_h\cdot\boldsymbol{n}))\xi = 0\,, \tag{63b}$$

with $(\eta,\,\xi)\in\boldsymbol{M}_h\times M_h$ basis-functions on the faces. Equation (63) is discretized on the plane (x,y). We define the following matrices:

$$\begin{aligned}
\mathbb{F}^F_{ij} &= \int_F \varphi_i^K\psi_j^F\,dS\,, \qquad \mathbb{Q}^F_{kij} = \int_F \varphi_i^K\psi_j^F\,n_k\,dS\,, \qquad \mathbb{L}^F_{klij} = \int_F \varphi_i^K\psi_j^F\,n_k\,n_l\,dS\,,\\
\mathbb{G}^F_{ij} &= \int_F \psi_i^F\psi_j^F\,dS\,, \qquad \mathbb{H}^F_{kij} = \int_F \psi_i^F\psi_j^F\,n_k\,dS\,, \qquad \mathbb{O}^F_{klij} = \int_F \psi_i^F\psi_j^F\,n_k\,n_l\,dS\,.
\end{aligned} \tag{64}$$

with $k = x, y$, and $l = x, y$.

6.1 Discretization of condition (63a)

Starting from equation (63a):

$$\int_F (\hat{\boldsymbol{\tau}}_h\,\boldsymbol{n} + (\mathbf{X}_1(\hat{\mathbf{u}}_h\cdot\boldsymbol{n}) + \mathbf{X}_2(\hat{\mathbf{w}}_h\cdot\boldsymbol{n}))\,\boldsymbol{n} + \mathbf{X}_3(\hat{\mathbf{u}}_h\cdot\mathbf{t})\,\mathbf{t})\cdot\eta = 0\,, \tag{65}$$

and replacing the numerical traces $\hat{\boldsymbol{\tau}}_h$, $\hat{\mathbf{w}}_h$ using equation (59), we obtain

$$\begin{aligned}
&\int_F(\boldsymbol{\tau}_h\,\boldsymbol{n})\cdot\eta - \int_F \boldsymbol{S}_1(\mathbf{u}_h-\boldsymbol{\lambda}_1)\cdot\eta - \int_F(\mathrm{p}_h-\lambda_2)(\boldsymbol{S}_3\,\boldsymbol{n})\cdot\eta\\
&+\int_F\Big((\mathbf{X}_1(\boldsymbol{\lambda}_1\cdot\boldsymbol{n})\boldsymbol{n} + \mathbf{X}_2\Big((\mathbf{w}_h\cdot\boldsymbol{n}) - (\mathrm{p}_h-\lambda_2)(\boldsymbol{S}_2\,\boldsymbol{n})\cdot\boldsymbol{n} - \boldsymbol{S}_4(\mathbf{u}_h-\boldsymbol{\lambda}_1)\cdot\boldsymbol{n}\Big)\boldsymbol{n} + \mathbf{X}_3(\boldsymbol{\lambda}_1\cdot\mathbf{t})\,\mathbf{t}\Big)\cdot\eta = 0\,.
\end{aligned}$$

We replace the test-functions η, ξ by basis functions, and we decompose the unknowns as given in equations (62a) and (62b). The discretization of the equation on (x,y) is written as follows:

$$\begin{aligned}
&\int_F \underline{\tau}^K_{xx}n_x\varphi_j^K\psi_i^{\beta(K,l)}dS + \int_F \underline{\tau}^K_{xy}n_y\varphi_j^K\psi_i^{\beta(K,l)}dS - \int_F \gamma_1\varphi_j^K\,\underline{\mathrm{u}}_x^K\psi_i^{\beta(K,l)}dS + \int_F \gamma_1\psi_j^{\beta(K,l)}\underline{\lambda}_{1x}^{\beta(K,l)}\psi_i^{\beta(K,l)}dS\\
&-\int_F \gamma_3 n_x\underline{\mathrm{p}}^K\varphi_j^K\psi_i^{\beta(K,l)}dS + \int_F \gamma_3 n_x\underline{\lambda}_2^{\beta(K,l)}\psi_j^{\beta(K,l)}\psi_i^{\beta(K,l)}dS + \int_F \mathbf{X}_1\,(\underline{\lambda}_{1x}^{\beta(K,l)}n_x + \underline{\lambda}_{1y}^{\beta(K,l)}n_y)n_x\,\psi_j^{\beta(K,l)}\,\psi_i^{\beta(K,l)}dS\\
&+\int_F \mathbf{X}_2\,\underline{\mathrm{w}}_x^K\,n_x^2\varphi_j^K\,\psi_i^{\beta(K,l)}dS + \int_F \mathbf{X}_2\,\underline{\mathrm{w}}_y^K\,n_xn_y\varphi_j^K\,\psi_i^{\beta(K,l)}dS - \int_F \mathbf{X}_2\,\gamma_2\underline{\mathrm{p}}^K\,(n_x^2+n_y^2)n_x\varphi_j^K\,\psi_i^{\beta(K,l)}dS\\
&+\int_F \mathbf{X}_2\,\gamma_2\underline{\lambda}_2^{\beta(K,l)}\,(n_x^2+n_y^2)n_x\,\psi_j^{\beta(K,l)}\,\psi_i^{\beta(K,l)}dS - \int_F \mathbf{X}_2\,\gamma_4\,(\underline{\mathrm{u}}_x^K n_x + \underline{\mathrm{u}}_y^K n_y)n_x\,\varphi_j^K\,\psi_i^{\beta(K,l)}dS\\
&+\int_F \mathbf{X}_2\,\gamma_4\,(\underline{\lambda}_{1x}^{\beta(K,l)}n_x + \underline{\lambda}_{1y}^{\beta(K,l)}n_y)n_x\,\psi_j^{\beta(K,l)}\,\psi_i^{\beta(K,l)}dS + \int_F \mathbf{X}_3\,(\underline{\lambda}_{1x}^{\beta(K,l)}n_y^2 - \underline{\lambda}_{1y}^{\beta(K,l)}n_xn_y)\psi_j^{\beta(K,l)}\psi_i^{\beta(K,l)} = 0\,,
\end{aligned} \tag{66a}$$

$$\int_F \underline{\tau}_{xy}^K n_x \varphi_j^K \psi_i^{\beta(K,l)} dS + \int_F \underline{\tau}_{yy}^K n_y \varphi_j^K \psi_i^{\beta(K,l)} dS - \int_F \gamma_1 \varphi_j^K \underline{\mathrm{u}}_y^K \psi_i^{\beta(K,l)} dS + \int_F \gamma_1 \varphi_j^K \underline{\lambda}_{1y}^{\beta(K,l)} \psi_i^{\beta(K,l)} dS$$
$$- \int_F \gamma_3 n_y \underline{\mathrm{p}}^K \varphi_j^K \psi_i^{\beta(K,l)} dS + \int_F \gamma_3 n_y \underline{\lambda}_2^K \psi_j^{\beta(K,l)} \psi_i^{\beta(K,l)} dS + \int_F \mathbf{X}_1 \, (\underline{\lambda}_{1x}^{\beta(K,l)} n_x + \underline{\lambda}_{1y}^{\beta(K,l)} n_y) n_y \, \psi_j^{\beta(K,l)} \, \psi_i^{\beta(K,l)} dS$$
$$+ \int_F \mathbf{X}_2 \, \underline{\mathrm{w}}_x^K \, n_x n_y \varphi_j^K \, \psi_i^{\beta(K,l)} dS + \int_F \mathbf{X}_2 \, \underline{\mathrm{w}}_y^K \, n_y^2 \varphi_j^K \, \psi_i^{\beta(K,l)} dS - \int_F \mathbf{X}_2 \, \gamma_2 \underline{\mathrm{p}}^K \, (n_x^2 + n_y^2) n_y \varphi_j^K \, \psi_i^{\beta(K,l)} dS$$
$$+ \int_F \mathbf{X}_2 \, \gamma_2 \underline{\lambda}_2^{\beta(K,l)} \, (n_x^2 + n_y^2) n_y \, \psi_j^{\beta(K,l)} \, \psi_i^{\beta(K,l)} dS - \int_F \mathbf{X}_2 \, \gamma_4 \, (\underline{\mathrm{u}}_x^K n_x + \underline{\mathrm{u}}_y^K n_y) n_y \, \varphi_j^K \, \psi_i^{\beta(K,l)} dS$$
$$+ \int_F \mathbf{X}_2 \, \gamma_4 \, (\underline{\lambda}_{1x}^{\beta(K,l)} n_x + \underline{\lambda}_{1y}^{\beta(K,l)} n_y) n_y \, \psi_j^{\beta(K,l)} \, \psi_i^{\beta(K,l)} dS + \int_F \mathbf{X}_3 \, (-\underline{\lambda}_{1x}^{\beta(K,l)} n_x n_y + \underline{\lambda}_{1y}^{\beta(K,l)} n_x^2) \psi_j^{\beta(K,l)} \psi_i^{\beta(K,l)} = 0 \, . \tag{66b}$$

The two above equations can be written using matrix vector products:

$$(\mathbb{Q}_{xl}^{\beta(K,l)})^T \underline{\tau}_{xx}^K + (\mathbb{Q}_{yl}^{\beta(K,l)})^T \underline{\tau}_{xy}^K - \gamma_1 (\mathbb{F}_l^{\beta(K,l)})^T \underline{\mathrm{u}}_x^K + \gamma_1 \mathbb{G}^{\beta(K,l)} \underline{\lambda}_{1x}^{\beta(K,l)} - \gamma_3 (\mathbb{Q}_{xl}^{\beta(K,l)})^T \underline{\mathrm{p}}^K + \gamma_3 \mathbb{H}_x^{\beta(K,l)} \underline{\lambda}_2^{\beta(K,l)}$$
$$+ \mathbb{O}_{xx}^{\beta(K,l)} \mathbf{X}_1 \, \underline{\lambda}_{1x}^{\beta(K,l)} + \mathbb{O}_{xy}^{\beta(K,l)} \mathbf{X}_1 \underline{\lambda}_{1y}^{\beta(K,l)} + (\mathbb{L}_{xxl}^{\beta(K,l)})^T \mathbf{X}_2 \, \underline{\mathrm{w}}_x^K + (\mathbb{L}_{xyl}^{\beta(K,l)})^T \mathbf{X}_2 \, \underline{\mathrm{w}}_y^K$$
$$- (\mathbb{Q}_{xl}^{\beta(K,l)})^T \mathbf{X}_2 \, \gamma_2 \underline{\mathrm{p}}^K + \mathbb{H}_{xl}^{\beta(K,l)} \mathbf{X}_2 \, \gamma_2 \underline{\lambda}_2^{\beta(K,l)} - (\mathbb{L}_{xxl}^{\beta(K,l)})^T \mathbf{X}_2 \, \gamma_4 \, \underline{\mathrm{u}}_x^K - (\mathbb{L}_{xyl}^{\beta(K,l)})^T \mathbf{X}_2 \, \gamma_4^{\beta(K,l)} \underline{\mathrm{u}}_y^K$$
$$+ \mathbb{O}_{xx}^{\beta(K,l)} \mathbf{X}_2 \, \underline{\lambda}_{1x}^{\beta(K,l)} + \mathbb{O}_{xy}^{\beta(K,l)} \mathbf{X}_2 \underline{\lambda}_{1y}^{\beta(K,l)} + \mathbb{O}_{yy}^{\beta(K,l)} \mathbf{X}_3 \, \underline{\lambda}_{1x}^{\beta(K,l)} - \mathbb{O}_{xy}^{\beta(K,l)} \mathbf{X}_3 \, \underline{\lambda}_{1y}^{\beta(K,l)} = 0 \, , \tag{67a}$$

$$(\mathbb{Q}_{xl}^{\beta(K,l)})^T \underline{\tau}_{xy}^K + (\mathbb{Q}_{yl}^{\beta(K,l)})^T \underline{\tau}_{yy}^K - \gamma_1 (\mathbb{F}_l^{\beta(K,l)})^T \underline{\mathrm{u}}_y^K + \gamma_1 \mathbb{G}^{\beta(K,l)} \underline{\lambda}_{1y}^{\beta(K,l)} - \gamma_3 (\mathbb{Q}_{yl}^{\beta(K,l)})^T \underline{\mathrm{p}}^K + \gamma_3 \mathbb{H}_y^{\beta(K,l)} \underline{\lambda}_2^{\beta(K,l)}$$
$$+ \mathbb{O}_{xy}^{\beta(K,l)} \mathbf{X}_1 \, \underline{\lambda}_{1x}^{\beta(K,l)} + \mathbb{O}_{yy}^{\beta(K,l)} \mathbf{X}_1 \underline{\lambda}_{1y}^{\beta(K,l)} + (\mathbb{L}_{xyl}^{\beta(K,l)})^T \mathbf{X}_2 \, \underline{\mathrm{w}}_x^K + (\mathbb{L}_{yyl}^{\beta(K,l)})^T \mathbf{X}_2 \, \underline{\mathrm{w}}_y^K$$
$$- (\mathbb{Q}_{yl}^{\beta(K,l)})^T \mathbf{X}_2 \, \gamma_2 \underline{\mathrm{p}}^K + \mathbb{H}_{yl}^K \mathbf{X}_2 \, \gamma_2 \underline{\lambda}_2^{\beta(K,l)} - (\mathbb{L}_{xyl}^{\beta(K,l)})^T \mathbf{X}_2 \, \gamma_4 \, \underline{\mathrm{u}}_x^K - (\mathbb{L}_{yyl}^{\beta(K,l)})^T \mathbf{X}_2 \, \gamma_4 \underline{\mathrm{u}}_y^K$$
$$+ \mathbb{O}_{xy}^{\beta(K,l)} \mathbf{X}_2 \, \underline{\lambda}_{1x}^{\beta(K,l)} + \mathbb{O}_{yy}^{\beta(K,l)} \mathbf{X}_2 \underline{\lambda}_{1y}^{\beta(K,l)} - \mathbb{O}_{xy}^{\beta(K,l)} \mathbf{X}_3 \, \underline{\lambda}_{1x}^{\beta(K,l)} + \mathbb{O}_{xx}^{\beta(K,l)} \mathbf{X}_3 \, \underline{\lambda}_{1y}^{\beta(K,l)} = 0 \, . \tag{67b}$$

6.2 Discretization of condition (63b)

From equation (63b), we have:

$$\int_F (\hat{\mathrm{p}}_h + \mathbf{X}_4(\hat{\mathbf{u}}_h \cdot \boldsymbol{n}) + \mathbf{X}_5(\hat{\mathbf{w}}_h \cdot \boldsymbol{n})) \, \xi = 0 \, .$$

Replacing the numerical traces using equation (59), we have:

$$\int_F \Big(\lambda_2 + \mathbf{X}_4(\boldsymbol{\lambda}_1 \cdot \boldsymbol{n}) + \mathbf{X}_5 \Big((\mathbf{w}_h \cdot \boldsymbol{n}) - (\mathrm{p}_h - \lambda_2)(\boldsymbol{S}_2 \cdot \boldsymbol{n}) \cdot \boldsymbol{n} - \boldsymbol{S}_4(\mathbf{u}_h - \boldsymbol{\lambda}_1) \cdot \boldsymbol{n} \Big) \Big) \, \xi = 0 \, .$$

The equation is discretized on (x, y) and the local solutions and lagrange operators are expressed with (62a) and (62b).

$$\int_F \underline{\lambda}_2^{\beta(K,l)} \psi_j^{\beta(K,l)} \psi_i^{\beta(K,l)} + \int_F \mathbf{X}_4 (\underline{\lambda}_{1x}^{\beta(K,l)} n_x + \underline{\lambda}_{1y}^{\beta(K,l)} n_y) \psi_j^{\beta(K,l)} \psi_i^{\beta(K,l)} + \int_F \mathbf{X}_5 (\underline{\mathrm{w}}_x^K n_x + \underline{\mathrm{w}}_y^K n_y) \varphi_j^K \psi_i^{\beta(K,l)}$$
$$- \int_F \mathbf{X}_5 \, \gamma_2 \underline{\mathrm{p}}^K \, (n_x^2 + n_y^2) \, \varphi_j^K \, \psi_i^{\beta(K,l)} dS + \int_F \mathbf{X}_5 \, \gamma_2 \underline{\lambda}_2^{\beta(K,l)} \, (n_x^2 + n_y^2) \, \psi_j^{\beta(K,l)} \, \psi_i^{\beta(K,l)} dS \tag{68}$$
$$- \int_F \mathbf{X}_5 \, \gamma_4 \, (\underline{\mathrm{u}}_x^K n_x + \underline{\mathrm{u}}_y^K n_y) \, \varphi_j^K \, \psi_i^{\beta(K,l)} dS + \int_F \mathbf{X}_5 \, \gamma_4 \, (\underline{\lambda}_{1x}^{\beta(K,l)} n_x + \underline{\lambda}_{1y}^{\beta(K,l)} n_y) \, \psi_j^{\beta(K,l)} \, \psi_i^{\beta(K,l)} dS = 0 \, .$$

Using the elementary matrices defined in (64), we obtain:

$$\mathbb{G}^{\beta(K,l)}\underline{\lambda}_2^{\beta(K,l)} + \mathbb{H}_{xl}^{\beta(K,l)}\mathbf{X}_4\underline{\lambda}_{1x}^{\beta(K,l)} + \mathbb{H}_{yl}^{\beta(K,l)}\mathbf{X}_4\underline{\lambda}_{1y}^{\beta(K,l)} + (\mathbb{Q}_{xl}^{\beta(K,l)})^T\mathbf{X}_5\underline{\mathrm{w}}_x^K + (\mathbb{Q}_{yl}^{\beta(K,l)})^T\mathbf{X}_5\underline{\mathrm{w}}_y^K - (\mathbb{F}_l^{\beta(K,l)})^T\mathbf{X}_5\,\gamma_2\underline{\mathrm{p}}^K$$
$$+ \mathbb{G}_l^{\beta(K,l)}\mathbf{X}_5\,\gamma_2\underline{\lambda}_2^{\beta(K,l)} - (\mathbb{Q}_{xl}^{\beta(K,l)})^T\mathbf{X}_5\,\gamma_4\,\underline{\mathrm{u}}_x^K - (\mathbb{Q}_{yl}^{\beta(K,l)})^T\mathbf{X}_5\,\gamma_4\,\underline{\mathrm{u}}_y^K + \mathbb{H}_{xl}^{\beta(K,l)}\mathbf{X}_5\,\gamma_4\,\underline{\lambda}_{1x}^{\beta(K,l)} + \mathbb{H}_{yl}^{\beta(K,l)}\mathbf{X}_5\,\gamma_4\,\underline{\lambda}_{1y}^{\beta(K,l)} = 0\,. \tag{69}$$

Algorithm 1 Resolution with HDG Method

Step 1: Construction of the stiffness matrix
for $K = 1, N_{elem}$ **do**
Compute the matrices $\mathbb{M}^K$ and $\mathbb{D}_v^K$, with $v = x, y$.
for $l = 1, 3$ (4) **do**
Compute the matrices $\mathbb{E}_l^K$, $\mathbb{F}_l^K$, $\mathbb{G}_l^K$, $\mathbb{Q}_{lv}^K$, $\mathbb{J}_{lv}^K$, $\mathbb{H}_{lv}^K$, $\mathbb{N}_{lv}^K$, $\mathbb{O}_{lv}^K$, $\mathbb{L}_{lv}^K$ with $v = x, y$.
end for
Compute the matrices $\mathbb{A}^K$,$(\mathbb{A}^K)^{-1}$, $\mathbb{B}^K$.
Compute $(\mathbb{A}^K)^{-1}\mathbb{B}$.
Compute $\mathbb{P}^K$, and $\mathbb{T}^K$ with BC.
Compute $\mathbb{K}^K = \mathbb{P}^K(\mathbb{A}^K)^{-1}\mathbb{B}^K + \mathbb{T}^K$.
Use the $\mathcal{A}_{HDG}$ operator to know the global degrees of freedom of the element and fill the global matrix $\mathbb{K}$.
end for

Step 2: Construction of the source term
for $K = 1, N_{elem}$ **do**
Compute the local matrices $\mathbb{C}_{\text{source}}^K$ and $\mathbb{S}_{\text{inc}}^K$.
Compute $\mathbb{P}^K(\mathbb{A}^K)^{-1}\mathbb{C}_{\text{source}}^K$.
Use the $\mathcal{A}_{HDG}$ operator to know the global degrees of freedom of the element and fill the global matrix $\mathbb{S}$.
end for

Step 3: Resolution of the global system
Resolution of $\mathbb{K}\underline{\Lambda} = \mathbb{S}$ with MUMPS .

Step 4: Reconstruction of the solution
for $K = 1, N_{elem}$ **do**
Compute the solutions $\underline{W}^K$ using the $\mathcal{A}_{HDG}^K$ operator:
$\underline{W}^K = -(\mathbb{A}^K)^{-1}\mathbb{B}^K\mathcal{A}_{HDG}^K\underline{\Lambda}$.
end for

6.3 Elementary matrices

Supposing that the first face of the element K is on Γ_{abs}, matrices $\mathbb{P}^K$ and $\mathbb{T}^K$ read then as:

$$\mathbb{P}^K = \begin{pmatrix} -\gamma_1(\mathbb{F}_1^{\beta(K,1)})^T - \gamma_4\mathbf{X}_2(\mathbb{L}_{xx1}^{\beta(K,1)})^T & -\gamma_4\mathbf{X}_2(\mathbb{L}_{xy1}^{\beta(K,1)})^T & \mathbf{X}_2(\mathbb{L}_{xx1}^{\beta(K,1)})^T & \mathbf{X}_2(\mathbb{L}_{xy1}^{\beta(K,1)})^T & \dots \\ -\gamma_1(\mathbb{F}_2^{\beta(K,2)})^T & 0 & 0 & 0 & \dots \\ -\gamma_1(\mathbb{F}_3^{\beta(K,3)})^T & 0 & 0 & 0 & \dots \\ -\gamma_4\mathbf{X}_2(\mathbb{L}_{xy1}^{\beta(K,1)})^T & -\gamma_1(\mathbb{F}_1^{\beta(K,1)})^T - \gamma_4\mathbf{X}_2(\mathbb{L}_{yy1}^{\beta(K,1)})^T & \mathbf{X}_2(\mathbb{L}_{xy1}^{\beta(K,1)})^T & \mathbf{X}_2(\mathbb{L}_{yy1}^{\beta(K,1)})^T & \dots \\ 0 & -\gamma_1(\mathbb{F}_2^{\beta(K,2)})^T & 0 & 0 & \dots \\ 0 & -\gamma_1(\mathbb{F}_3^{\beta(K,3)})^T & 0 & 0 & \dots \\ -(\mathbb{Q}_{x1}^{\beta(K,1)})\mathbf{X}_5\,\gamma_4 & -(\mathbb{Q}_{y1}^{\beta(K,1)})^T\mathbf{X}_5\,\gamma_4 & (\mathbb{Q}_{x1}^{\beta(K,1)})^T\mathbf{X}_5 & (\mathbb{Q}_{y1}^{\beta(K,2)})^T\mathbf{X}_5 & \dots \\ -(\mathbb{Q}_x^{\beta(K,2)})^T\gamma_4 & -(\mathbb{Q}_y^{\beta(K,2)})^T\gamma_4 & (\mathbb{Q}_{x2}^{\beta(K,2)})^T & (\mathbb{Q}_{y2}^{\beta(K,2)})^T & \dots \\ -(\mathbb{Q}_x^{\beta(K,3)})^T\gamma_4 & -(\mathbb{Q}_y^{\beta(K,3)})^T\gamma_4 & (\mathbb{Q}_{x3}^{\beta(K,2)})^T & (\mathbb{Q}_{y3}^{\beta(K,2)})^T & \dots \end{pmatrix}$$

$$\begin{pmatrix}
\dots & (\mathbb{Q}_{x1}^{\beta(K,1)})^T & 0 & (\mathbb{Q}_{y1}^{\beta(K,1)})^T & -\gamma_3(\mathbb{Q}_{x1}^{\beta(K,1)})^T - \gamma_2\mathbf{X}_2(\mathbb{Q}_{x1}^{\beta(K,1)})^T \\
\dots & (\mathbb{Q}_{x2}^{\beta(K,2)})^T & 0 & (\mathbb{Q}_{y2}^{\beta(K,2)})^T & -\gamma_3(\mathbb{Q}_{x2}^{\beta(K,2)})^T \\
\dots & (\mathbb{Q}_{x3}^{\beta(K,3)})^T & 0 & (\mathbb{Q}_{y3}^{\beta(K,3)})^T & -\gamma_3(\mathbb{Q}_{x3}^{\beta(K,3)})^T \\
\dots & 0 & (\mathbb{Q}_{y1}^{\beta(K,1)})^T & (\mathbb{Q}_{x1}^{\beta(K,1)})^T & -\gamma_3(\mathbb{Q}_{y1}^{\beta(K,1)})^T - \gamma_2\mathbf{X}_2(\mathbb{Q}_{y1}^{\beta(K,1)})^T \\
\dots & 0 & (\mathbb{Q}_{y2}^{\beta(K,2)})^T & (\mathbb{Q}_{x2}^{\beta(K,2)})^T & -\gamma_3(\mathbb{Q}_{y2}^{\beta(K,2)})^T \\
\dots & 0 & (\mathbb{Q}_{y3}^{\beta(K,3)})^T & (\mathbb{Q}_{x3}^{\beta(K,3)})^T & -\gamma_3(\mathbb{Q}_{y3}^{\beta(K,3)})^T \\
\dots & 0 & 0 & 0 & -\gamma_2\mathbf{X}_5(\mathbb{F}_1^{\beta(K,1)})^T \\
\dots & 0 & 0 & 0 & -\gamma_2(\mathbb{F}_2^{\beta(K,2)})^T \\
\dots & 0 & 0 & 0 & -\gamma_2(\mathbb{F}_3^{\beta(K,3)})^T
\end{pmatrix},$$

and

$$\mathbb{T}^K = \begin{pmatrix}
\gamma_1\mathbb{G}^{\beta(K,1)} + \mathbb{O}_{xx}^{\beta(K,2)}\gamma_4\mathbf{X}_2 + \mathbb{O}_{xx}^{\beta(K,2)}\mathbf{X}_1 + \mathbb{O}_{yy}^{\beta(K,2)}\mathbf{X}_3 & 0 & 0 & \mathbb{O}_{xy}^{\beta(K,2)}\gamma_4\mathbf{X}_2 + \mathbb{O}_{xy}^{\beta(K,2)}\mathbf{X}_1 - \mathbb{O}_{xy}^{\beta(K,2)}\mathbf{X}_3 & \dots \\
0 & \gamma_1\mathbb{G}^{\beta(K,2)} & 0 & 0 & \dots \\
0 & 0 & \gamma_1\mathbb{G}^{\beta(K,3)} & 0 & \dots \\
\mathbb{O}_{xy}^{\beta(K,2)}\gamma_4\mathbf{X}_2 + \mathbb{O}_{xy}^{\beta(K,2)}\mathbf{X}_1 - \mathbb{O}_{xy}^{\beta(K,2)}\mathbf{X}_3 & 0 & 0 & \gamma_1\mathbb{G}^{\beta(K,1)} + \mathbb{O}_{yy}^{\beta(K,2)}\gamma_4\mathbf{X}_2 + \mathbb{O}_{yy}^{\beta(K,2)}\mathbf{X}_1 + \mathbb{O}_{xx}^{\beta(K,2)}\mathbf{X}_3 & \dots \\
0 & 0 & 0 & 0 & \dots \\
0 & 0 & 0 & 0 & \dots \\
\mathbb{H}_{x1}^{\beta(K,2)}\mathbf{X}_4 + \mathbb{H}_{x1}^{\beta(K,2)}\mathbf{X}_5\gamma_4 & 0 & 0 & \mathbb{H}_{y1}^{\beta(K,2)}\mathbf{X}_4 + \mathbb{H}_{y1}^{\beta(K,2)}\mathbf{X}_5\gamma_4 & \dots \\
0 & \gamma_4\mathbb{H}_x^{\beta(K,2)} & 0 & 0 & \dots \\
0 & 0 & \gamma_4\mathbb{H}_x^{\beta(K,3)} & 0 & \dots
\end{pmatrix}$$

$$\begin{pmatrix}
\dots & 0 & 0 & \gamma_3\mathbb{H}_x^{\beta(K,1)} + \mathbb{H}_{xl}^{\beta(K,1)}\mathbf{X}_2\ \gamma_2 & 0 & 0 \\
\dots & 0 & 0 & 0 & \gamma_3\mathbb{H}_x^{\beta(K,2)} & 0 \\
\dots & 0 & 0 & 0 & 0 & \gamma_3\mathbb{H}_x^{\beta(K,3)} \\
\dots & 0 & 0 & \gamma_3\mathbb{H}_y^{\beta(K,1)} + \mathbb{H}_{y1}^{\beta(K,2)}\mathbf{X}_2\ \gamma_2 & 0 & 0 \\
\dots & \gamma_1\mathbb{G}^{\beta(K,2)} & 0 & 0 & \gamma_3\mathbb{H}_y^{\beta(K,2)} & 0 \\
\dots & 0 & \gamma_1\mathbb{G}^{\beta(K,3)} & 0 & 0 & \gamma_3\mathbb{H}_y^{\beta(K,3)} \\
\dots & 0 & 0 & \mathbb{G}^{\beta(K,1)}(1 + \mathbf{X}_5\gamma_2) & 0 & 0 \\
\dots & \gamma_4\mathbb{H}_y^{\beta(K,2)} & 0 & 0 & \gamma_2\mathbb{G}^{\beta(K,2)} & 0 \\
\dots & 0 & \gamma_4\mathbb{H}_y^{\beta(K,3)} & 0 & 0 & \gamma_2\mathbb{G}^{\beta(K,3)}
\end{pmatrix}.$$

7 HDG method with PML

In this section, we apply a Perfectly Matched Layer (PML) to the discretization of poroelastic equations (2) using HDG method. The perfectly matched layer is an artificial absorbing layer on the edges of the computational domain. It absorbs the outgoing waves and prevents the reflections. In the formulation, we use two absorbing functions α and β that represent the attenuation of the wave in the absorbing layer. The attenuation functions α and β are taken equal to zero outside of the absorbing layers, and the more the considered points in the layers are far from the part with no attenuation, the more their values grow. In practice, we replace the derivatives

$$\frac{\partial}{\partial x} \to \frac{i\,\omega}{i\,\omega + \alpha(x)}\frac{\partial}{\partial x}, \qquad \text{and} \qquad \frac{\partial}{\partial y} \to \frac{i\,\omega}{i\,\omega + \beta(y)}\frac{\partial}{\partial y}.$$

We consider a two-dimensional porous domain Ω with the boundary Γ on the plane (x, y). $(\mathbf{u},\, \mathbf{w},\, \boldsymbol{\tau},\, \mathrm{p})$ solve the poroelastic equations (2) on Ω. We consider a triangulation $\mathcal{T}_h$ of Ω, and $\mathcal{F}_h$ the set of all the faces. K is a triangle element of $\mathcal{T}_h$ and F is a face of K. We use the approximation spaces defined in section 6. The local unknowns $(\mathbf{u}_h,\, \mathbf{w}_h,\, \boldsymbol{\tau}_h,\, \mathrm{p}_h) \in (\boldsymbol{V}_h^p \times \boldsymbol{V}_h^p \times \boldsymbol{\Sigma}_h^p \times V_h^p)$ solve the poroelastic equations (2) on $\mathcal{T}_h$. The HDG discretization of the poroelastic equations (2) is modified. The transmission conditions are not modified and stay the same as the one used in HDG method with no PML, see [4].

We consider an element $K \in \mathcal{T}_h$, $(\tilde{\boldsymbol{u}},\, \tilde{\boldsymbol{w}},\, \tilde{\boldsymbol{\tau}},\, \tilde{\mathrm{p}}) \in (\boldsymbol{V}_h^p \times \boldsymbol{V}_h^p \times \boldsymbol{\Sigma}_h^p \times V_h^p)$ test-functions. We multiply equations

(2) by the test-functions and integrate on the element K:

$$\int_K \mathrm{i}\,\omega\rho_a \mathrm{u}_x^K \tilde{u}_x + \int_K \mathrm{i}\,\omega\rho_a \mathrm{u}_y^K \tilde{u}_y + \int_K \mathrm{i}\,\omega\rho_f \mathrm{w}_x^K \tilde{u}_x + \int_K \mathrm{i}\,\omega\rho_f \mathrm{w}_y^K \tilde{u}_y - \int_K \left(\frac{i\,\omega}{i\,\omega+\alpha(x)} \frac{\partial \tau_{xx}^K}{\partial x} + \frac{i\,\omega}{i\,\omega+\beta(y)} \frac{\partial \tau_{xy}^K}{\partial y} \right) \tilde{u}_x$$
$$- \int_K \left(\frac{i\,\omega}{i\,\omega+\alpha(x)} \frac{\partial \tau_{xy}^K}{\partial x} + \frac{i\,\omega}{i\,\omega+\beta(y)} \frac{\partial \tau_{yy}^K}{\partial y} \right) \tilde{u}_y = 0\,,$$

$$\int_K \mathrm{i}\omega\rho_f \mathrm{u}_x^K \tilde{w}_x + \int_K \mathrm{i}\omega\rho_f \mathrm{u}_y^K \tilde{w}_y + \int_K \mathrm{i}\omega\tilde{\rho} \mathrm{w}_x^K \tilde{w}_x + \int_K \mathrm{i}\omega\tilde{\rho} \mathrm{w}_y^K \tilde{w}_y + \int_K \frac{i\,\omega}{i\,\omega+\alpha(x)} \frac{\partial \mathrm{p}}{\partial x} \tilde{w}_x + \int_K \frac{i\,\omega}{i\,\omega+\beta(y)} \frac{\partial \mathrm{p}}{\partial y} \tilde{w}_y = 0\,,$$

$$\int_K \mathrm{i}\omega\tau_{xx}^K \tilde{\tau}_{xx} + \int_K \mathrm{i}\omega\alpha_{11}\mathrm{p}_h\tilde{\tau}_{xx} - \int_K C_{11} \frac{i\,\omega}{i\,\omega+\alpha(x)} \frac{\partial \mathrm{u}_x^K}{\partial x} \tilde{\tau}_{xx} - \int_K C_{12} \frac{i\,\omega}{i\,\omega+\beta(y)} \frac{\partial \mathrm{u}_y^K}{\partial y} \tilde{\tau}_{xx}$$
$$- \int_K C_{13} \left(\frac{i\,\omega}{i\,\omega+\alpha(x)} \frac{\partial \mathrm{u}_y^K}{\partial x} + \frac{i\,\omega}{i\,\omega+\beta(y)} \frac{\partial \mathrm{u}_x^K}{\partial y} \right) \tilde{\tau}_{xx}$$
$$+ \int_K \mathrm{i}\omega\tau_{yy}^K \tilde{\tau}_{yy} + \int_K \mathrm{i}\omega\alpha_{22}\mathrm{p}_h\tilde{\tau}_{yy} - \int_K C_{12} \frac{i\,\omega}{i\,\omega+\alpha(x)} \frac{\partial \mathrm{u}_x^K}{\partial x} \tilde{\tau}_{yy} - \int_K C_{22} \frac{i\,\omega}{i\,\omega+\beta(y)} \frac{\partial \mathrm{u}_y^K}{\partial y} \tilde{\tau}_{yy}$$
$$- \int_K C_{23} \left(\frac{i\,\omega}{i\,\omega+\alpha(x)} \frac{\partial \mathrm{u}_y^K}{\partial x} + \frac{i\,\omega}{i\,\omega+\beta(y)} \frac{\partial \mathrm{u}_x^K}{\partial y} \right) \tilde{\tau}_{yy}$$
$$+ \int_K \mathrm{i}\omega\tau_{xy}^K \tilde{\tau}_{xy} + \int_K \mathrm{i}\omega\alpha_{12}\mathrm{p}_h\tilde{\tau}_{xy} - \int_K C_{13} \frac{i\,\omega}{i\,\omega+\alpha(x)} \frac{\partial \mathrm{u}_x^K}{\partial x} \tilde{\tau}_{xy} - \int_K C_{23} \frac{i\,\omega}{i\,\omega+\beta(y)} \frac{\partial \mathrm{u}_y^K}{\partial y} \tilde{\tau}_{xy}$$
$$- \int_K C_{33} \left(\frac{i\,\omega}{i\,\omega+\alpha(x)} \frac{\partial \mathrm{u}_y^K}{\partial x} + \frac{i\,\omega}{i\,\omega+\beta(y)} \frac{\partial \mathrm{u}_x^K}{\partial y} \right) \tilde{\tau}_{xy} = 0\,,$$

and

$$\int_K \mathrm{i}\omega\mathrm{p}_h\tilde{\mathrm{p}} + \int_K M \left(\frac{i\,\omega}{i\,\omega+\alpha(x)} \frac{\partial \mathrm{w}_x^K}{\partial x} + \frac{i\,\omega}{i\,\omega+\beta(y)} \frac{\partial \mathrm{w}_y^K}{\partial y} \right) \tilde{\mathrm{p}} + \int_K M\alpha_{11} \frac{i\,\omega}{i\,\omega+\alpha(x)} \frac{\partial \mathrm{u}_x^K}{\partial x} \tilde{\mathrm{p}}$$
$$+ \int_K M\alpha_{22} \frac{i\,\omega}{i\,\omega+\beta(y)} \frac{\partial \mathrm{u}_y^K}{\partial y} \tilde{\mathrm{p}} + \int_K M\alpha_{12} \left(\frac{i\,\omega}{i\,\omega+\beta(y)} \frac{\partial \mathrm{u}_x^K}{\partial y} + \frac{i\,\omega}{i\,\omega+\alpha(x)} \frac{\partial \mathrm{u}_y^K}{\partial x} \right) \tilde{\mathrm{p}} = 0\,.$$

By integrating by parts, we obtain:

$$\int_K \mathrm{i}\omega\rho_a \mathrm{u}_x^K \tilde{u}_x + \int_K \mathrm{i}\omega\rho_a \mathrm{u}_y^K \tilde{u}_y + \int_K \mathrm{i}\omega\rho_f \mathrm{w}_x^K \tilde{u}_x + \int_K \mathrm{i}\omega\rho_f \mathrm{w}_y^K \tilde{u}_y + \int_K \frac{i\,\omega}{i\,\omega+\alpha(x)} \tau_{xx}^K \frac{\partial \tilde{u}_x}{\partial x} + \int_K \frac{i\,\omega}{i\,\omega+\beta(y)} \tau_{xy}^K \frac{\partial \tilde{u}_x}{\partial y}$$
$$- \int_F \frac{i\,\omega}{i\,\omega+\alpha(x)} \hat{\tau}_{xx}^K n_x \tilde{u}_x - \int_F \frac{i\,\omega}{i\,\omega+\beta(y)} \hat{\tau}_{xy}^K n_y \tilde{u}_x + \int_K \frac{i\,\omega}{i\,\omega+\alpha(x)} \tau_{xy}^K \frac{\partial \tilde{u}_y}{\partial x} + \int_K \frac{i\,\omega}{i\,\omega+\beta(y)} \tau_{yy}^K \frac{\partial \tilde{u}_y}{\partial y}$$
$$- \int_F \frac{i\,\omega}{i\,\omega+\alpha(x)} \hat{\tau}_{xy}^K n_x \tilde{u}_y - \int_F \frac{i\,\omega}{i\,\omega+\beta(y)} \hat{\tau}_{yy}^K n_y \tilde{u}_y = 0\,,$$

$$\int_K \mathrm{i}\omega\rho_f \mathrm{u}_x^K \tilde{w}_x + \int_K \mathrm{i}\omega\rho_f \mathrm{u}_y^K \tilde{w}_y + \int_K \mathrm{i}\omega\tilde{\rho} \mathrm{w}_x^K \tilde{w}_x + \int_K \mathrm{i}\omega\tilde{\rho} \mathrm{w}_y^K \tilde{w}_y - \int_K \frac{i\,\omega}{i\,\omega+\alpha(x)} \mathrm{p} \frac{\partial \tilde{w}_x}{\partial x} + \int_F \frac{i\,\omega}{i\,\omega+\alpha(x)} \hat{\mathrm{p}}_h n_x \tilde{w}_x$$
$$- \int_K \frac{i\,\omega}{i\,\omega+\beta(y)} \mathrm{p} \frac{\partial \tilde{w}_y}{\partial y} + \int_F \frac{i\,\omega}{i\,\omega+\beta(y)} \hat{\mathrm{p}}_h n_y \tilde{w}_y = 0\,,$$

$$
\begin{aligned}
&\int_K \mathrm{i}\omega\tau_{xx}^K\,\tilde{\tau}_{xx} + \int_K \mathrm{i}\omega\alpha_{11}\mathrm{p}_h\tilde{\tau}_{xx} + \int_K C_{11}\frac{i\,\omega}{i\,\omega+\alpha(x)}\mathrm{u}_x^K\frac{\partial\tilde{\tau}_{xx}}{\partial x} - \int_F C_{11}\frac{i\,\omega}{i\,\omega+\alpha(x)}\hat{\mathrm{u}}_x^K n_x\tilde{\tau}_{xx}\\
&+\int_K C_{12}\frac{i\,\omega}{i\,\omega+\beta(y)}\mathrm{u}_y^K\frac{\partial\tilde{\tau}_{xx}}{\partial y} - \int_F C_{12}\frac{i\,\omega}{i\,\omega+\beta(y)}\hat{\mathrm{u}}_y^K n_y\tilde{\tau}_{xx} + \int_K C_{13}\frac{i\,\omega}{i\,\omega+\alpha(x)}\mathrm{u}_y^K\frac{\partial\tilde{\tau}_{xx}}{\partial x}\\
&-\int_F C_{13}\frac{i\,\omega}{i\,\omega+\alpha(x)}\hat{\mathrm{u}}_y^K n_x\tilde{\tau}_{xx} + \int_K C_{13}\frac{i\,\omega}{i\,\omega+\beta(y)}\mathrm{u}_x^K\frac{\partial\tilde{\tau}_{xx}}{\partial y} - \int_F C_{13}\frac{i\,\omega}{i\,\omega+\beta(y)}\hat{\mathrm{u}}_x^K n_y\tilde{\tau}_{xx}\\
&+\int_K \mathrm{i}\omega\tau_{yy}^K\,\tilde{\tau}_{yy} + \int_K \mathrm{i}\omega\alpha_{22}\mathrm{p}_h\tilde{\tau}_{yy} + \int_K C_{12}\frac{i\,\omega}{i\,\omega+\alpha(x)}\mathrm{u}_x^K\frac{\partial\tilde{\tau}_{yy}}{\partial x} - \int_F C_{12}\frac{i\,\omega}{i\,\omega+\alpha(x)}\hat{\mathrm{u}}_x^K n_x\tilde{\tau}_{yy}\\
&+\int_K C_{22}\frac{i\,\omega}{i\,\omega+\beta(y)}\mathrm{u}_y^K\frac{\partial\tilde{\tau}_{yy}}{\partial y} - \int_F C_{22}\frac{i\,\omega}{i\,\omega+\beta(y)}\hat{\mathrm{u}}_y^K n_y\tilde{\tau}_{yy} + \int_K C_{23}\frac{i\,\omega}{i\,\omega+\alpha(x)}\mathrm{u}_y^K\frac{\partial\tilde{\tau}_{yy}}{\partial x}\\
&-\int_F C_{23}\frac{i\,\omega}{i\,\omega+\alpha(x)}\hat{\mathrm{u}}_y^K n_x\tilde{\tau}_{yy} + \int_K C_{23}\frac{i\,\omega}{i\,\omega+\beta(y)}\mathrm{u}_x^K\frac{\partial\tilde{\tau}_{yy}}{\partial y} - \int_F C_{23}\frac{i\,\omega}{i\,\omega+\beta(y)}\hat{\mathrm{u}}_x^K n_y\tilde{\tau}_{yy}\\
&+\int_K \mathrm{i}\omega\tau_{xy}^K\,\tilde{\tau}_{xy} + \int_K \mathrm{i}\omega\alpha_{12}\mathrm{p}_h\tilde{\tau}_{xy} + \int_K C_{13}\frac{i\,\omega}{i\,\omega+\alpha(x)}\mathrm{u}_x^K\frac{\partial\tilde{\tau}_{xy}}{\partial x} - \int_F C_{13}\frac{i\,\omega}{i\,\omega+\alpha(x)}\hat{\mathrm{u}}_x^K n_x\tilde{\tau}_{xy}\\
&+\int_K C_{23}\frac{i\,\omega}{i\,\omega+\beta(y)}\mathrm{u}_y^K\frac{\partial\tilde{\tau}_{xy}}{\partial y} - \int_F C_{23}\frac{i\,\omega}{i\,\omega+\beta(y)}\hat{\mathrm{u}}_y^K n_y\tilde{\tau}_{xy} + \int_K C_{33}\frac{i\,\omega}{i\,\omega+\alpha(x)}\mathrm{u}_y^K\frac{\partial\tilde{\tau}_{xy}}{\partial x}\\
&-\int_F C_{33}\frac{i\,\omega}{i\,\omega+\alpha(x)}\hat{\mathrm{u}}_y^K n_x\tilde{\tau}_{xy} + \int_K C_{33}\frac{i\,\omega}{i\,\omega+\beta(y)}\mathrm{u}_x^K\frac{\partial\tilde{\tau}_{xy}}{\partial y} - \int_F C_{33}\frac{i\,\omega}{i\,\omega+\beta(y)}\hat{\mathrm{u}}_x^K n_y\tilde{\tau}_{xy} = 0\,,
\end{aligned}
$$

$$
\begin{aligned}
&\int_K \mathrm{i}\omega\mathrm{p}_h\tilde{\mathrm{p}} - \int_K M\frac{i\,\omega}{i\,\omega+\alpha(x)}\mathrm{w}_x^K\frac{\partial\tilde{\mathrm{p}}}{\partial x} + \int_F M\frac{i\,\omega}{i\,\omega+\alpha(x)}\hat{\mathrm{w}}_x^K n_x\tilde{\mathrm{p}} - \int_K M\frac{i\,\omega}{i\,\omega+\beta(y)}\mathrm{w}_y^K\frac{\partial\tilde{\mathrm{p}}}{\partial y}\\
&+\int_F M\frac{i\,\omega}{i\,\omega+\beta(y)}\hat{\mathrm{w}}_y^K n_y\tilde{\mathrm{p}} - \int_K M\alpha_{11}\frac{i\,\omega}{i\,\omega+\alpha(x)}\mathrm{u}_x^K\frac{\partial\tilde{\mathrm{p}}}{\partial x} + \int_F M\alpha_{11}\frac{i\,\omega}{i\,\omega+\alpha(x)}\hat{\mathrm{u}}_x^K n_x\tilde{\mathrm{p}}\\
&-\int_K M\alpha_{22}\frac{i\,\omega}{i\,\omega+\beta(y)}\mathrm{u}_y^K\frac{\partial\tilde{\mathrm{p}}}{\partial y} + \int_F M\alpha_{22}\frac{i\,\omega}{i\,\omega+\beta(y)}\hat{\mathrm{u}}_y^K n_y\tilde{\mathrm{p}} - \int_K M\alpha_{12}\frac{i\,\omega}{i\,\omega+\beta(y)}\mathrm{u}_x^K\frac{\partial\tilde{\mathrm{p}}}{\partial y}\\
&+\int_F M\alpha_{12}\frac{i\,\omega}{i\,\omega+\beta(y)}\hat{\mathrm{u}}_x^K n_y\tilde{\mathrm{p}} - \int_K M\alpha_{12}\frac{i\,\omega}{i\,\omega+\alpha(x)}\mathrm{u}_y^K\frac{\partial\tilde{\mathrm{p}}}{\partial x} + \int_F M\alpha_{12}\frac{i\,\omega}{i\,\omega+\alpha(x)}\hat{\mathrm{u}}_y^K n_x\tilde{\mathrm{p}} = 0\,.
\end{aligned}
$$

Next we replace the numerical traces $\hat{\mathbf{u}}_h$, $\hat{\mathbf{w}}_h$, $\hat{\boldsymbol{\tau}}_h$ and $\hat{\mathrm{p}}_h$ by the expressions from equation (59):

$$
\begin{aligned}
&\int_K \mathrm{i}\omega\rho_a\mathrm{u}_x^K\tilde{u}_x + \int_K \mathrm{i}\omega\rho_a\mathrm{u}_y^K\tilde{u}_y + \int_K \mathrm{i}\omega\rho_f\mathrm{w}_x^K\tilde{u}_x + \int_K \mathrm{i}\omega\rho_f\mathrm{w}_y^K\tilde{u}_y - \int_K\frac{i\,\omega}{i\,\omega+\alpha(x)}\frac{\partial\tau_{xx}^K}{\partial x}\tilde{u}_x\\
&+\int_F\gamma_1\frac{i\,\omega}{i\,\omega+\alpha(x)}(\mathrm{u}_x^K-\lambda_{1x})n_x^2\tilde{u}_x + \int_F\gamma_3\frac{i\,\omega}{i\,\omega+\alpha(x)}(\mathrm{p}_h-\lambda_2)n_x\tilde{u}_x - \int_K\frac{i\,\omega}{i\,\omega+\beta(y)}\frac{\partial\tau_{xy}^K}{\partial y}\tilde{u}_x\\
&+\int_F\gamma_1\frac{i\,\omega}{i\,\omega+\beta(y)}(\mathrm{u}_x^K-\lambda_{1x})n_y^2\tilde{u}_x - \int_K\frac{i\,\omega}{i\,\omega+\alpha(x)}\frac{\partial\tau_{xy}^K}{\partial x}\tilde{u}_y + \int_F\gamma_1\frac{i\,\omega}{i\,\omega+\alpha(x)}(\mathrm{u}_y^K-\lambda_{1y})n_x^2\tilde{u}_y\\
&-\int_K\frac{i\,\omega}{i\,\omega+\beta(y)}\frac{\partial\tau_{yy}^K}{\partial y}\tilde{u}_y + \int_F\gamma_1\frac{i\,\omega}{i\,\omega+\beta(y)}(\mathrm{u}_y^K-\lambda_{1y})n_y^2\tilde{u}_y + \int_F\gamma_3\frac{i\,\omega}{i\,\omega+\beta(y)}(\mathrm{p}_h-\lambda_2)n_y\tilde{u}_y = 0\,,
\end{aligned}
$$

$$
\begin{aligned}
&\int_K \mathrm{i}\,\omega\rho_f\mathrm{u}_x^K\tilde{w}_x + \int_K \mathrm{i}\,\omega\rho_f\mathrm{u}_y^K\tilde{w}_y + \int_K \mathrm{i}\,\omega\tilde{\rho}\mathrm{w}_x^K\tilde{w}_x + \int_K \mathrm{i}\,\omega\tilde{\rho}\mathrm{w}_y^K\tilde{w}_y - \int_K\frac{i\,\omega}{i\,\omega+\alpha(x)}\mathrm{p}\frac{\partial\tilde{w}_x}{\partial x} + \int_F\frac{i\,\omega}{i\,\omega+\alpha(x)}\lambda_2 n_x\tilde{w}_x\\
&-\int_K\frac{i\,\omega}{i\,\omega+\beta(y)}\mathrm{p}\frac{\partial\tilde{w}_y}{\partial y} + \int_F\frac{i\,\omega}{i\,\omega+\beta(y)}\lambda_2 n_y\tilde{w}_y = 0\,,
\end{aligned}
$$

$$
\begin{aligned}
&\int_K \mathrm{i}\omega\tau_{xx}^K\,\tilde\tau_{xx} + \int_K \mathrm{i}\omega\alpha_{11}\mathrm{p}_h\tilde\tau_{xx} + \int_K C_{11}\frac{i\,\omega}{i\,\omega+\alpha(x)}\mathrm{u}_x^K\frac{\partial\tilde\tau_{xx}}{\partial x} - \int_F C_{11}\frac{i\,\omega}{i\,\omega+\alpha(x)}\lambda_{1x}n_x\tilde\tau_{xx}\\
&+\int_K C_{12}\frac{i\,\omega}{i\,\omega+\beta(y)}\mathrm{u}_y^K\frac{\partial\tilde\tau_{xx}}{\partial y} - \int_F C_{12}\frac{i\,\omega}{i\,\omega+\beta(y)}\lambda_{1y}n_y\tilde\tau_{xx} + \int_K C_{13}\frac{i\,\omega}{i\,\omega+\alpha(x)}\mathrm{u}_y^K\frac{\partial\tilde\tau_{xx}}{\partial x}\\
&-\int_F C_{13}\frac{i\,\omega}{i\,\omega+\alpha(x)}\lambda_{1y}n_x\tilde\tau_{xx} + \int_K C_{13}\frac{i\,\omega}{i\,\omega+\beta(y)}\mathrm{u}_x^K\frac{\partial\tilde\tau_{xx}}{\partial y} - \int_F C_{13}\frac{i\,\omega}{i\,\omega+\beta(y)}\lambda_{1x}n_y\tilde\tau_{xx}\\
&+\int_K \mathrm{i}\omega\tau_{yy}^K\,\tilde\tau_{yy} + \int_K \mathrm{i}\omega\alpha_{22}\mathrm{p}_h\tilde\tau_{yy} + \int_K C_{12}\frac{i\,\omega}{i\,\omega+\alpha(x)}\mathrm{u}_x^K\frac{\partial\tilde\tau_{yy}}{\partial x} - \int_F C_{12}\frac{i\,\omega}{i\,\omega+\alpha(x)}\lambda_{1x}n_x\tilde\tau_{yy}\\
&+\int_K C_{22}\frac{i\,\omega}{i\,\omega+\beta(y)}\mathrm{u}_y^K\frac{\partial\tilde\tau_{yy}}{\partial y} - \int_F C_{22}\frac{i\,\omega}{i\,\omega+\beta(y)}\lambda_{1y}n_y\tilde\tau_{yy} + \int_K C_{23}\frac{i\,\omega}{i\,\omega+\alpha(x)}\mathrm{u}_y^K\frac{\partial\tilde\tau_{yy}}{\partial x}\\
&-\int_F C_{23}\frac{i\,\omega}{i\,\omega+\alpha(x)}\lambda_{1y}n_x\tilde\tau_{yy} + \int_K C_{23}\frac{i\,\omega}{i\,\omega+\beta(y)}\mathrm{u}_x^K\frac{\partial\tilde\tau_{yy}}{\partial y} - \int_F C_{23}\frac{i\,\omega}{i\,\omega+\beta(y)}\lambda_{1x}n_y\tilde\tau_{yy}\\
&+\int_K \mathrm{i}\omega\tau_{xy}^K\,\tilde\tau_{xy} + \int_K \mathrm{i}\omega\alpha_{12}\mathrm{p}_h\tilde\tau_{xy} + \int_K C_{13}\frac{i\,\omega}{i\,\omega+\alpha(x)}\mathrm{u}_x^K\frac{\partial\tilde\tau_{xy}}{\partial x} - \int_F C_{13}\frac{i\,\omega}{i\,\omega+\alpha(x)}\lambda_{1x}n_x\tilde\tau_{xy}\\
&+\int_K C_{23}\frac{i\,\omega}{i\,\omega+\beta(y)}\mathrm{u}_y^K\frac{\partial\tilde\tau_{xy}}{\partial y} - \int_F C_{23}\frac{i\,\omega}{i\,\omega+\beta(y)}\lambda_{1y}n_y\tilde\tau_{xy} + \int_K C_{33}\frac{i\,\omega}{i\,\omega+\alpha(x)}\mathrm{u}_y^K\frac{\partial\tilde\tau_{xy}}{\partial x}\\
&-\int_F C_{33}\frac{i\,\omega}{i\,\omega+\alpha(x)}\lambda_{1y}n_x\tilde\tau_{xy} + \int_K C_{33}\frac{i\,\omega}{i\,\omega+\beta(y)}\mathrm{u}_x^K\frac{\partial\tilde\tau_{xy}}{\partial y} - \int_F C_{33}\frac{i\,\omega}{i\,\omega+\beta(y)}\lambda_{1x}n_y\tilde\tau_{xy} = 0\,,
\end{aligned}
$$

$$
\begin{aligned}
&\int_K \mathrm{i}\omega\mathrm{p}_h\tilde{\mathrm{p}} + \int_K M\frac{i\,\omega}{i\,\omega+\alpha(x)}\frac{\partial\mathrm{w}_x^K}{\partial x}\tilde{\mathrm{p}} - \int_F M\gamma_2\frac{i\,\omega}{i\,\omega+\alpha(x)}(\mathrm{p}_h-\lambda_2)n_x^2\tilde{\mathrm{p}} - \int_F M\gamma_4\frac{i\,\omega}{i\,\omega+\alpha(x)}(\mathrm{u}_x^K-\lambda_{1x})n_x\tilde{\mathrm{p}}\\
&+\int_K M\frac{i\,\omega}{i\,\omega+\beta(y)}\frac{\partial\mathrm{w}_y^K}{\partial y}\tilde{\mathrm{p}} - \int_F M\gamma_2\frac{i\,\omega}{i\,\omega+\beta(y)}(\mathrm{p}_h-\lambda_2)n_y^2\tilde{\mathrm{p}} - \int_F M\gamma_4\frac{i\,\omega}{i\,\omega+\beta(y)}(\mathrm{u}_y^K-\lambda_{1y})n_y\tilde{\mathrm{p}}\\
&-\int_K M\alpha_{11}\frac{i\,\omega}{i\,\omega+\alpha(x)}\mathrm{u}_x^K\frac{\partial\tilde{\mathrm{p}}}{\partial x} + \int_F M\alpha_{11}\frac{i\,\omega}{i\,\omega+\alpha(x)}\lambda_{1x}n_x\tilde{\mathrm{p}} - \int_K M\alpha_{22}\frac{i\,\omega}{i\,\omega+\beta(y)}\mathrm{u}_y^K\frac{\partial\tilde{\mathrm{p}}}{\partial y}\\
&+\int_F M\alpha_{22}\frac{i\,\omega}{i\,\omega+\beta(y)}\lambda_{1y}n_y\tilde{\mathrm{p}} - \int_K M\alpha_{12}\frac{i\,\omega}{i\,\omega+\beta(y)}\mathrm{u}_x^K\frac{\partial\tilde{\mathrm{p}}}{\partial y} + \int_F M\alpha_{12}\frac{i\,\omega}{i\,\omega+\beta(y)}\lambda_{1x}n_y\tilde{\mathrm{p}}\\
&-\int_K M\alpha_{12}\frac{i\,\omega}{i\,\omega+\alpha(x)}\mathrm{u}_y^K\frac{\partial\tilde{\mathrm{p}}}{\partial x} + \int_F M\alpha_{12}\frac{i\,\omega}{i\,\omega+\alpha(x)}\lambda_{1y}n_x\tilde{\mathrm{p}} = 0\,.
\end{aligned}
$$

Then, we replace the local unknowns and the local test-functions using equations (62a) and (62b). We obtain:

$$
\begin{aligned}
&\int_K \mathrm{i}\,\omega\rho_a\underline{\mathrm{u}}_x^K\,\varphi_j^K\varphi_i^K + \int_K \mathrm{i}\,\omega\rho_f\underline{\mathrm{w}}_x^K\,\varphi_j^K\varphi_i^K - \int_K\frac{i\,\omega}{i\,\omega+\alpha(x)}\frac{\partial\underline{\tau}_{xx}^K}{\partial x}\varphi_j^K\varphi_i^K + \int_F\gamma_1\frac{i\,\omega}{i\,\omega+\alpha(x)}(\underline{\mathrm{u}}_x^K\varphi_j^K-\underline{\lambda}_{1x}\psi_j^{\beta(K,l)})n_x^2\varphi_i^K\\
&+\int_F\gamma_3\frac{i\,\omega}{i\,\omega+\alpha(x)}(\underline{\mathrm{p}}^K\varphi_j^K-\underline{\lambda}_2\psi_j^{\beta(K,l)})n_x\varphi_i^K - \int_K\frac{i\,\omega}{i\,\omega+\beta(y)}\frac{\partial\underline{\tau}_{xy}^K}{\partial y}\varphi_j^K\varphi_i^K + \int_F\gamma_1\frac{i\,\omega}{i\,\omega+\beta(y)}(\underline{\mathrm{u}}_x^K\varphi_j^K-\underline{\lambda}_{1x}\psi_j^{\beta(K,l)})n_y^2\varphi_i^K =
\end{aligned}
$$

$$
\begin{aligned}
&\int_K \mathrm{i}\omega\rho_a\underline{\mathrm{u}}_y^K\,\varphi_j^K\varphi_i^K + \int_K \mathrm{i}\omega\rho_f\underline{\mathrm{w}}_y^K\varphi_j^K\varphi_i^K - \int_K\frac{i\,\omega}{i\,\omega+\alpha(x)}\underline{\tau}_{xy}^K\frac{\partial\varphi_j^K}{\partial x}\varphi_i^K + \int_F\gamma_1\frac{i\,\omega}{i\,\omega+\alpha(x)}(\underline{\mathrm{u}}_y^K\varphi_j^K-\underline{\lambda}_{1y}\psi_j^{\beta(K,l)})n_x^2\varphi_i^K\\
&-\int_K\frac{i\,\omega}{i\,\omega+\beta(y)}\frac{\partial\underline{\tau}_{yy}^K}{\partial y}\varphi_j^K\varphi_i^K + \int_F\gamma_1\frac{i\,\omega}{i\,\omega+\beta(y)}(\underline{\mathrm{u}}_y^K\varphi_j^K-\underline{\lambda}_{1y}\psi_j^{\beta(K,l)})n_y^2\varphi_i^K + \int_F\gamma_3\frac{i\,\omega}{i\,\omega+\beta(y)}(\underline{\mathrm{p}}^K\varphi_j^K-\underline{\lambda}_2\psi_j^{\beta(K,l)})n_y\varphi_i^K =
\end{aligned}
$$

$$
\begin{aligned}
&\int_K \mathrm{i}\omega\rho_f\underline{\mathrm{u}}_x^K\varphi_j^K\varphi_i^K + \int_K \mathrm{i}\omega\tilde\rho\underline{\mathrm{w}}_x^K\varphi_j^K\varphi_i^K - \int_K\frac{i\,\omega}{i\,\omega+\alpha(x)}\underline{\mathrm{p}}^K\varphi_j^K\frac{\partial\varphi_i^K}{\partial x} + \int_F\frac{i\,\omega}{i\,\omega+\alpha(x)}\underline{\lambda}_2\psi_j^{\beta(K,l)}n_x\varphi_i^K = 0\,,\\
&\int_K \mathrm{i}\omega\rho_f\underline{\mathrm{u}}_y^K\varphi_j^K\varphi_i^K + \int_K \mathrm{i}\omega\tilde\rho\underline{\mathrm{w}}_y^K\varphi_j^K\varphi_i^K - \int_K\frac{i\,\omega}{i\,\omega+\beta(y)}\underline{\mathrm{p}}^K\varphi_j^K\frac{\partial\varphi_i^K}{\partial y} + \int_F\frac{i\,\omega}{i\,\omega+\beta(y)}\underline{\lambda}_2\psi_j^{\beta(K,l)}n_y\varphi_i^K = 0\,,
\end{aligned}
$$

$$\int_K \mathrm{i}\omega \underline{\tau}_{xx}^K \varphi_j^K \varphi_i^K + \int_K \mathrm{i}\omega\alpha_{11}\underline{\mathrm{p}}^K \varphi_j^K \varphi_i^K + \int_K C_{11}\frac{i\,\omega}{i\,\omega+\alpha(x)}\underline{\mathrm{u}}_x^K \varphi_j^K \frac{\partial \varphi_i^K}{\partial x} - \int_F C_{11}\frac{i\,\omega}{i\,\omega+\alpha(x)}\underline{\lambda}_{1x}\psi_j^{\beta(K,l)} n_x \varphi_i^K$$
$$+ \int_K C_{12}\frac{i\,\omega}{i\,\omega+\beta(y)}\underline{\mathrm{u}}_y^K \varphi_j^K \frac{\partial \varphi_i^K}{\partial y} - \int_F C_{12}\frac{i\,\omega}{i\,\omega+\beta(y)}\underline{\lambda}_{1y}\psi_j^{\beta(K,l)} n_y \varphi_i^K + \int_K C_{13}\frac{i\,\omega}{i\,\omega+\alpha(x)}\underline{\mathrm{u}}_y^K \varphi_j^K \frac{\partial \varphi_i^K}{\partial x}$$
$$- \int_F C_{13}\frac{i\,\omega}{i\,\omega+\alpha(x)}\underline{\lambda}_{1y}\psi_j^{\beta(K,l)} n_x \varphi_i^K + \int_K C_{13}\frac{i\,\omega}{i\,\omega+\beta(y)}\underline{\mathrm{u}}_x^K \varphi_j^K \frac{\partial \varphi_i^K}{\partial y} - \int_F C_{13}\frac{i\,\omega}{i\,\omega+\beta(y)}\underline{\lambda}_{1x}\psi_j^{\beta(K,l)} n_y \varphi_i^K = 0\,,$$

$$\int_K \mathrm{i}\omega \underline{\tau}_{yy}^K \varphi_j^K \varphi_i^K + \int_K \mathrm{i}\omega\alpha_{22}\underline{\mathrm{p}}^K \varphi_j^K \varphi_i^K + \int_K C_{12}\frac{i\,\omega}{i\,\omega+\alpha(x)}\underline{\mathrm{u}}_x^K \varphi_j^K \frac{\partial \varphi_i^K}{\partial x} - \int_F C_{12}\frac{i\,\omega}{i\,\omega+\alpha(x)}\underline{\lambda}_{1x}\psi_j^{\beta(K,l)} n_x \varphi_i^K$$
$$+ \int_K C_{22}\frac{i\,\omega}{i\,\omega+\beta(y)}\underline{\mathrm{u}}_y^K \varphi_j^K \frac{\partial \varphi_i^K}{\partial y} - \int_F C_{22}\frac{i\,\omega}{i\,\omega+\beta(y)}\underline{\lambda}_{1y}\psi_j^{\beta(K,l)} n_y \varphi_i^K + \int_K C_{23}\frac{i\,\omega}{i\,\omega+\alpha(x)}\underline{\mathrm{u}}_y^K \varphi_j^K \frac{\partial \varphi_i^K}{\partial x}$$
$$- \int_F C_{23}\frac{i\,\omega}{i\,\omega+\alpha(x)}\underline{\lambda}_{1y}\psi_j^{\beta(K,l)} n_x \varphi_i^K + \int_K C_{23}\frac{i\,\omega}{i\,\omega+\beta(y)}\underline{\mathrm{u}}_x^K \varphi_j^K \frac{\partial \varphi_i^K}{\partial y} - \int_F C_{23}\frac{i\,\omega}{i\,\omega+\beta(y)}\underline{\lambda}_{1x}\psi_j^{\beta(K,l)} n_y \varphi_i^K = 0\,,$$

$$\int_K \mathrm{i}\omega \underline{\tau}_{yy}^K \varphi_j^K \varphi_i^K + \int_K \mathrm{i}\omega\alpha_{22}\mathrm{p}_h \varphi_j^K \varphi_i^K + \int_K C_{13}\frac{i\,\omega}{i\,\omega+\alpha(x)}\underline{\mathrm{u}}_x^K \varphi_j^K \frac{\partial \varphi_i^K}{\partial x} - \int_F C_{13}\frac{i\,\omega}{i\,\omega+\alpha(x)}\underline{\lambda}_{1x}\psi_j^{\beta(K,l)} n_x \varphi_i^K$$
$$+ \int_K C_{23}\frac{i\,\omega}{i\,\omega+\beta(y)}\underline{\mathrm{u}}_y^K \varphi_j^K \frac{\partial \varphi_i^K}{\partial y} - \int_F C_{23}\frac{i\,\omega}{i\,\omega+\beta(y)}\underline{\lambda}_{1y}\psi_j^{\beta(K,l)} n_y \varphi_i^K + \int_K C_{33}\frac{i\,\omega}{i\,\omega+\alpha(x)}\underline{\mathrm{u}}_y^K \varphi_j^K \frac{\partial \varphi_i^K}{\partial x}$$
$$- \int_F C_{33}\frac{i\,\omega}{i\,\omega+\alpha(x)}\underline{\lambda}_{1y}\psi_j^{\beta(K,l)} n_x \varphi_i^K + \int_K C_{33}\frac{i\,\omega}{i\,\omega+\beta(y)}\underline{\mathrm{u}}_x^K \varphi_j^K \frac{\partial \varphi_i^K}{\partial y} - \int_F C_{33}\frac{i\,\omega}{i\,\omega+\beta(y)}\underline{\lambda}_{1x}\psi_j^{\beta(K,l)} n_y \varphi_i^K = 0\,,$$

$$\int_K \mathrm{i}\omega \underline{\mathrm{p}}^K \varphi_j^K \varphi_i^K + \int_K M\frac{i\,\omega}{i\,\omega+\alpha(x)}\underline{\mathrm{w}}_x^K \frac{\partial \varphi_j^K}{\partial x}\varphi_i^K - \int_F M\gamma_2\frac{i\,\omega}{i\,\omega+\alpha(x)}(\underline{\mathrm{p}}^K \varphi_j^K - \underline{\lambda}_2\psi_j^{\beta(K,l)}) n_x^2 \varphi_i^K$$
$$- \int_F M\gamma_4\frac{i\,\omega}{i\,\omega+\alpha(x)}(\underline{\mathrm{u}}_x^K \varphi_j^K - \underline{\lambda}_{1x}\psi_j^{\beta(K,l)}) n_x \varphi_i^K + \int_K M\frac{i\,\omega}{i\,\omega+\beta(y)}\underline{\mathrm{w}}_y^K \frac{\partial \varphi_j^K}{\partial y}\varphi_i^K - \int_F M\gamma_2\frac{i\,\omega}{i\,\omega+\beta(y)}(\underline{\mathrm{p}}^K \varphi_j^K - \underline{\lambda}_2\psi_j^{\beta(K,l)}) n_y^2 \varphi_i^K$$
$$- \int_F M\gamma_4\frac{i\,\omega}{i\,\omega+\beta(y)}(\underline{\mathrm{u}}_y^K \varphi_j^K - \underline{\lambda}_{1y}\psi_j^{\beta(K,l)}) n_y \varphi_i^K - \int_K M\alpha_{11}\frac{i\,\omega}{i\,\omega+\alpha(x)}\underline{\mathrm{u}}_x^K \varphi_j^K \frac{\partial \varphi_i^K}{\partial x} + \int_F M\alpha_{11}\frac{i\,\omega}{i\,\omega+\alpha(x)}\underline{\lambda}_{1x}\psi_j^{\beta(K,l)} n_x \varphi_i^K$$
$$- \int_K M\alpha_{22}\frac{i\,\omega}{i\,\omega+\beta(y)}\underline{\mathrm{u}}_y^K \varphi_j^K \frac{\partial \varphi_i^K}{\partial y} + \int_F M\alpha_{22}\frac{i\,\omega}{i\,\omega+\beta(y)}\underline{\lambda}_{1y}\psi_j^{\beta(K,l)} n_y \varphi_i^K - \int_K M\alpha_{12}\frac{i\,\omega}{i\,\omega+\beta(y)}\underline{\mathrm{u}}_x^K \varphi_j^K \frac{\partial \varphi_i^K}{\partial y}$$
$$+ \int_F M\alpha_{12}\frac{i\,\omega}{i\,\omega+\beta(y)}\underline{\lambda}_{1x}\psi_j^{\beta(K,l)} n_y \varphi_i^K - \int_K M\alpha_{12}\frac{i\,\omega}{i\,\omega+\alpha(x)}\underline{\mathrm{u}}_y^K \varphi_j^K \frac{\partial \varphi_i^K}{\partial x} + \int_F M\alpha_{12}\frac{i\,\omega}{i\,\omega+\alpha(x)}\underline{\lambda}_{1y}\psi_j^{\beta(K,l)} n_x \varphi_i^K = 0\,,$$

We define and recall the following matrices:

$$\begin{aligned}
&\mathbb{M}_{ij}^K = \int_K \varphi_i^K \varphi_j^K dX\,, \qquad \mathbb{D}_{vij}^K = \int_K \varphi_j^K \frac{\partial \varphi_i^K}{\partial l} dX\,, \qquad \mathbb{J}_{vij}^F = \int_F \varphi_i^K \varphi_j^K n_v\, dS\,,\\
&\mathbb{Q}_{vij}^F = \int_F \varphi_i^K \psi_j^F n_u\, dS\,, \qquad \mathbb{L}_{uvij}^F = \int_F \varphi_i^K \psi_j^F n_u n_v dS\,, \qquad \mathbb{N}_{uvij}^F = \int_F \varphi_i^K \varphi_j^K n_u n_v dS\,,
\end{aligned} \tag{71}$$

with $u = x, y$, $v = x, y$. The elementary matrices $\mathbb{A}^K$ and $\mathbb{B}^K$ are then expressed as follows:

$$\mathbb{A}^K = \begin{pmatrix} \mathbb{A}_1^K & \mathbb{A}_2^K & \mathbb{A}_3^K & \mathbb{A}_4^K & \mathbb{A}_5^K & \mathbb{A}_6^K & \mathbb{A}_7^K & \mathbb{A}_8^K \end{pmatrix}, \tag{72}$$

with

$$\mathbb{A}_1^K = \begin{pmatrix} \mathrm{i}\,\omega\rho_a^K\mathbb{M}^K + \sum_{l=1}^{3}\gamma_1\left(\frac{i\,\omega}{i\,\omega+\alpha(x)}\mathbb{N}_{xl}^K + \frac{i\,\omega}{i\,\omega+\beta(y)}\mathbb{N}_{yl}^K\right) \\ 0 \\ \mathrm{i}\,\omega\rho_f^K\mathbb{M}^K \\ 0 \\ \left(C_{11}\frac{i\,\omega}{i\,\omega+\alpha(x)}\mathbb{D}_x^K + C_{13}\frac{i\,\omega}{i\,\omega+\beta(y)}\mathbb{D}_y^K\right) \\ \left(C_{12}\frac{i\,\omega}{i\,\omega+\alpha(x)}\mathbb{D}_x^K + C_{23}\frac{i\,\omega}{i\,\omega+\beta(y)}\mathbb{D}_y^K\right) \\ \left(C_{13}\frac{i\,\omega}{i\,\omega+\alpha(x)}\mathbb{D}_x^K + C_{33}\frac{i\,\omega}{i\,\omega+\beta(y)}\mathbb{D}_y^K\right) \\ -M\left(\sum_{l=1}^{3}\gamma_4\frac{i\,\omega}{i\,\omega+\alpha(x)}\mathbb{J}_{xl}^K + \alpha_{11}\frac{i\,\omega}{i\,\omega+\alpha(x)}\mathbb{D}_x^K + \alpha_{12}\frac{i\,\omega}{i\,\omega+\beta(y)}\mathbb{D}_y^K\right) \end{pmatrix},$$

$$\mathbb{A}_2^K = \begin{pmatrix} 0 \\ \mathrm{i}\,\omega\rho_a^K\mathbb{M}^K + \sum_{l=1}^{3}\gamma_1\left(\frac{i\,\omega}{i\,\omega+\alpha(x)}\mathbb{N}_{xl}^K + \frac{i\,\omega}{i\,\omega+\beta(y)}\mathbb{N}_{yl}^K\right) \\ 0 \\ \mathrm{i}\,\omega\rho_f^K\mathbb{M}^K \\ \left(C_{13}\frac{i\,\omega}{i\,\omega+\alpha(x)}\mathbb{D}_x^K + C_{12}\frac{i\,\omega}{i\,\omega+\beta(y)}\mathbb{D}_y^K\right) \\ \left(C_{23}\frac{i\,\omega}{i\,\omega+\alpha(x)}\mathbb{D}_x^K + C_{22}\frac{i\,\omega}{i\,\omega+\beta(y)}\mathbb{D}_y^K\right) \\ \left(C_{33}\frac{i\,\omega}{i\,\omega+\alpha(x)}\mathbb{D}_x^K + C_{23}\frac{i\,\omega}{i\,\omega+\beta(y)}\mathbb{D}_y^K\right) \\ -M\left(\sum_{l=1}^{3}\gamma_4\frac{i\,\omega}{i\,\omega+\beta(y)}\mathbb{J}_{yl}^K + \alpha_{12}\frac{i\,\omega}{i\,\omega+\alpha(x)}\mathbb{D}_x^K + \alpha_{22}\frac{i\,\omega}{i\,\omega+\beta(y)}\mathbb{D}_y^K\right) \end{pmatrix},$$

$$\mathbb{A}_3^K = \begin{pmatrix} \mathrm{i}\,\omega\rho_f^K\mathbb{M}^K \\ 0 \\ \mathrm{i}\,\omega\tilde{\rho}^K\mathbb{M}^K \\ 0 \\ 0 \\ 0 \\ 0 \\ M\frac{i\,\omega}{i\,\omega+\alpha(x)}\mathbb{D}_x^{K^T} \end{pmatrix}, \qquad \mathbb{A}_4^K = \begin{pmatrix} 0 \\ \mathrm{i}\,\omega\rho_f^K\mathbb{M}^K \\ 0 \\ \mathrm{i}\,\omega\tilde{\rho}^K\mathbb{M}^K \\ 0 \\ 0 \\ 0 \\ M\frac{i\,\omega}{i\,\omega+\beta(y)}\mathbb{D}_y^{K^T} \end{pmatrix},$$

$$\mathbb{A}_5^K = \begin{pmatrix} -\frac{i\,\omega}{i\,\omega+\alpha(x)}\mathbb{D}_x^{K^T} \\ 0 \\ 0 \\ 0 \\ \mathrm{i}\,\omega\mathbb{M}^K \\ 0 \\ 0 \\ 0 \end{pmatrix}, \qquad \mathbb{A}_6^K = \begin{pmatrix} 0 \\ -\frac{i\,\omega}{i\,\omega+\beta(y)}\mathbb{D}_y^{K^T} \\ 0 \\ 0 \\ 0 \\ \mathrm{i}\,\omega\mathbb{M}^K \\ 0 \\ 0 \end{pmatrix}, \qquad \mathbb{A}_7^K = \begin{pmatrix} -\frac{i\,\omega}{i\,\omega+\beta(y)}\mathbb{D}_y^{K^T} \\ -\frac{i\,\omega}{i\,\omega+\alpha(x)}\mathbb{D}_x^{K^T} \\ 0 \\ 0 \\ 0 \\ 0 \\ \mathrm{i}\,\omega\mathbb{M}^K \\ 0 \end{pmatrix},$$

$$\mathbb{A}_8^K = \begin{pmatrix} \sum_{l=1}^{3} \gamma_3 \frac{i\,\omega}{i\,\omega + \alpha(x)} \mathbb{J}_{xl}^K \\ \sum_{l=1}^{3} \gamma_3 \frac{i\,\omega}{i\,\omega + \beta(y)} \mathbb{J}_{yl}^K \\ -\frac{i\,\omega}{i\,\omega + \alpha(x)} \mathbb{D}_x^K \\ -\frac{i\,\omega}{i\,\omega + \beta(y)} \mathbb{D}_y^K \\ \mathrm{i}\omega \alpha_{11}^K \mathbb{M}^K \\ \mathrm{i}\,\omega \alpha_{22}^K \mathbb{M}^K \\ \mathrm{i}\,\omega \alpha_{12}^K \mathbb{M}^K \\ \mathrm{i}\,\omega \mathbb{M}^K - \sum_{l=1}^{3} M \gamma_2 \left(\frac{i\,\omega}{i\,\omega + \alpha(x)} \mathbb{N}_{xl}^K + \frac{i\,\omega}{i\,\omega + \beta(y)} \mathbb{N}_{yl}^K \right) \end{pmatrix},$$

and

$$\mathbb{B}^K = \begin{pmatrix} \mathbb{B}_{1,1}^K & \mathbb{B}_{1,2}^K & \mathbb{B}_{1,3}^K & \mathbb{B}_{2,1}^K & \mathbb{B}_{2,2}^K & \mathbb{B}_{2,3}^K & \mathbb{B}_{3,1}^K & \mathbb{B}_{3,2}^K & \mathbb{B}_{3,3}^K \end{pmatrix}, \tag{73}$$

with

$$\mathbb{B}_{1,f}^K = \begin{pmatrix} -\gamma_1 \left(\frac{i\,\omega}{i\,\omega + \alpha(x)} \mathbb{L}_{xf}^K + \frac{i\,\omega}{i\,\omega + \beta(y)} \mathbb{L}_{yf}^K \right) \\ 0 \\ 0 \\ 0 \\ \left(-C_{11} \frac{i\,\omega}{i\,\omega + \alpha(x)} \mathbb{Q}_{xf}^K - C_{13} \frac{i\,\omega}{i\,\omega + \beta(y)} \mathbb{Q}_{yf}^K \right) \\ \left(-C_{12} \frac{i\,\omega}{i\,\omega + \alpha(x)} \mathbb{Q}_{xf}^K - C_{23} \frac{i\,\omega}{i\,\omega + \beta(y)} \mathbb{Q}_{yf}^K \right) \\ \left(-C_{13} \frac{i\,\omega}{i\,\omega + \alpha(x)} \mathbb{Q}_{xf}^K - C_{33} \frac{i\,\omega}{i\,\omega + \beta(y)} \mathbb{Q}_{yf}^K \right) \\ M \left((\gamma_4 + \alpha_{11}) \frac{i\,\omega}{i\,\omega + \alpha(x)} \mathbb{Q}_{xf}^K + \alpha_{12} \frac{i\,\omega}{i\,\omega + \beta(y)} \mathbb{Q}_{yf}^K \right) \end{pmatrix}, \text{ for } f = 1, 2, 3,$$

$$\mathbb{B}_{2,f}^K = \begin{pmatrix} 0 \\ -\gamma_1 \left(\frac{i\,\omega}{i\,\omega + \alpha(x)} \mathbb{L}_{xf}^K + \frac{i\,\omega}{i\,\omega + \beta(y)} \mathbb{L}_{yf}^K \right) \\ 0 \\ 0 \\ \left(-C_{13} \frac{i\,\omega}{i\,\omega + \alpha(x)} \mathbb{Q}_{xf}^K - C_{12} \frac{i\,\omega}{i\,\omega + \beta(y)} \mathbb{Q}_{yf}^K \right) \\ \left(-C_{23} \frac{i\,\omega}{i\,\omega + \alpha(x)} \mathbb{Q}_{xf}^K - C_{22} \frac{i\,\omega}{i\,\omega + \beta(y)} \mathbb{Q}_{yf}^K \right) \\ \left(-C_{33} \frac{i\,\omega}{i\,\omega + \alpha(x)} \mathbb{Q}_{xf}^K - C_{23} \frac{i\,\omega}{i\,\omega + \beta(y)} \mathbb{Q}_{yf}^K \right) \\ M \left(\alpha_{12} \frac{i\,\omega}{i\,\omega + \alpha(x)} \mathbb{Q}_{xf}^K + (\gamma_4 + \alpha_{22}) \frac{i\,\omega}{i\,\omega + \beta(y)} \mathbb{Q}_{yf}^K \right) \end{pmatrix}, \text{ for } f = 1, 2, 3,$$

$$\mathbb{B}^K_{3,f} = \begin{pmatrix} -\gamma_3 \dfrac{i\,\omega}{i\,\omega+\alpha(x)}\mathbb{Q}^K_{xf} \\ -\gamma_3 \dfrac{i\,\omega}{i\,\omega+\beta(y)}\mathbb{Q}^K_{yf} \\ \dfrac{i\,\omega}{i\,\omega+\alpha(x)}\mathbb{Q}^K_{xf} \\ \dfrac{i\,\omega}{i\,\omega+\beta(y)}\mathbb{Q}^K_{yf} \\ 0 \\ 0 \\ 0 \\ M\gamma_2\left(\dfrac{i\,\omega}{i\,\omega+\alpha(x)}\mathbb{L}^K_{xf} + \dfrac{i\,\omega}{i\,\omega+\beta(y)}\mathbb{L}^K_{yf}\right) \end{pmatrix}, \text{ for } f = 1,2,3\,.$$

8 Numerical tests using HDG discretization

This section aims at evaluating the performance of the HDG discretization of poroelastic equations with absorbing boundary conditions or PML, which are detailed in sections 6 and 7. We first consider the influence of the geometry of the domain on the result of the numerical solution with absorbing boundary conditions in section 8.1. Then in section 8.2, we compare the two methods, absorbing boundary conditions and PML, using the analytical solution, for several configurations.

8.1 Influence of the geometry of the domain

In this section, we test the accuracy of the HDG discretization with absorbing boundary conditions. The boundary conditions have been developed for a circular geometry, and we want to test if those absorbing boundary conditions remain efficient on a different geometry. We consider an infinite porous medium, in which there is a solid obstacle, and we set artificial boundaries, in one case, circular boundaries, and in the second case squared boundaries. We run a test on an annulus described in figure 1, and for a square with a hole, see Fig. 27. The solutions are displayed in Fig. 26.

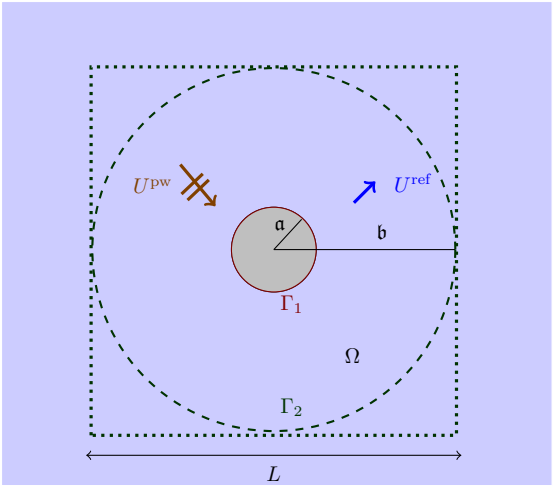

Figure 25: Scattering of a plane wave by an impenetrable solid immersed in a porous medium. The cross section of the inclusion is a disc of radius denoted by $\mathfrak{a}$. The artificial boundaries are build either on the circle $r = \mathfrak{b}$ or on the square of length L.

For the numerical tests, we use $\mathfrak{a} = 1$m and $\mathfrak{b} = 10$m, $L = 20$m (see Fig. 25). For a porous medium composed of sandstone at $f = 1$kHz, we compare the L2 error of the solution for an order of discretization between 1 and 3, for different values of viscosity and for two boundary conditions. We compare the L2 error

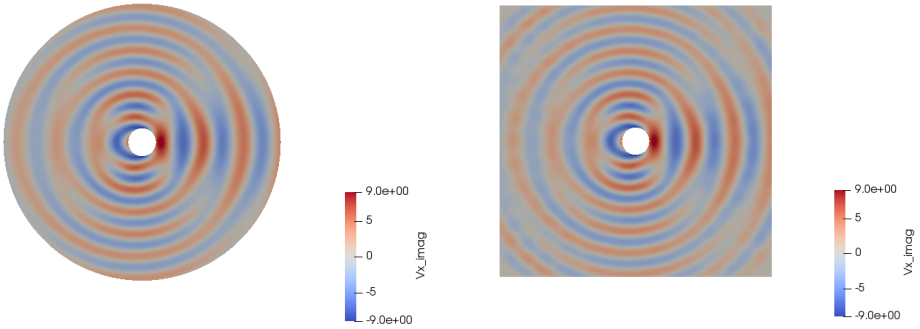

(a) $\mathfrak{b} = 10$m (b) $\mathfrak{b} = 10$m

Figure 26: Imaginary part of the solid velocity $\mathbf{u}_x$ (10^3 m.s^{-1}) of the reflected wave for absorbing boundary conditions for a porous medium composed of inviscid sandstone with $f = 1.5$ kHz and boundary conditions 3 for two different domains, with $\mathfrak{a} = 1$m and $\mathfrak{b} = 10$m, $L = 20$m.

between the analytic solution and the results with HDG for an annulus, and for a square with a hole *cf.* Table 3.

BC1	Square	Annulus
$\eta = 0$ Pa.s^{-1}	7.70	3.03
$\eta = 10^{-3}$ Pa.s^{-1}	6.09	2.16

BC3	Square	Annulus
$\eta = 0$ Pa.s^{-1}	8.26	4.00
$\eta = 10^{-3}$ Pa.s^{-1}	6.53	2.75

Table 3: L2 relative error (%) on the solid velocity between the analytic solution with absorbing conditions and the numeric solution with order of discretization 3 for $\eta = 0$ Pa.s^{-1} and $\eta = 10^{-3}$ Pa.s^{-1}. We display the solution for the scattering of a P plane wave for boundary conditions of type 1 and 3, with $\mathfrak{a} = 1$m and $\mathfrak{b} = 10$m, $L = 20$m.

As expected, for a circular geometry, the discretization of absorbing boundary conditions is efficient. For a square geometry, the absorbing boundaries remain efficient, however, the error is greater than for circular geometry, (see tab. 3). We also observe that the presence of viscosity improves the accuracy of the solution. The error is between 5 to 10%, which is comparable to the results for the LK condition in elasticity ([Tab. 7,8 [21]).

8.2 Comparison of HDG methods using ABC or PML

In this section, we compare the two methods of absorbing boundary conditions that we presented in sections 6 and 7 : low order ABC and PML applied on the HDG discretization. In the code, we use for the absorption functions (see section 7): $\alpha(x) = \beta_0\, d(x)$ and $\beta(y) = \beta_0\, d(y)$, with d the horizontal or vertical distance between the considered point and the artificial boundary. First, we compare the results on a square domain with an impenetrable obstacle, then we consider a domain composed of two porous layers.

8.2.1 Square with a hole

We consider an infinite porous medium, with a solid inclusion Γ, see Fig. 27. Here, the artificial boundary is a square.

For the two different cases, PML or absorbing boundary conditions, an outgoing wave is scattered on the obstacle, and we study the reflected solution. In this case we can compare with the analytical outgoing solution. Figure 28 shows the solution with the two different absorbing conditions. In Table 4, we present the L2 error between the solution with absorbing boundary conditions and the exact outgoing solution. We denote "ABC" for the solution with absorbing boundary conditions, "PML" for the solution with PML on the boundaries, and "exact" for the analytic outgoing solution. Note that the error is calculated only on the part of the domain

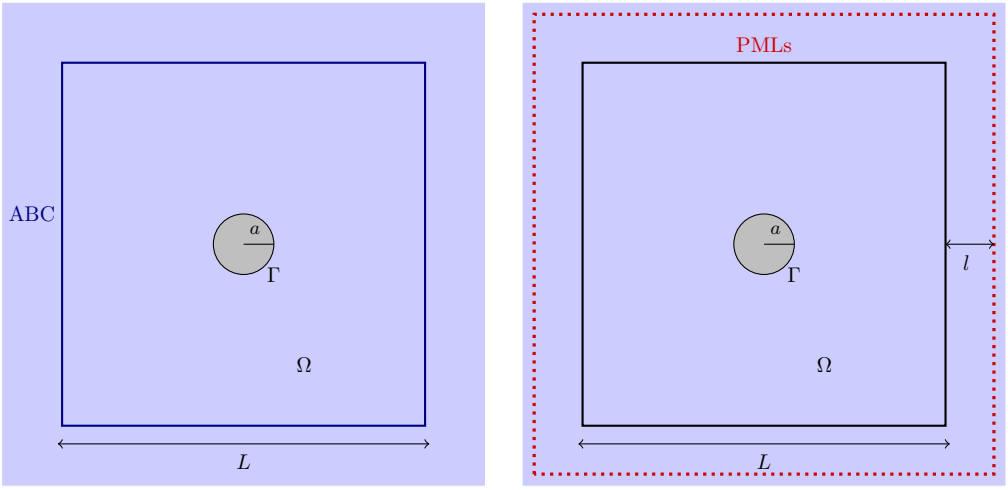

(a) Domain with ABC (b) Domain with PML

Figure 27: Infinite porous domain with a solid obstacle used for the numerical tests, in which we build absorbing boundary conditions. In the tests, we take : $a = 1\text{m}$, $L = 20\text{m}$, $\beta_0 = 6.39$, and $l = 3\text{m}$ or $l = 6\text{m}$. We can use either PML or ABC.

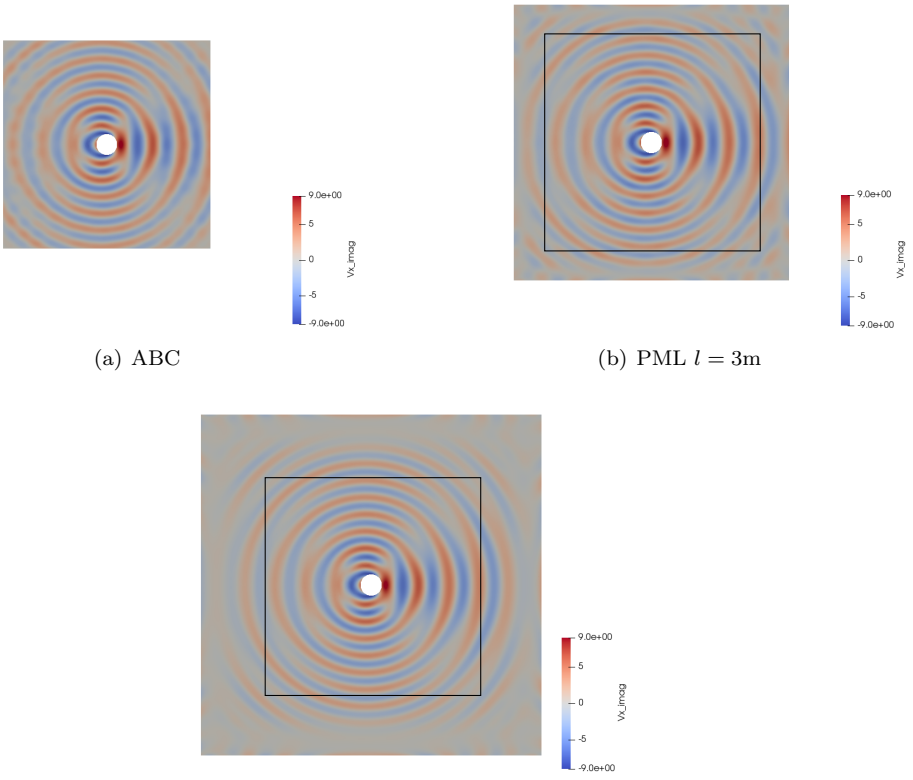

(a) ABC (b) PML $l = 3\text{m}$

(c) PML $l = 6\text{m}$

Figure 28: Imaginary part of the solid velocity $\mathbf{u}_x$ (10^3 m.s^{-1}) of the reflected wave for the scattering of a P-wave on an obstacle with boundary conditions 3 at the interior radius, for a porous medium composed of inviscid sandstone with $f = 1.5$ kHz for a domain with absorbing boundary condition and a domain with PML.

where the original is actually solved and which coincides with the domain used for the case with absorbing

boundary conditions.

BC3	ABC	PML $l = 3$m	PML $l = 6$m
$\eta = 0$ Pa.s^{-1}	7.70	10.8	3.65
$\eta = 10^{-3}$ Pa.s^{-1}	6.09	9.82	2.8

BC3	ABC	PML $l = 3$m	PML $l = 6$m
$\eta = 0$ Pa.s^{-1}	8.26	9.52	3.81
$\eta = 10^{-3}$ Pa.s^{-1}	6.53	8.72	2.78

Table 4: L2 error (%) on $\mathbf{u}_x$ between the analytic solution with absorbing conditions and the numeric solution for $\eta = 0$ Pa.s^{-1} and $\eta = 10^{-3}$ Pa.s^{-1}. We display the error for the scattering of a P plane wave for boundary conditions of type 1 and 3 on the interior radius.

	ABC	PML $l = 3$m	PML $l = 6$m
Number of edges	10974	17448	25581
Number of dof	43896	69792	102324

Table 5: Number of degrees of freedom for the three cases shown in Fig. 28, with interpolation order equals to 3.

We observe from table 4 that the PML solution with $l = 3$m generates slightly greater errors than absorbing boundary conditions and needs more computational time. However, when the size of the layer increases, ($l = 6$m), the error is lower than for the solution with ABC. It also leads to an important increase of the computational time because we need to compute the program on a larger domain (see Tab. 5).

8.2.2 Stratified domain

Secondly, we investigate the case of a two-layer stratified plane domain. We consider the configuration detailed in Fig. 29. A point-source is located in the upper medium of the domain. The four edges are non-reflective, either by a PML or Absorbing boundary condition. Table 6 gives the size of the linear system solved by the program. The size of discretization is the same in both meshes. The solutions are presented in Fig. 30.

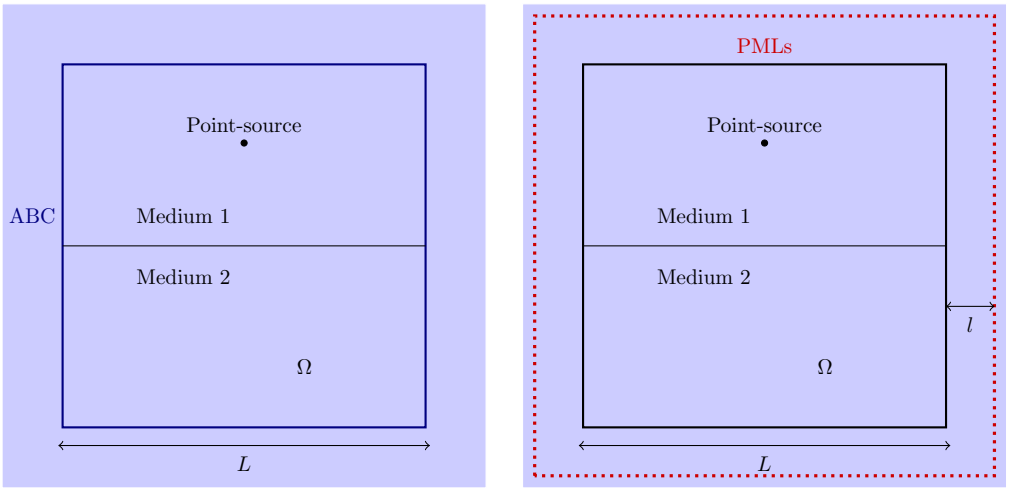

(a) Domain with ABC (b) Domain with PML

Figure 29: Stratified porous domain used for the numerical tests, in which we build absorbing boundary conditions. Here, the upper medium is composed of shale while the lower medium is composed of sandstone. The parameters of the media are detailed in Table 1. In the tests, we take : $L = 20$m, $l = 3$m.

Figures 30, 30(a) and 30(b) present similar results in the region outside of the PML. In figure 30(b) all the wave are absorbed in the PML region. However, in Fig. 30(c), with a different value of absorption parameter, the wave is not absorbed in the PML, and we observe many reflections which worsen the accuracy of the solution. Moreover, Fig. 30(d) shows that for high values of the absorbing coefficients, the energy in the PML explodes.

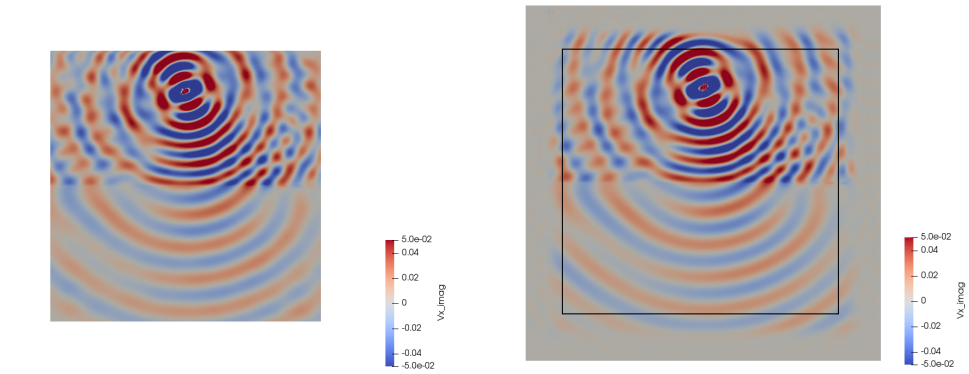

(a) ABC (b) PML with $\beta_0 = 6.39$

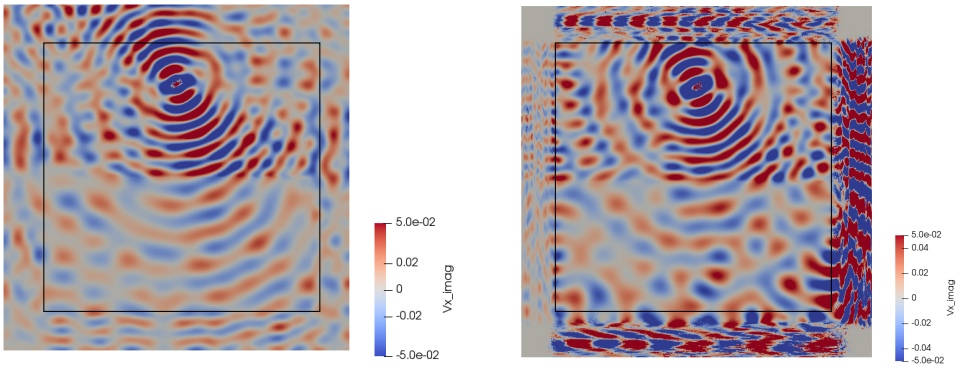

(c) PML with $\beta_0 = 0.096$ (d) PML with $\beta_0 = 63.9$

Figure 30: Imaginary part of the solid velocity $\mathbf{u}_x$ (10^3 m.s^{-1}) of the reflected wave for absorbing boundary conditions for a porous medium composed of inviscid sandstone with $f = 1$ kHz for a domain with absorbing boundary conditions and for domain with PML with different values of the absorbing coefficient.

	ABC	PML
Number of edges	9380	15949
Number of dof	37520	63796

Table 6: Number of degrees of freedom for the cases shown in Fig 30, with interpolation order equals to 3.

Indeed, the size of the layer and the value of the coefficient of absorption can have an impact on the accuracy of the solution, and the values of these parameters depend on the configuration of the test.

9 Conclusion

In this report, we have built a low-order absorbing condition for isotropic poroelastic wave equations in frequency domain. The performance of this ABC has been evaluated in two groups of numerical investigation. In the first one, in the setting of planewave scattering by circular obstacles, we compare how well the analytical solution associated to the ABC approximates the restriction of the true outgoing solution on the truncated domain. We have an overall conclusion that that our ABC has comparable robustness to LK for elasticity and Sommerfeld condition for acoustic equation, in the sense that the error is less than 10 % for most cases. In the second investigation, the absorbing condition has been implemented in a hybridizable dicontinuous Galerkin (HDG) formulation. We have also applied perfectly matched layers (PML) on the HDG discretization of the poroelastic equations. We then compare the performance of our ABC with the PML technique on different configurations. PML can be an alternative to the absorbing condition, however its performance depends on parameters that are specific to each experiment. If the size of the PML is not large enough, the performance is deteriorated. To obtain better results than ABC, the PML can be taken larger but this doubles the degrees of freedom and incurs substantial increase of the computational time, while the gain in accuracy is not considerable. This work will be used as a basis to develop ABC for porous-electromagnetic wave equations in an upcoming work.

A Expansion of an outgoing solution

In the following, we detail the system solved by ($\mathbf{u}$, $\mathbf{w}$, $\boldsymbol{\tau}$, p) with the expansion of the potentials in the case of an outgoing solution. Consider the scattering of a time-harmonic plane wave by an impenetrable infinite cylinder (see figure 31). The total wave is a superposition of the incident plane wave and the reflected wave with each quantity satisfying poroelastic equations (2) in $\mathbb{R}^2 \setminus \mathbb{B}_{(0,\mathfrak{a})}$, also listed below in (75) and (80), according to the type of boundary conditions. For $\bullet$ = total, ref, pw, we denote by

$$\mathfrak{U}^\bullet = \begin{pmatrix} \mathbf{u}^\bullet \\ \mathbf{w}^\bullet \\ \boldsymbol{\tau}^\bullet \\ \mathrm{p}^\bullet \end{pmatrix}$$

the total wave, the reflected wave and the incident plane wave correspondingly.

The unknown is the reflected wave which is outgoing, this means that it satisfies the Sommerfeld radiation condition(74), and is in addition uniquely determined by how the obstacle scatters the plane wave. For $\bullet = \mathrm{P}, \mathrm{B}, \mathrm{S}$, $\chi_\bullet$ is called $\mathsf{k}_\bullet$-outgoing if it satisfies the Sommerfeld radiation condition at wave number $\mathsf{k}_\bullet$ uniformly,

$$\lim_{r\to\infty} \sqrt{r} \left(\frac{\partial \chi_\bullet}{\partial r} - \mathrm{i}\, \mathsf{k}_\bullet\, \chi_\bullet \right) = 0\,. \tag{74}$$

Hence, the solutions $(\mathbf{u}, \mathbf{w}, \boldsymbol{\tau}, \mathrm{p})$ are given by equation (18), while the potentials are given by:

$$\begin{aligned}
\chi_{\mathrm{P}}(\boldsymbol{x}) &= \sum_{k\in\mathbb{Z}} a_k^\infty\, \mathrm{H}_k^{(1)}(\omega\, \mathsf{s}_{\mathrm{P}}\, |\boldsymbol{x}|)\; e^{\mathrm{i}\, k\, \theta}\,, \\
\chi_{\mathrm{B}}(\boldsymbol{x}) &= \sum_{k\in\mathbb{Z}} b_k^\infty\, \mathrm{H}_k^{(1)}(\omega\, \mathsf{s}_{\mathrm{B}}\, |\boldsymbol{x}|)\; e^{\mathrm{i}\, k\, \theta}\,, \\
\chi_{\mathrm{S}}(\boldsymbol{x}) &= \sum_{k\in\mathbb{Z}} c_k^\infty\, \mathrm{H}_k^{(1)}(\omega\, \mathsf{s}_{\mathrm{S}}\, |\boldsymbol{x}|)\; e^{\mathrm{i}\, k\, \theta}\,.
\end{aligned}$$

The series coefficients a_k^∞, b_k^∞, c_k^∞ are then determined by the boundary conditions imposed on the interface Γ. We will consider the boundary conditions of type 1 in A.1 and of type 3 in A.2.

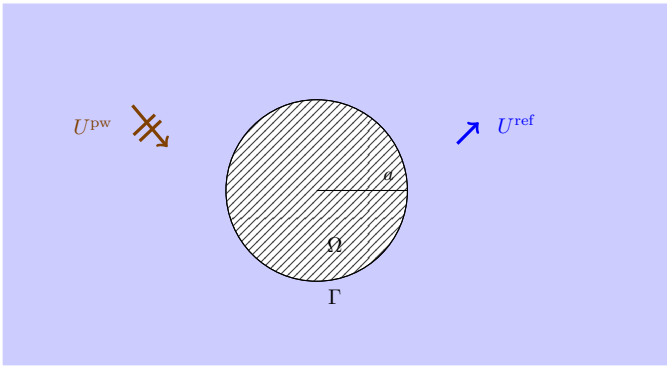

Figure 31: Scattering of a plane wave by an impenetrable solid inclusion. The inclusion occupies the domain denoted by Ω. The cross section of the inclusion is a disc of radius denoted by $\mathfrak{a}$. How the obstacle scatters the plane wave is mathematically described by boundary conditions, for example (3a) or (3c).

A.1 Boundary conditions of type 1

The unknown reflected wave solves the poroelastic problem:

$$\begin{cases} \mathfrak{U}^{\text{ref}} \text{ solves the poroelastic equations (2) in } \mathbb{R}^2 \setminus \Omega\,; \\ \mathfrak{U}^{\text{ref}} \text{ is outgoing by definition (74);} \\ \text{Boundary conditions on the interface } \Gamma \\ \quad \mathbf{w}^{\text{pw}} \cdot \mathbf{n} + \mathbf{w}^{\text{ref}} \cdot \mathbf{n} = 0 \quad , \quad \partial\mathbb{B}_{(0,\mathfrak{a})}\,; \\ \quad \boldsymbol{\tau}^{\text{pw}} \cdot \mathbf{n} + \boldsymbol{\tau}^{\text{ref}} \cdot \mathbf{n} = 0 \quad , \quad \partial\mathbb{B}_{(0,\mathfrak{a})}\,. \end{cases} \tag{75}$$

In the current geometry, $\boldsymbol{n} = \mathbf{e}_r$. Hence,

$$\begin{aligned} \mathbf{w} \cdot \boldsymbol{n} &= \mathbf{w}_r\,, & \boldsymbol{\tau} \cdot \boldsymbol{n} &= \boldsymbol{\tau}_{rr}\,\mathbf{e}_r + \boldsymbol{\tau}_{r\theta}\,\mathbf{e}_\theta\,, \\ \mathbf{w}^{\text{pw}} \cdot \boldsymbol{n} &= \mathbf{w}^{\text{pw}}_r\,, & \boldsymbol{\tau}^{\text{pw}} \cdot \boldsymbol{n} &= \boldsymbol{\tau}^{\text{pw}}_{rr}\,\mathbf{e}_r + \boldsymbol{\tau}^{\text{pw}}_{r\theta}\,\mathbf{e}_\theta\,. \end{aligned}$$

For convenience, the boundary conditions are written as:

$$\mathrm{i}\,\omega\,\mathbf{w}_r \;=\; \mathrm{i}\,\omega\,\mathbf{w}^{\text{pw}}_r\,, \quad \omega^2\,\boldsymbol{\tau}_{rr} \;=\; \omega^2\,\boldsymbol{\tau}^{\text{pw}}_{rr}\,, \quad \omega^2\,\boldsymbol{\tau}_{r\theta} \;=\; \omega^2\,\boldsymbol{\tau}^{\text{pw}}_{r\theta} \quad , \quad \partial\mathbb{B}_{(0,\mathfrak{a})}\,. \tag{76}$$

Next we expand the coefficients of each component in Fourier series. For the right hand-side,

$$\mathbf{w}^{\text{pw}}_r = \sum_{k\in\mathbb{Z}} \mathbf{w}^{\text{pw}}_{r,k}\,e^{\mathrm{i}\,k\,\theta}\,, \quad \boldsymbol{\tau}^{\text{pw}}_{rr} = \sum_{k\in\mathbb{Z}} \boldsymbol{\tau}^{\text{pw}}_{rr,k}\,e^{\mathrm{i}\,k\,\theta}\,, \quad ,\boldsymbol{\tau}^{\text{pw}}_{r\theta} = \sum_{k\in\mathbb{Z}} \boldsymbol{\tau}^{\text{pw}}_{r\theta,k}\,e^{\mathrm{i}\,k\,\theta}\,.$$

For the unknowns:

$$\mathbf{w}_r = \sum_{k\in\mathbb{Z}} \mathbf{w}_{r,k}\,e^{\mathrm{i}\,k\,\theta}\,, \quad \boldsymbol{\tau}_{rr} = \sum_{k\in\mathbb{Z}} \boldsymbol{\tau}_{rr,k}\,e^{\mathrm{i}\,k\,\theta}\,, \quad \boldsymbol{\tau}_{r\theta} = \sum_{k\in\mathbb{Z}} \boldsymbol{\tau}_{r\theta,k}\,e^{\mathrm{i}\,k\,\theta}\,.$$

Using (18), we have:

$$
\begin{aligned}
\mathrm{i}\,\omega\,\mathbf{w}_{r,k} =& a_k^\infty\,\frac{\beta_{\mathrm{P}}}{\mathsf{s}_{\mathrm{P}}}\,\omega\,\mathrm{H}_k^{(1)'}(\omega\,\mathsf{s}_{\mathrm{P}}\,|\boldsymbol{x}|)\,e^{\mathrm{i}k\theta}\;+\;b_k^\infty\,\frac{\beta_{\mathrm{B}}}{\mathsf{s}_{\mathrm{B}}}\,\omega\,\mathrm{H}_k^{(1)'}(\omega\,\mathsf{s}_{\mathrm{B}}\,|\boldsymbol{x}|)\,e^{\mathrm{i}k\theta}\;+\;c_k^\infty\,\frac{\rho_f\,\mu_{\mathrm{fr}}}{\det A}\,\frac{\mathrm{i}k}{|\boldsymbol{x}|}\mathrm{H}_k^{(1)}(\omega\,\mathsf{s}_{\mathrm{S}}\,|\boldsymbol{x}|)\,e^{\mathrm{i}k\theta},\\
\omega^2\boldsymbol{\tau}_{rr,k} =& -\frac{2\mu_{\mathrm{fr}}\,\omega}{\mathsf{s}_{\mathrm{P}}\,|\boldsymbol{x}|}\,a_k^\infty\,\mathrm{H}_{k+1}^{(1)}(\omega\,\mathsf{s}_{\mathrm{P}}\,|\boldsymbol{x}|)\,e^{\mathrm{i}\,k\,\theta}\;+\;\frac{2\,\mu_{\mathrm{fr}}\,k}{\mathsf{s}_{\mathrm{P}}^2\,|\boldsymbol{x}|^2}\,a_k^\infty\,\mathrm{H}_k^{(1)}(\omega\,\mathsf{s}_{\mathrm{P}}\,|\boldsymbol{x}|)\,e^{\mathrm{i}\,k\,\theta}\;+2\mu_{\mathrm{fr}}\,a_k^\infty\,\omega^2\,\mathrm{H}_k^{(1)}(\omega\,\mathsf{s}_{\mathrm{P}}\,|\boldsymbol{x}|)\,e^{\mathrm{i}\,k\,\theta}\\
&-\frac{2\,\mu_{\mathrm{fr}}\,k^2}{\mathsf{s}_{\mathrm{P}}^2\,|\boldsymbol{x}|^2}\,a_k^\infty\,\mathrm{H}_k^{(1)}(\omega\,\mathsf{s}_{\mathrm{P}}\,|\boldsymbol{x}|)\,e^{\mathrm{i}\,k\,\theta}-\frac{2\,\mu_{\mathrm{fr}}\,\omega}{\mathsf{s}_{\mathrm{B}}\,|\boldsymbol{x}|}\,b_k^\infty\,\mathrm{H}_{k+1}^{(1)}(\omega\,\mathsf{s}_{\mathrm{B}}\,|\boldsymbol{x}|)\,e^{\mathrm{i}\,k\,\theta}\;+\;\frac{2\mu_{\mathrm{fr}}\,k}{\mathsf{s}_{\mathrm{B}}^2\,|\boldsymbol{x}|^2}b_k^\infty\,\mathrm{H}_k^{(1)}(\omega\,\mathsf{s}_{\mathrm{B}}\,|\boldsymbol{x}|)\,e^{\mathrm{i}\,k\,\theta}\\
&+2\mu_{\mathrm{fr}}\,b_k^\infty\,\omega^2\,\mathrm{H}_k^{(1)}(\omega\,\mathsf{s}_{\mathrm{B}}\,|\boldsymbol{x}|)\,e^{\mathrm{i}\,k\,\theta}\;-\;\frac{2\,\mu_{\mathrm{fr}}\,k^2}{\mathsf{s}_{\mathrm{B}}^2\,|\boldsymbol{x}|^2}b_k^\infty\,\mathrm{H}_k^{(1)}(\omega\,\mathsf{s}_{\mathrm{B}}\,|\boldsymbol{x}|)\,e^{\mathrm{i}\,k\,\theta}\;+\;\frac{2\,\mu_{\mathrm{fr}}}{\mathsf{s}_{\mathrm{S}}^2 r}c_k^\infty\,\omega\,\mathsf{s}_{\mathrm{S}}\,\mathrm{i}k\,\mathrm{H}_k^{(1)'}(\omega\,\mathsf{s}_{\mathrm{S}}\,|\boldsymbol{x}|)\,e^{\mathrm{i}\,k\,\theta}\\
&+\omega^2\,\left(-\tfrac{2}{3}\mu_{\mathrm{fr}}\;+\;\mathrm{k}_{\mathrm{fr}}\;+\;M\alpha^2\;+\;\alpha\,M\beta_{\mathrm{P}}\right)\;a_k^\infty\,\mathrm{H}_k^{(1)}(\omega\,\mathsf{s}_{\mathrm{P}}\,|\boldsymbol{x}|)\;e^{\mathrm{i}\,k\,\theta}\\
&+\omega^2\,\left(-\tfrac{2}{3}\mu_{\mathrm{fr}}\;+\;\mathrm{k}_{\mathrm{fr}}\;+\;M\alpha^2\;+\;\alpha\,M\beta_{\mathrm{B}}\right)\;b_k^\infty\,\mathrm{H}_k^{(1)}(\omega\,\mathsf{s}_{\mathrm{B}}\,|\boldsymbol{x}|)\;e^{\mathrm{i}\,k\,\theta},\\
\omega^2\,\boldsymbol{\tau}_{r\theta,k} =& -\frac{2\mu_{\mathrm{fr}}\omega\,\mathrm{i}k}{|\boldsymbol{x}|\mathsf{s}_{\mathrm{P}}}a_k^\infty\mathrm{H}_k^{(1)'}(\omega\,\mathsf{s}_{\mathrm{P}}|\boldsymbol{x}|)\,e^{\mathrm{i}\,k\,\theta}+\frac{2\mathrm{i}\,\mu_{\mathrm{fr}}k}{|\boldsymbol{x}|^2\,\mathsf{s}_{\mathrm{P}}^2}a_k^\infty\mathrm{H}_k^{(1)}(\omega\,\mathsf{s}_{\mathrm{P}}\,|\boldsymbol{x}|)\,e^{\mathrm{i}\,k\,\theta}\;-\;\frac{2\mu_{\mathrm{fr}}\omega\,\mathrm{i}\,k}{|\boldsymbol{x}|\,\mathsf{s}_{\mathrm{B}}}b_k^\infty\mathrm{H}_k^{(1)'}(\omega\,\mathsf{s}_{\mathrm{B}}|\boldsymbol{x}|)\,e^{\mathrm{i}\,k\,\theta}\\
&+\frac{2\,\mathrm{i}\,\mu_{\mathrm{fr}}\,k}{|\boldsymbol{x}|^2\mathsf{s}_{\mathrm{B}}^2}\,b_k^\infty\,\mathrm{H}_k^{(1)}(\omega\,\mathsf{s}_{\mathrm{B}}|\boldsymbol{x}|)\;e^{\mathrm{i}\,k\,\theta}\;-\;\frac{\mu_{\mathrm{fr}}\,k^2}{|\boldsymbol{x}|^2\,\mathsf{s}_{\mathrm{S}}^2}\,c_k^\infty\,\mathrm{H}_k^{(1)}(\omega\,\mathsf{s}_{\mathrm{S}}\,|\boldsymbol{x}|)\;e^{\mathrm{i}\,k\,\theta}\;+\;\frac{\mu_{\mathrm{fr}}\,\omega}{|\boldsymbol{x}|\,\mathsf{s}_{\mathrm{S}}}\,c_k^\infty\,\mathrm{H}_k^{(1)'}(\omega\,\mathsf{s}_{\mathrm{S}}\,|\boldsymbol{x}|)\;e^{\mathrm{i}\,k\,\theta}\\
&-\mu_{\mathrm{fr}}\,\frac{\omega}{\mathsf{s}_{\mathrm{S}}\,|\boldsymbol{x}|}\,c_k^\infty\,\mathrm{H}_{k+1}^{(1)}(\omega\,\mathsf{s}_{\mathrm{S}}\,|\boldsymbol{x}|)\;e^{\mathrm{i}\,k\,\theta}\;+\mu_{\mathrm{fr}}\,\frac{k}{\mathsf{s}_{\mathrm{S}}^2\,|\boldsymbol{x}|^2}c_k^\infty\,\mathrm{H}_k^{(1)}(\omega\,\mathsf{s}_{\mathrm{S}}\,|\boldsymbol{x}|)\;e^{\mathrm{i}\,k\,\theta}\\
&+\omega^2\,c_k^\infty\,\mathrm{H}_k^{(1)}(\omega\,\mathsf{s}_{\mathrm{S}}\,|\boldsymbol{x}|)\;e^{\mathrm{i}\,k\,\theta}\;-\;\mu_{\mathrm{fr}}\,\frac{k^2}{\mathsf{s}_{\mathrm{S}}^2\,|\boldsymbol{x}|^2}\,c_k^\infty\,\mathrm{H}_k^{(1)}(\omega\,\mathsf{s}_{\mathrm{S}}\,|\boldsymbol{x}|)\;e^{\mathrm{i}\,k\,\theta}.
\end{aligned}
\tag{77}
$$

Here, the second derivatives of the Hankel functions are replaced using equation (21). Imposing (76), we obtain a linear system satisfied by a_k^∞, b_k^∞, c_k^∞ in each mode k.

$$
\mathbb{A}_k^{\mathbf{w},\boldsymbol{\tau}}\begin{pmatrix}a_k^\infty\\ b_k^\infty\\ c_k^\infty\end{pmatrix}=\begin{pmatrix}-\,\mathrm{i}\,\omega\,\mathbf{w}_r^{\mathrm{pw}}\\ -\omega^2\,\boldsymbol{\tau}_{rr}^{\mathrm{pw}}\\ -\omega^2\,\boldsymbol{\tau}_{r\theta}^{\mathrm{pw}}\end{pmatrix},
\tag{78}
$$

where the coefficient matrix is defined as:

$$
\mathbb{A}_k^{\mathbf{w},\boldsymbol{\tau}}=\begin{pmatrix}A_{11}&A_{12}&A_{13}\\ A_{21}&A_{22}&A_{23}\\ A_{31}&A_{32}&A_{33}\end{pmatrix}
\tag{79}
$$

with

$$
\begin{aligned}
A_{11} =& \frac{\beta_{\mathrm{P}}}{\mathsf{s}_{\mathrm{P}}}\,\omega\,\mathrm{H}_k^{(1)'}(\omega\,\mathsf{s}_{\mathrm{P}}\mathfrak{a}),\qquad A_{12}=\frac{\beta_{\mathrm{B}}}{\mathsf{s}_{\mathrm{B}}}\,\omega\,\mathrm{H}_k^{(1)'}(\omega\,\mathsf{s}_{\mathrm{S}}\mathfrak{a})\qquad A_{13}=\frac{\rho_f\,\mu_{\mathrm{fr}}}{\det A}\,\frac{\mathrm{i}k}{\mathfrak{a}}\mathrm{H}_k^{(1)}(\omega\,\mathsf{s}_{\mathrm{S}}\mathfrak{a}),\\
A_{21} =& -\frac{2\,\mu_{\mathrm{fr}}\,\omega}{\mathsf{s}_{\mathrm{P}}\,\mathfrak{a}}\,\mathrm{H}_{k+1}^{(1)}(\omega\,\mathsf{s}_{\mathrm{P}}\,\mathfrak{a})\;e^{\mathrm{i}\,k\,\theta}\;+\;\frac{2\,\mu_{\mathrm{fr}}\,k}{\mathsf{s}_{\mathrm{P}}^2\,\mathfrak{a}^2}\,\mathrm{H}_k^{(1)}(\omega\,\mathsf{s}_{\mathrm{P}}\,\mathfrak{a})\;+\;2\,\mu_{\mathrm{fr}}\,\omega^2\,\mathrm{H}_k^{(1)}(\omega\,\mathsf{s}_{\mathrm{P}}\,\mathfrak{a})\\
&-\;\frac{2\,\mu_{\mathrm{fr}}\,k^2}{\mathsf{s}_{\mathrm{P}}^2\,\mathfrak{a}^2}\,\mathrm{H}_k^{(1)}(\omega\,\mathsf{s}_{\mathrm{P}}\,\mathfrak{a})\;+\omega^2\,\left(-\tfrac{2}{3}\mu_{\mathrm{fr}}\;+\;\mathrm{k}_{\mathrm{fr}}\;+\;M\alpha^2\;+\;\alpha\,M\beta_{\mathrm{P}}\right)\mathrm{H}_k^{(1)}(\omega\,\mathsf{s}_{\mathrm{P}}\mathfrak{a}),\\
A_{22} =& -\frac{2\,\mu_{\mathrm{fr}}\,\omega}{\mathsf{s}_{\mathrm{B}}\,\mathfrak{a}}\,\mathrm{H}_{k+1}^{(1)}(\omega\,\mathsf{s}_{\mathrm{B}}\,\mathfrak{a})\;+\;\frac{2\,\mu_{\mathrm{fr}}\,k}{\mathsf{s}_{\mathrm{B}}^2\,\mathfrak{a}^2}\,\mathrm{H}_k^{(1)}(\omega\,\mathsf{s}_{\mathrm{B}}\,\mathfrak{a})\;+\;2\,\mu_{\mathrm{fr}}\,\omega^2\,\mathrm{H}_k^{(1)}(\omega\,\mathsf{s}_{\mathrm{B}}\,\mathfrak{a})\\
&-\;\frac{2\,\mu_{\mathrm{fr}}\,k^2}{\mathsf{s}_{\mathrm{B}}^2\,\mathfrak{a}^2}\,\mathrm{H}_k^{(1)}(\omega\,\mathsf{s}_{\mathrm{B}}\,\mathfrak{a})\;+\omega^2\,\left(-\tfrac{2}{3}\mu_{\mathrm{fr}}\;+\;\mathrm{k}_{\mathrm{fr}}\;+\;M\alpha^2\;+\;\alpha\,M\beta_{\mathrm{B}}\right)\mathrm{H}_k^{(1)}(\omega\,\mathsf{s}_{\mathrm{B}}\mathfrak{a}),
\end{aligned}
$$

and

$$
\begin{aligned}
A_{23} &= \frac{2\mu_{\rm fr}}{\mathsf{s}_{\rm S}\mathfrak{a}}\,\omega\,\mathrm{i}k\,\mathrm{H}_k^{(1)'}(\omega\,\mathsf{s}_{\rm S}\mathfrak{a})\,,\\
A_{31} &= -\frac{2\omega\,\mu_{\rm fr}\mathrm{i}k}{\mathfrak{a}\mathsf{s}_{\rm P}}\mathrm{H}_k^{(1)'}(\omega\,\mathsf{s}_{\rm P}\mathfrak{a}) + \frac{2\,\mu_{\rm fr}\mathrm{i}k}{\mathfrak{a}^2\mathsf{s}_{\rm P}^2}\mathrm{H}_k^{(1)}(\omega\,\mathsf{s}_{\rm P}\mathfrak{a})\,,\\
A_{32} &= -\frac{2\omega\,\mu_{\rm fr}\mathrm{i}k}{\mathfrak{a}\mathsf{s}_{\rm B}}\mathrm{H}_k^{(1)'}(\omega\,\mathsf{s}_{\rm B}\mathfrak{a}) + \frac{2\mu_{\rm fr}\mathrm{i}k}{\mathfrak{a}^2\mathsf{s}_{\rm B}^2}\mathrm{H}_k^{(1)}(\omega\,\mathsf{s}_{\rm B}\mathfrak{a})\,,\\
A_{33} &= -\frac{k^2\mu_{\rm fr}}{\mathfrak{a}^2\mathsf{s}_{\rm S}^2}\mathrm{H}_k^{(1)}(\omega\,\mathsf{s}_{\rm S}\,\mathfrak{a}) + \frac{\omega\,\mu_{\rm fr}}{\mathfrak{a}\mathsf{s}_{\rm S}}\mathrm{H}_k^{(1)'}(\omega\,\mathsf{s}_{\rm S}\,\mathfrak{a}) \;-\; \frac{\omega}{\mathsf{s}_{\rm S}\,\mathfrak{a}}\,\mathrm{H}_{k+1}^{(1)}(\mathsf{s}_{\rm S}\,\mathfrak{a}) \;+\; \frac{k}{\mathsf{s}_{\rm S}^2\,\mathfrak{a}^2}\,\mathrm{H}_k^{(1)}(\omega\,\mathsf{s}_{\rm S}\,\mathfrak{a})\;,\\
&\quad +\,\omega^2\,\mathrm{H}_k^{(1)}(\omega\,\mathsf{s}_{\rm S}\,\mathfrak{a})\;e^{\mathrm{i}\,k\,\theta} \;-\; \frac{k^2}{\mathsf{s}_{\rm S}^2\,\mathfrak{a}^2}\,\mathrm{H}_k^{(1)}(\omega\,\mathsf{s}_{\rm S}\,\mathfrak{a})\;.
\end{aligned}
$$

A.2 Boundary conditions of type 3

In this case, the unknown reflected wave solves the following poroelastic problem:

$$
\begin{cases}
\mathfrak{U}^{\rm ref} \text{ solves the poroelastic equations (2) in } \mathbb{R}^2\setminus\Omega\,;\\[2ex]
\mathfrak{U}^{\rm ref} \text{ is outgoing by definition (74) ;}\\[2ex]
\text{Boundary conditions on the interface } \Gamma\\
\quad \mathbf{v}^{\rm pw}+\mathbf{v}^{\rm ref}=0 \;\text{ on }\Gamma\,,\\
\quad \mathrm{p}^{\rm pw}+\mathrm{p}^{\rm ref}=0 \;\text{ on }\Gamma\,.
\end{cases}
\tag{80}
$$

We work in polar coordinates, $\mathbf{u}^{\rm pw}=\mathbf{u}_r^{\rm pw}\mathbf{e}_r+\mathbf{u}_\theta^{\rm pw}\,\mathbf{e}_\theta$ and $\mathbf{u}=\mathbf{u}_r\mathbf{e}_r+\mathbf{u}_\theta\,\mathbf{e}_\theta$. The boundary conditions are written as:

$$
\mathrm{i}\,\omega\,\mathbf{u}_r \;=\; -\,\mathrm{i}\,\omega\,\mathbf{u}_r^{\rm pw}\,,\quad \mathrm{i}\,\omega\,\mathbf{u}_\theta \;=\; -\,\mathrm{i}\,\omega\,\mathbf{u}_\theta^{\rm pw}\,,\quad \mathrm{p}\;=\;-\,\mathrm{p}^{\rm pw}\quad,\quad \partial\mathbb{B}_{(0,\mathfrak{a})}\,. \tag{81}
$$

We expand the coefficient of each component in Fourier series. For the right hand-side,

$$
\mathbf{u}_r^{\rm pw}=\sum_{k\in\mathbb{Z}}\mathbf{u}_{r,k}^{\rm pw}\,e^{\mathrm{i}\,k\,\theta}\,,\quad \mathbf{u}_\theta^{\rm pw}=\sum_{k\in\mathbb{Z}}\mathbf{u}_{\theta,k}^{\rm pw}\,e^{\mathrm{i}\,k\,\theta}\,,\quad \mathrm{p}^{\rm pw}=\sum_{k\in\mathbb{Z}}\mathrm{p}_k^{\rm pw}\,e^{\mathrm{i}\,k\,\theta}\,.
$$

For the unknowns:

$$
\mathbf{u}_r=\sum_{k\in\mathbb{Z}}\mathbf{u}_{r,k}\,e^{\mathrm{i}\,k\,\theta}\,,\quad \mathbf{u}_\theta=\sum_{k\in\mathbb{Z}}\mathbf{u}_{\theta,k}\,e^{\mathrm{i}\,k\,\theta}\,,\quad \mathrm{p}_k=\sum_{k\in\mathbb{Z}}\mathrm{p}_k\,e^{\mathrm{i}\,k\,\theta}\,.
$$

Using (18), we have:

$$
\begin{aligned}
\mathrm{i}\,\omega\,\mathbf{u}_{r,k} \;&=\; a_k^\infty\;\mathsf{s}_{\rm P}^{-1}\,\omega\,\mathrm{H}_k^{(1)'}(\omega\,\mathsf{s}_{\rm P}\,|\boldsymbol{x}|)e^{\mathrm{i}k\theta} \;+\; b_k^\infty\;\mathsf{s}_{\rm B}^{-1}\,\omega\,\mathrm{H}_k^{(1)'}(\omega\,\mathsf{s}_{\rm B}\,|\boldsymbol{x}|)e^{\mathrm{i}k\theta} \;-\; c_k^\infty\;\mathsf{s}_{\rm S}^{-2}\,\frac{\mathrm{i}k}{|\boldsymbol{x}|}\mathrm{H}_k^{(1)}(\omega\,\mathsf{s}_{\rm S}\,|\boldsymbol{x}|)e^{\mathrm{i}k\theta}\,,\\
\mathrm{i}\,\omega\,\mathbf{u}_{\theta,k} \;&=\; a_k^\infty\;\mathsf{s}_{\rm P}^{-2}\,\frac{\mathrm{i}k}{|\boldsymbol{x}|}\mathrm{H}_k^{(1)}(\omega\,\mathsf{s}_{\rm P}\,|\boldsymbol{x}|)e^{\mathrm{i}k\theta} \;+\; b_k^\infty\;\mathsf{s}_{\rm B}^{-2}\,\frac{\mathrm{i}k}{|\boldsymbol{x}|}\mathrm{H}_k^{(1)}(\omega\,\mathsf{s}_{\rm B}\,|\boldsymbol{x}|)e^{\mathrm{i}k\theta} \;+\; c_k^\infty\;\mathsf{s}_{\rm S}^{-1}\,\omega\,\mathrm{H}_k^{(1)'}(\omega\,\mathsf{s}_{\rm S}\,|\boldsymbol{x}|)e^{\mathrm{i}k\theta}\,,\\
\mathrm{p}_k \;&=\; -\,a_k^\infty\,M\,\big(\beta_{\rm P}\;+\;\alpha\big)\,\mathrm{H}_k^{(1)}(\omega\,\mathsf{s}_{\rm P}\,|\boldsymbol{x}|)\,e^{\mathrm{i}\,k\,\theta} \;-\; b_k^\infty\,M\,\big(\beta_{\rm B}\;+\;\alpha\big)\,\mathrm{H}_k^{(1)}(\omega\,\mathsf{s}_{\rm P}\,|\boldsymbol{x}|)\,e^{\mathrm{i}\,k\,\theta}\;.
\end{aligned}
\tag{82}
$$

Imposing (81), we obtain the following linear system satisfied by a_k^∞, b_k^∞, c_k^∞ in each mode k:

$$
\mathbb{A}_k^{\mathbf{u},\mathrm{p}}\begin{pmatrix}a_k^\infty\\ b_k^\infty\\ c_k^\infty\end{pmatrix}=\begin{pmatrix}-\,\mathrm{i}\,\omega\,\mathbf{u}_{r,k}^{\rm pw}\\ -\,\mathrm{i}\,\omega\,\mathbf{u}_{\theta,k}^{\rm pw}\\ -\mathrm{p}_k^{\rm pw}\end{pmatrix}\,, \tag{83}
$$

where the coefficients matrix is defined as:

$$
\mathbb{A}_k^{\mathbf{u},\mathrm{p}}=\begin{pmatrix}
\mathsf{s}_{\rm P}^{-1}\,\omega\,\mathrm{H}_k^{(1)'}(\omega\,\mathsf{s}_{\rm P}\,\mathfrak{a}) & \mathsf{s}_{\rm B}^{-1}\,\omega\,\mathrm{H}_k^{(1)'}(\omega\,\mathsf{s}_{\rm B}\,\mathfrak{a}) & -\,\mathsf{s}_{\rm S}^{-2}\,\dfrac{\mathrm{i}k}{\mathfrak{a}}\mathrm{H}_k^{(1)}(\omega\,\mathsf{s}_{\rm S}\,\mathfrak{a})\\
\mathsf{s}_{\rm P}^{-2}\,\dfrac{\mathrm{i}k}{\mathfrak{a}}\mathrm{H}_k^{(1)}(\omega\,\mathsf{s}_{\rm P}\,\mathfrak{a}) & \mathsf{s}_{\rm B}^{-2}\,\dfrac{\mathrm{i}k}{\mathfrak{a}}\mathrm{H}_k^{(1)}(\omega\,\mathsf{s}_{\rm B}\,\mathfrak{a}) & \mathsf{s}_{\rm S}^{-1}\,\omega\,\mathrm{H}_k^{(1)'}(\omega\,\mathsf{s}_{\rm S}\,\mathfrak{a})\\
-M\,\big(\beta_{\rm P}\;+\;\alpha\big)\,\mathrm{H}_k^{(1)}(\omega\,\mathsf{s}_{\rm P}\,\mathfrak{a}) & -\,M\,\big(\beta_{\rm B}\;+\;\alpha\big)\,\mathrm{H}_k^{(1)}(\omega\,\mathsf{s}_{\rm P}\,\mathfrak{a}) & 0
\end{pmatrix}\,. \tag{84}
$$

Contents

References

[1] T. Akiyoshi, K. Fuchida, and H. Fang, *Absorbing boundary conditions for dynamic analysis of fluid-saturated porous media*, Soil Dynamics and Earthquake Engineering, 13 (1994), pp. 387–397.

[2] T. Akiyoshi, X. Sun, and K. Fuchida, *General absorbing boundary conditions for dynamic analysis of fluid-saturated porous media*, Soil Dynamics and Earthquake Engineering, 17 (1998), pp. 397–406.

[3] H. Barucq, J. Diaz, R.-C. Meyer, and H. Pham, *Analytic solutions and transmission eigenvalues in isotropic poroelasticity for bounded domain, scattering of obstacles and fluid-solid interaction problems in 2d*, 2019.

[4] ——, *Implementation of HDG method for 2D anisotropic poroelastic first-order harmonic equations*, 2020.

[5] J.-P. Berenger, *A perfectly matched layer for the absorption of electromagnetic waves*, Journal of computational physics, 114 (1994), pp. 185–200.

[6] Biot, *General theory of three-dimensional consolidation*, Journal of Applied Physics, 12, (1941).

[7] ——, *General solutions of the equations of elasticity and consolidation for a porous material*, Journal of Applied Mechanics, (1956).

[8] ——, *Generalized theory of acoustic propagation in porous dissipative media*, Journal of the Acoustical Society of America, (1962).

[9] M. A. Biot, *Theory of elasticity and consolidation for a porous anisotropic solid*, Journal of Applied Physics, (1955).

[10] Biot-Willis, *The elastic coefficients of the theory of consolidation*, Journal od Applied Mechanics, (1957).

[11] L. Boillot, *Contributions à la modélisation mathématique et à l'algorithmique parallèle pour l'optimisation d'un propagateur d'ondes élastiques en milieu anisotrope*, PhD thesis, Pau, 2014.

[12] M. Bonnasse-Gahot, *High order discontinuous Galerkin methods for time-harmonic elastodynamics*, PhD thesis, 2015.

[13] J. M. Carcione, *Wave fields in real media: Wave propagation in anisotropic, anelastic, porous and electromagnetic media*, vol. 38, Elsevier, 3 ed., 2015.

[14] J. de la Puente, M. Dumbser, M. Käser, and H. Igel, *Discontinuous Galerkin methods for wave propagation in poroelastic media*, Geophysics, 73 (2008), pp. T77–T97.

[15] G. Degrande and G. De Roeck, *An absorbing boundary condition for wave propagation in saturated poroelastic mediaPart I: Formulation and efficiency evaluation*, Soil Dynamics and Earthquake Engineering, 12 (1993), pp. 411–421.

[16] ——, *An absorbing boundary condition for wave propagation in saturated poroelastic mediaPart II: Finite element formulation*, Soil Dynamics and Earthquake Engineering, 12 (1993), pp. 423–432.

[17] *NIST Digital Library of Mathematical Functions*. http://dlmf.nist.gov/, Release 1.0.24 of 2019-09-15. F. W. J. Olver, A. B. Olde Daalhuis, D. W. Lozier, B. I. Schneider, R. F. Boisvert, C. W. Clark, B. R. Miller, B. V. Saunders, H. S. Cohl, and M. A. McClain, eds.

[18] B. Dupuy, L. De Barros, S. Garambois, and J. Virieux, *Wave propagation in heterogeneous porous media formulated in the frequency-space domain using a discontinuous Galerkin method*, Geophysics, 76 (2011), pp. N13–N28.

[19] S. Garambois and M. Dietrich, *Full waveform numerical simulations of seismoelectromagnetic wave conversions in fluid-saturated stratified porous media*, Journal of geophysical research, (2002).

[20] Y. He, T. Chen, and J. Gao, *Unsplit perfectly matched layer absorbing boundary conditions for second-order poroelastic wave equations*, Wave Motion, 89 (2019), pp. 116–130.

[21] V. Mattesi, M. Darbas, and C. Geuzaine, *A high-order absorbing boundary condition for 2D time-harmonic elastodynamic scattering problems*, Computers & Mathematics with Applications, 77 (2019), pp. 1703–1721.

[22] T. B. A. Senior and J. L. Volakis, *Approximate boundary conditions in electromagnetics*, Institution of Electrical Engineers, London, 1995. OCLC: ocm32509096.

[23] Y. Zeng, J. He, and Q. Liu, *The application of the perfectly matched layer in numerical modeling of wave propagation in poroelastic media*, Geophysics, 66 (2001), pp. 1258–1266.

Acknowledgments

This project has received funding from the European Unions Horizon 2020 research and innovation program under the Marie Sklodowska-Curie grant agreement No 777778 (MATHROCKS).

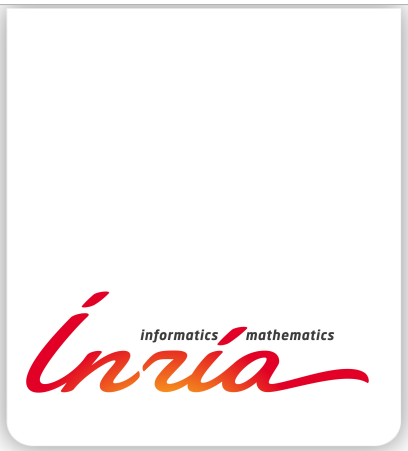

RESEARCH CENTRE
BORDEAUX – SUD-OUEST

200 avenue de la Vieille Tour
33405 Talence Cedex

Publisher
Inria
Domaine de Voluceau - Rocquencourt
BP 105 - 78153 Le Chesnay Cedex
inria.fr

ISSN 0249-6399